University of Alberta

Tumor necrosis factor triggers the expression and activation of matrix metalloproteinases through NADPH-dependent superoxide production

by

Ahmed Awad

A thesis submitted to the Faculty of Graduate Studies and Research
in partial fulfillment of the requirements for the degree of
Master of Science

in

Physiology

Ahmed Awad

Edmonton, Alberta

Examining Committee members:

Supervisor:	Dr. Zamaneh Kassiri, Physiology
Committee member:	Dr. Richard Schulz, Pediatrics and Pharmacology
Committee member:	Dr. Sandra Davidge, Obstetrics/Gynecology and Physiology
External examiner:	Dr. Nadia Jahroudi, Medicine

Dedication

to

My grandmother Nefoos

&

My parents, Elsayed & Fadia

Abstract

Tumor necrosis factor (TNF) is upregulated in a number of cardiomyopathies. This thesis investigates TNF in triggering the expression and activation of matrix metalloproteinases (MMPs) in pressure overload cardiac disease, and explores the role of superoxide.

Cardiac pressure overload was generated in adult wild-type and $TNF^{-/-}$ mice by transverse aortic constriction. Isolated cardiomyocytes and cardiofibroblasts from neonatal mice ventricles were treated with recombinant TNF (rTNF), and MMP induction and activation were assessed, with and without apocynin (a NADPH-oxidase inhibitor).

$TNF^{-/-}$ mice showed less superoxide production and MMP activation, compared to wild-type mice, following pressure overload. rTNF upregulated the production of NADPH-dependent superoxide in cardiomyocytes as early as 1 hour (24 hours in cardiofibroblasts). rTNF also increased the expression of MMP-9 and MMP-12 in cardiomyocytes more than in cardiofibroblasts, and MMP-8 and MMP-13 more in cardiofibroblasts. This induction in both cardiac cell types was concomitant with superoxide production.

Acknowledgements

I would like to thank my supervisor, Dr. Zamaneh Kassiri without whom this work would not have been a reality. I want to express my gratitude to her for inspiration and patience during the period of my research.

My next appreciation goes to my supervisory committee members, Dr. Richard Schulz and Dr. Sandra Davidge for their kindness, guidance, support, and valuable suggestions.

My gratitude also goes to all members in Dr. Kassiri's lab and Dr. Oudit's lab for their help during this study. I would like to thank Vijay Kandalam, Danny Guo, and Fung Lan Chow who offered support and help in numerous ways.

I am thankful to my parents, Elsayed Elhefny and Fadial Aboelmal, and to my sisters, Dina and Nehal, for their ongoing support and encouragement. I thank all my friends who stood behind me in times of hardship. Finally, thanks to my wife, Aya Mowafy, for being by my side.

Table of Contents

List of Figures

List of Tables

List of Abbreviations

AP-1	activator protein-1
BSA	bovine serum albumin
DHE	dihydroethidium
DPI	diphenyleneiodonium sulfate
FBS	fetal bovine serum
IKB	inhibitor of NF-κB
IKK	inhibitor of κB kinase
JNK	c-Jun-NH2 terminal kinase
LDH	lactate dehydrogenase
LV	left ventricle
MAPK	mitogen activated protein kinase
MEKK	mitogen activated protein kinase kinase
MMPs	matrix metalloproteinases
MT-MMP	membrane-type MMP
NF-κB	nuclear factor-kappaB
NO	nitric oxide
NOS	nitric oxide synthase
RAIDD	RIP-associated ICH-1/CED-3-homologous protein with a death domain
RIP	receptor interacting protein
RNS	reactive nitrogen species

ROS	reactive oxygen species
SDS	sodium dodecyl sulfate
SOD	superoxide dismutase
SODD	silencer of death domain, inhibitory protein
TAC	transverse aortic constriction
TACE	tumor necrosis alpha converting enzyme; also known as disintegrin or metalloproteinase-17 (ADAM-17)
TIMPs	tissue inhibitors metalloproteinases
TIMPs	tissue inhibitor of metalloproteinases
TNF	tumor necrosis factor
TNF-R1	tumor necrosis factor receptor-1
TRADD	TNF receptor-associated death domain
TRAF2	TNF receptor-associated factor-2
WT	wild type

Chapter 1. Introduction

1.1 Cardiac Diseases: Overview

Despite the immense progress in research, cardiovascular diseases remain a major cause of morbidity and mortality around the world.[1] The World Health Organization (WHO) reports that cardiovascular diseases contribute to the deaths of 17 million people of all ages each year.[2] In developing countries, they cause twice as many deaths as HIV, malaria, and tuberculosis combined.[3] The burden of cardiovascular diseases strike not only the developing countries but developed countries as well.[4] In the US, according to the National Health and Nutrition Examination Survey, over 80 million American adults suffer from one or more types of cardiovascular disease,[5] and in Canada, cardiovascular diseases contribute to 30% of all mortalities.[6]

Cardiovascular disease is a general term that refers to a variety of different conditions affecting heart and blood vessels such as myocardial ischemia, pericardial and endocardial diseases, congenital heart defects, arrhythmia, hypertension and atherosclerosis.[7] Since cardiac disease and remodeling can progress to heart failure if not treated, elucidation of the mechanisms underlying these conditions are important and can lead to new strategies for diagnosis, prevention, and/or treatment of cardiovascular diseases. This can, in turn, reduce the economic cost of long-term drug treatment and frequent hospitalization of patients.[8] Nearly all medications currently used clinically for the treatment of

heart failure target the neurohormonal systems such as catecholaminergic and renin/angiotensin.[9] Unfortunately, no treatment is available for maladaptive cardiac remodeling, which is characterized by a progressive degradation of extracellular matrix structure initiating an adverse remodeling process that leads to cardiac dilation dysfunction.[10] Hence, determining the molecular pathways underlying cardiac remodeling remains a challenge for researchers.

1.1.1 Cardiac hypertrophy and remodeling

The heart is a dynamic organ with the ability to adjust to sustained increase in hemodynamic load as it occurs with chronic hypertension, valve stenosis, or in conditioned athletes with regulated cardiac output.[11] Cardiac remodeling is best described as structural changes in one or more cardiac chambers,[12] as well as dynamic changes in ventricular size and shape as a result of hemodynamic and metabolic insults to the heart.[13] Left ventricular (LV) remodeling is a complex process in the pathogenesis of heart failure, and is characterized by cardiac hypertrophy and interstitial fibrosis.[14] Cardiac hypertrophy is a fundamental adaptation of the heart to an increased hemodynamic overload. This adaptation is characterized by an increase in the size and protein content of cardiomyocytes.[15] With little to no capacity for proliferation, an increase in cardiomyocyte size maintains pressure through normalization of wall stress. This relationship is governed by the Law of LaPlace:[16]

$$j=pr/2h$$

where j=wall stress, p=ventricular pressure, r=internal radius of chamber, and h=thickness of LV chamber. Hypertrophy is categorized by its geometry, being either concentric or eccentric. Eccentric hypertrophy is characterized by an increase in ventricular wall thickness (h) accompanied by an increase in chamber size (r). This phenotype is created through addition of sarcomeres in series rather than in parallel (width), and has been associated with physiological growth as well as pathophysiological growth resulting from volume overload.[17, 18] Concentric hypertrophy is characterized by an increase in ventricular wall thickness (h) accompanied by a decrease in internal chamber size (r). Specifically, cardiomyocytes increase more in width than in length through parallel sarcomere addition.[17, 19] Concentric hypertrophy is considered pathological as it often develops into a decompensated state, characterized by systolic dysfunction and reduced left ventricular ejection fraction.[20] This decompensated state is characterized by a decrease in wall thickness (h) and an increase in internal chamber size (r).

Remodeling of the ventricular wall to a more dilated state marks the progression of cardiomyopathy to end-stage heart failure, which presently does not appear to be reversible by conventional pharmacological therapies.[21] Thus, the development of novel strategies to specifically target the maladaptive features of left ventricular hypertrophy could provides a treatment for heart failure.

1.2 Left Ventricular Pressure Overload

1.2.1 Overview

Cardiac pressure overload occurs in response to excessive work load imposed on heart chambers by increased impedance to ejection.[22] Atrial pressure overload occurs due to valvular diseases such as mitral stenosis brought about by rheumatic fever[23] and affects the left atrium, whereas, the right atrium is affected by tricuspid stenosis, which can be caused by a tumor in the right atrium, a connective tissue disorder, or more rarely, a birth defect of the heart.[24] The right ventricle suffers pressure overload mainly secondary to pulmonary hypertension,[25] whereas, the causes of increased pressure overload on the left ventricle (LV) are systemic hypertension, obstruction in left ventricular blood flow as in coarctation of the aorta, or aortic stenosis.[14]

The causes of left ventricular pressure overload contribute to a large portion of cardiac diseases. Hypertension causes 62% of stroke and 49% of heart attack incidents, the two leading causes of death worldwide,[26] and is responsible for 7 million deaths each year.[26] The estimated total number of human adults worldwide with hypertension is expected to be 1.56 billion by 2025.[27] Aortic stenosis, defined as a narrowing of the aortic valve or the aorta, is the most dangerous of all valve lesions, and often leads to sudden death.[28] Approximately 2% of people over the age of 65, 3% of people over the age of 75, and 4% of people over the age of 85 have aortic stenosis disorder. Patients with chronic heart failure due to aortic stenosis have a 2-year mortality rate of 50% if the aortic

valve is not replaced.[29] The main causes of aortic stenosis include congenital birth defect of the aortic valve, progressive calcification, and to a lesser extent, scarring following rheumatic fever.[30] Coarctation of the aorta most often occurs as an isolated defect in about 6 to 8% of all children with congenital heart disease.[28]

1.2.2 Pressure overload-induced cardiac remodeling: Molecular mechanisms

Left ventricular hypertrophy is the initial compensatory response to pressure overload. The increased wall thickness normalizes wall stress according to the Law of Laplace, and aims to sustain the pumping function of the LV. Nevertheless, prolonged hemodynamic stress leads to maladaptive changes and pathological hypertrophy and eventual dilation.[11]

Cardiac response to left ventricular pressure overload involves complex molecular and cellular modifications.[31] Mechanical stress is transmitted through the myocardial extracellular matrix (ECM) to cardiomyocytes resulting in increased cardiomyocyte growth and hypertrophy[32, 33] as an adaptive response to the increased afterload and to maintain sufficient blood supply to the organs.[34,35] Cardiac hypertrophy has been reported to occur through upregulation of growth factors such as transforming growth factor beta[36, 37] and hormonal factors such as angiotensin II.[38] Increased activity of mitogen-activated protein kinase and protein kinase C isoforms have also been suggested to be involved in cardiomyocyte hypertrophy.[39, 40] Protein kinase C activation stimulates MAPK signaling, primarily through activation of ERK1/2 signaling, and weakly through JNK.[41, 42]

The importance of ERK signaling was reported since transgenic mice with cardiac-restricted overexpression of active MEK1 showed specific activation of ERK1/2 in the heart.[43] These mice developed concentric hypertrophy with no sign of interstitial cell fibrosis. In another study, increased p38 MAPK activity was reported during the development of left ventricular hypertrophy *in vivo* in hypertensive rats.[44]

Cardiac hypertrophy and heart failure are also associated with altered intracellular Ca^{2+} signaling.[45] The sarcoplasmic reticulum exhibits increased Ca^{2+}-uptake and release during the early stage of cardiac hypertrophy due to pressure overload.[45] Studies have shown that α-adrenergic receptor stimulation leads to phospholipase-C activation, resulting in the divergent activation of two signaling networks, one of which involves diacylglycerol-mediated activation of protein kinase C,[46] and the other involving the formation of inositol phosphates and release of calcium from intracellular sarcoplasmic calcium stores.[46] Both arms of the pathway have been implicated in hypertrophic regulation. In any case, persistent pressure overload leads to adverse ventricular remodeling, which is frequently associated with an increased rate of cardiomyocyte apoptosis, reduced contractile function, and increased collagen deposition,[47] leading to increased left ventricular wall stiffness and reduced compliance, and ultimately heart failure.[48] Moreover, pathological hypertrophy is also accompanied by the re-expression of a fetal gene program, which includes upregulation of atrial natriuretic factor, α-skeletal actin and ß-myosin heavy chain genes.[49]

Over the last 20 years, studies have revealed the activation and involvement of the immune system and inflammatory mediators in cardiac diseases.[50-56] Tumor necrosis factor-α (TNFα) plays a substantial role in cardiac remodeling in various cardiac diseases.[48, 53, 57] Levels of circulating TNFα were found to be elevated in patients with pressure overload, secondary to aortic stenosis.[58] Transgenic mice lacking TNFα were found to have a preserved cardiac function and develop less cardiac hypertrophy, dilation, and failure, compared to wild-type mice in response to pressure overload.[48, 59] Pressure overloaded cardiomyopathy is also associated with increased levels of ECM-degrading proteins and matrix metalloproteinases (MMPs). Cardiac MMP-9 activity was reported to be increased in wild-type mice subjected to aortic banding,[48] and a robust increase in the cardiac levels of MMP-2 and MMP-9 were observed in spontaneously hypertensive rats with heart failure, compared with wild-type rats. Another molecular mechanism that is activated in response to pressure overload is superoxide production, which can further contribute to cardiac dysfunction and heart failure.[60] Although increases in TNFα, MMPs, and superoxides have been reported in pressure-overload cardiomyopathy, a direct link between these three molecular pathways has not been demonstrated in the myocardium. Our study aimed to determine a relation between these three factors in pressure-overload cardiac disease.

1.3 Tumor Necrosis Factor-alpha (TNFα)

1.3.1 Overview

Tumor necrosis factor-alpha (TNFα) is a proinflammatory cytokine that was first isolated in an attempt to identify factors responsible for necrosis of sarcomas that were thought to be toxic for malignant cells.[61] TNFα is a major regulator of inflammatory responses and works through activating chemokines.[62] TNFα is comprised of 212 amino acids and was originally believed to be produced only by macrophages, lymphocytes, and neutrophils in response to inflammatory stimuli.[63, 64] Further studies revealed that TNF-α can also be produced by other cell types such as fibroblasts,[65] smooth muscle cells,[66] cardiomyocytes,[67, 68] epithelial cells,[69] and many other cell types. TNFβ, on the other hand, was found to be secreted by lymphocytes, hence, it was named 'lymphotoxin'. For the rest of this thesis, TNFα is referred to as TNF.

TNF is produced as a transmembrane protein (26 kDa), which is proteolytically cleaved by TACE (tumor necrosis alpha converting enzyme) also known as disintegrin and metalloproteinase-17 (ADAM-17),[70] into a circulating soluble form (17 kDa).[71] Activated TACE can be inhibited by TIMP-3.[72] In addition to TNF shedding,[73, 74] TACE also cleaves and releases TNF receptors[75] (TNF-R1 and TNF-R2) as well as other surface molecules such as transforming growth factor-alpha[76] and vascular adhesion molecule-1[77]. TNF receptors are expressed by almost all nucleated cells.[78] The cytotoxic deleterious effects on the heart caused by TNF are mediated via TNF-R1[56] (discussed in detail in Section

1.3.2). On the contrary, TNF-R2 appears to have protective functions, especially in the myocardium.[78, 79]

1.3.2 TNF signaling transduction pathways

TNF signaling has been implicated in many cardiac diseases. TNF acts by binding to its receptors, TNF-R1 (p55) and TNF-R2 (p75), on the cell surface. Soluble TNF preferentially binds to TNF-R1 due to its 30-fold higher dissociated rate from TNF-R2.[80] Hence, TNF-R1 is considered as the main receptor for soluble TNF, though it does not exclude TNF-R2.[81] Binding of the trimeric TNF to TNF-R1 and TNF-R2 induces a conformational change in the receptors leading to the dissociation of the inhibitory protein SODD (silencer of death domain) from the intracellular death domain and recruitment of several signaling proteins to the cytoplasmic domains of the receptors. Both TNF receptors can send survival and death signals to cells.[82] Binding of TNF to its two receptors, TNF-R1 and TNF-R2, results in recruitment of signal transducers that activate three effectors. Through complex signaling cascades and networks, these effectors lead to the activation of two transcription factors, activation protein-1 and nuclear factor-kappaB (NF-κB).[83] Initially, TRADD (TNF Receptor-Associated Death Domain) protein, binds to TNF-R2 and serves as a platform to recruit additional mediators.[84] TRADD recruits RAIDD (RIP-Associated ICH-1/CED-3-homologous protein with a Death Domain), MADD (MAPK-Activating Death Domain), and RIP (Receptor-Interacting Protein).[85] This event triggers phosphorylation of downstream signal transducers including mitogen activated

protein kinase (MAPK) kinase (MEK) and inhibitor of κB (IκB) kinase (IKK),[86] which, in turn, induces phosphorylation of MKK including c-Jun-NH2 terminal kinase (JNK) and the phosphorylational degradation of inhibitor of NF-κB (IκB). AP-1 proteins, activated by phosphorylated MAPK and NF-κB subunits (e.g., p50, p65) liberated from the IκB-NF-κB complex, would be subsequently translocalized into nuclei for DNA binding to modulate inflammatory effector gene expression including early-response cytokines (e.g., interleukin-1β), chemokines (e.g., macrophage inflammatory protein-2) and adhesion molecules (e.g., intercellular adhesion molecule-1).[87, 88]

TNF can activate another pathway involved in death signaling.[89] FADD (Fas-Associated Death Domain) binds to TRADD.[90] Binding of TRADD and FADD to TNF-R1 leads to the recruitment, oligomerization, and activation of caspase-8. Activated caspase-8 subsequently initiates a proteolytic cascade that includes other Caspases (caspases-3, 6, and 7) and ultimately induces apoptosis through DNA fragmentation and cytolysis. Furthermore, studies have shown that caspase-8 can proteolytically cleave RIP in its intermediate domain, resulting in an inhibition of NF-κB activity and enhanced TNF-induced apoptosis.[91] TNF-induced cell death plays a less significant role compared to its major function in the inflammatory process as death inducing capability is often masked by the anti-apoptotic effects of NF-κB.[92]

Interestingly, TNF-R2 is also the receptor for lymphotoxin or TNFβ. TNFβ is produced by activated lymphocytes and can be cytotoxic to many tumor

and other cells. In neutrophils, endothelial cells, and osteoclasts, TNFβ leads to increased expression of myocin heavy chain and adhesion molecules.[93] As most information regarding TNF signaling is derived from TNF-R1, the role of TNF-R2 is not fully understood, though it is suggested that TNF signaling, mediated via the TNF-R2 receptor, is protective in the myocardium.[79]

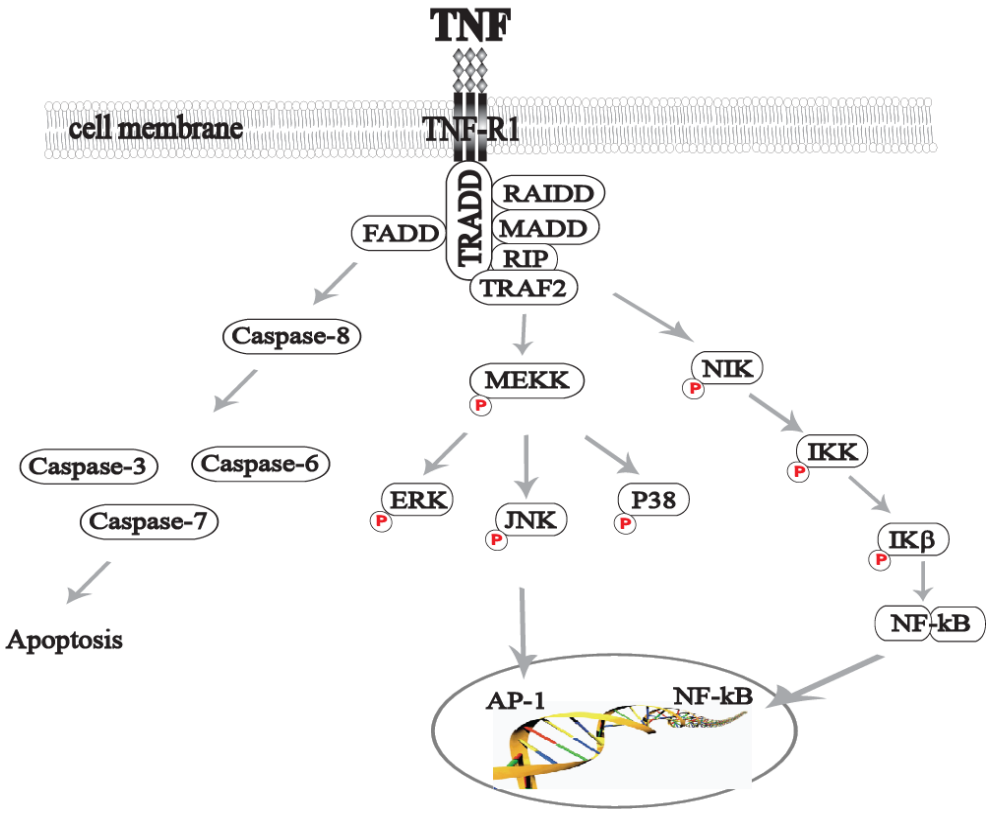

Figure 1.1: TNF signaling pathway through the TNF-R1 receptor. TNF can activate three different pathways: MAPK, NF-κB, and apoptosis.

The abbreviations in the diagrams are as follows: TNF (tumor necrosis factor), TNF-R1 (tumor necrosis factor receptor-1), TRADD (TNF Receptor-Associated Death Domain), FADD (Fas-Associated Death Domain), RAIDD (RIP-Associated ICH-1/CED-3-homologous protein with a Death Domain), MADD (MAPK-Activating Death Domain), RIP (Receptor-Interacting Protein), TRAF2 (TNF receptor-associated factor-2), MEKK (mitogen activated protein kinase kinase), ERK (extracellular signal-regulated kinase), JNK (c-Jun-NH2 terminal kinase), IKK (inhibitor of κB kinase), NIK (NF-κB inducing kinase), IKB (inhibitor of NF-κB), NF-κB (nuclear factor-kappaB), and AP-1(activator protein-1).

1.3.3 Role of TNF in cardiac diseases

TNF exerts a series of unfavorable effects in the heart such as the progression of left ventricular dysfunction, left ventricular remodeling,[94] pulmonary edema,[95] increased cardiac myocyte apoptosis,[96] abnormalities in myocardial metabolism,[97] cachexia,[98] the uncoupling of β-receptor from adenylate cyclase[99] and a triggering of platelet activation.[100] TNF signaling mostly involves intracellular signaling by NF-κB.[101]

TNF has been implicated in the pathogenesis of myocarditis, ischemic heart disease, and cardiac dysfunction.[102-104] Circulating levels of TNF were found to be increased in patients with chronic heart failure,[53] and transgenic mice overexpressing TNF, developed progressive left ventricular wall thinning and dilation accompanied by increased cardiomyocyte apoptosis.[105] Moreover, it was found that the plasma TNF levels increased significantly in patients post myocardial infarction.[106] In an animal study, rats receiving etanercept, a soluble dimerized TNF receptor that inhibits TNF, experienced reduced leukocyte infiltration and extracellular matrix turnover and preserved cardiac function.[107]

The impact of TNF on various cardiovascular diseases opens up opportunities for its use as a disease biomarker and a therapeutic agent.[108] TNF antagonists (e.g., infliximab, etanercept, and adalimumab) work thorough inhibiting the interaction between soluble TNF and its receptors (TNF-R1 and TNF-R2).[109] In a clinical study involving 2,048 patients with moderate-to-severe

congestive heart failure, patients were randomized to placebo or three different doses of etanercept, a highly specific anti-TNF blocking agent. The primary endpoint was the clinical benefit at 24-weeks, where no statistically significant difference was seen in cardiac function compared to the placebo group. In spite of the disappointing results of using anti-TNF as a therapeutic agent in patients with heart failure, the negative results do not necessarily argue against the cytokine hypothesis, but instead, reflect the complexity of the cytokine network, and underscore the challenges in developing treatments for heart disease. The lack of success with anti-TNF therapy[110, 111] may be attributable to application of the drug at a late stage of the disease, after TNF has already exerted its effects in disease progression at an earlier point, by triggering a number of signaling pathways. Hence, inhibiting TNF at the late stage of cardiac disease did not have any beneficial outcomes.

1.3.4 TNF in pressure-overload cardiac disease

Pressure overload is accompanied by a number of cardiac cellular and molecular changes that lead to myocardial remodeling and subsequent ventricular dysfunction. Cytokine signaling, involving TNF,[48] interleukin-6,[112] and their downstream effectors, was found to play a crucial role in the heart in response to pressure-overload. TNF was shown to be elevated in patients with cardiac pressure overload due to aortic stenosis,[58] and in animal models of pressure overload[59] and mechanical stress.[113] Enough evidence exists in the literature to support the function of TNF as a regulatory factor in the pathogenesis of cardiac

remodeling. TNF overexpression in mice results in heart failure,[114] cardiac hypertrophy,[115] and dilation,[116] while mice lacking TNF are less sensitive to hypertrophic signals, compared to the wild-type group, when subjected to mechanical stress.[48]

1.4 Matrix Metalloproteinases (MMPs)

1.4.1 MMPs, TIMPs, and the extracellular matrix (ECM): Overview

Matrix metalloproteinases (MMPs) are zinc-dependent endopeptidases that play a central role in tissue homeostasis and remodeling, and are responsible for degradation and turnover of the extracellular matrix (ECM).[117] By cleaving ECM substrates, MMPs stimulate matrix turnover and remodeling associated with wound healing, embryonic development, and bone growth. MMPs also regulate the bioavailability of important signaling molecules by causing the release of growth factors and cytokines sequestered in the ECM or attached to plasma membranes, permitting them to mediate cell signaling pathways.[118] In addition, the function of MMPs is suggested to regulate the homeostasis of the ECM and play an intracellular role.[119]

So far, 25 members of the MMP family have been identified[120] and collectively, all MMPs have been found to cleave most if not all of the constituents of the ECM.[121-132] MMPs are expressed as inactive zymogens with a pro-peptide domain that must be removed or unfolded to trigger the catalytic activity of the metalloproteinases.[133] The main physiological inhibitors of MMPs

are tissue inhibitors metalloproteinases (TIMPs). In vertebrates, four forms have been found: TIMP-1, TIMP-2, TIMP-3, and TIMP-4. In the adult murine heart, mRNA for TIMP-2 and TIMP-3, are most abundant, followed by TIMP4.[134, 135] All four TIMPs contains an N-terminal inhibitory domain and a C-terminal mediation domain.[136] The N-terminal domain of TIMPs contains residues that interact with the Zn^{2+}-binding region of the MMP catalytic domain, thereby, inhibiting the proteolytic activity of the MMPs.[137] TIMP-1 preferentially inhibits MMP-1, MMP-3, and MMP-9, while TIMP-2 inhibits MMP-2. TIMP-3 and TIMP-4 do not appear to have substrate preferences.[136, 138]

A balance between the function of MMPs and TIMPs determines the homeostasis of the ECM.[139] The cardiac ECM is a network comprised of highly organized protein structures, predominantly collagen type I and type III, and basement membrane components, including laminin, entactin, fibronectin, collagen type IV, fibrillin, and elastin.[140] The network of collagen fibers within the ECM exists at three levels: the *endomysium* surrounds individual muscle fibers; the *epimysium* is a network that surrounds a group of muscle fibers, and the *perimysium* consists of thick, spiral-shaped bundles of collagen that connect the epimysial and endomysial networks.[141] Collagenous “struts” connect adjacent myocytes, and connect the myocytes to the capillary endothelium to attain capillary stability in the presence of high intraventricular pressure. This structural arrangement of collagens prevents cardiomyocyte slippage and overstretching, while contributing to cardiac recoil.[141] The ECM provides the structural

framework for cardiomyocytes and the neighboring vessels and capillaries, and translates single cardiomyocyte contractility into a ventricular syncytium.[142] The ECM also bears most of the mechanical stress to which a tissue is subjected,[143] and provides a microenvironment for soluble, matrix-bound and cell surface proteins, that trigger the signaling pathways playing a fundamental role in the myocardial remodeling process,[140, 144, 145] which occurs with pressure overload.[146] For instance, TNF is initially present as a membrane-bound protein and its activation and signaling occurs primarily in the myocardial interstitium after being shed by TNF-alpha-converting enzyme (TACE or ADAM17),[10] while growth factors such as transforming growth factor-β are bound to the ECM, and are released by direct action of metalloproteinases[147, 148] or secondarily to disruption of the ECM structure.[152]

1.4.2 Classification of MMPs

The MMP family is collectively capable of digesting most of the ECM structural components, with each member having distinct, yet overlapping substrate specificity.[148] Family members differ from one another in terms of the presence or absence of domains that contribute to their substrate specificity, matrix binding, cellular localization, and inhibitor binding.[149] Generally, MMPs contain at least an N-terminal signal peptide followed by a prodomain, a catalytic domain, a hinge region, and a C-terminal hemopexin-like domain.[150] The signal peptide directs MMP translation to the rough endoplasmic reticulum where MMPs enter the secretory pathway and are ultimately expressed on the plasma

membrane (MT-MMPs) or secreted into the ECM. The function of the prodomain is to maintain MMP latency. The highly conserved PRCG(V/N)PD cysteine switch is located near the C-terminal end of the prodomain, and the cysteine within this sequence forms a critical bond with an essential Zn^{2+} ion located in the active site of the catalytic domain. The catalytic domain holds the MMP proteolytic machinery and contains the essential Zn^{2+} ion which is anchored to three histidine residues within the conserved peptide sequence HEXGHX(L/M)G(L/M)XH, located at the active site.[151] The hemopexin-like domain is a propeller structure involved in substrate recognition and in the recognition of MMPs by the tissue inhibitor of metalloproteinases (TIMPs).

MMPs have different molecular structures. MMP-7 and -26 (matrilysin-1 and -2) differ from other MMPs in that they lack the hemopexin domain and the hinge region. In addition to the common domains, several MMPs have other functionally important domains and peptide inserts. The gelatinases contain three fibronectin inserts within their catalytic domain, which assist in gelatin recognition.[152] MMP-9 also contains an extended hinge region that resembles the 012 chain of type V collagen.[153] The MT-MMPs are tethered to the plasma membrane by a single-pass, type I transmembrane domain or by glycosylphosphatidylinositol-anchored proteins, and also contain a furin cleavage site between the prodomain and the catalytic domain that is involved in intracellular MMP activation.[154] The furin-activated MMPs contain a recognition motif for intracellular activation by furin-like serine proteinases between their

propeptide and catalytic domain.[120] This motif is also found in the vitronectin-like insert MMPs and the MT-MMPs. [120]

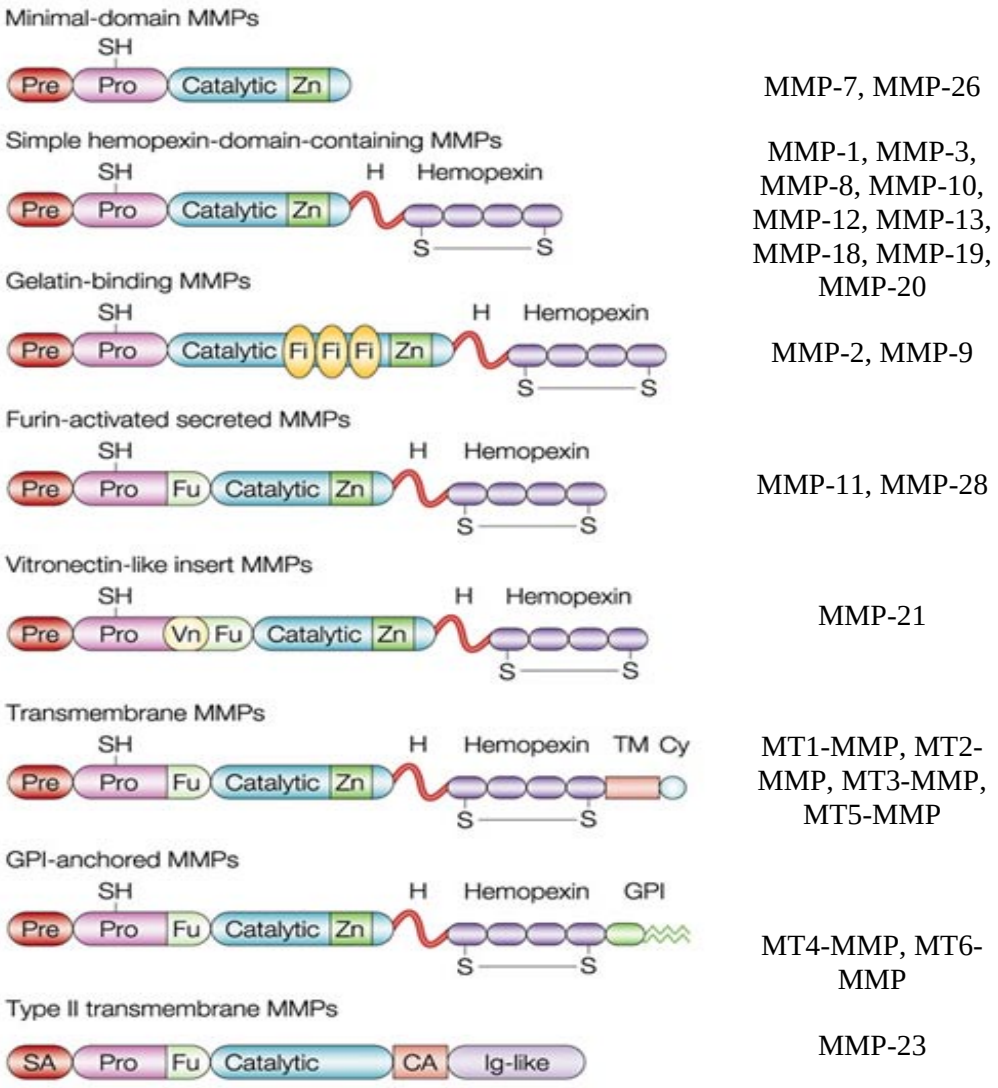

Figure 1.2: Schematic representation of the domain organizations of different structural classes of MMPs.

Adapted from Egeblad and Werb 2002.[155] The abbreviations in the diagrams are as follows: Pre (amino terminal signal sequence), Pro (propeptide), Zn (zinc binding site in the catalytic domain), H (hinge redion), SH (thiol group), S-S (disulphide bond), Fi (collagen type II repeats of fibronectin), Fu (furin recognition site), Vn (vitronectin-like insert), TM (transmembrane), Cy (short cytoplasmic tail), GPI-anchored (glycosylphoshatidylinositol), SA (n-terminal signal anchor), CA (cysteine array), and Ig-like (immunoglobulin-like domain).

MMPs are classified according to substrate preference into six different subfamilies: 1) collagenases, 2) gelatinases, 3) stromelysins, 4) matrilysins, 5) membrane-type MMPs, and 6) others (Table 1.1). The collagenases (including MMP-1, -8,-13, and -18) selectively degrade triple-helical fibrillar collagens,[156] while the stromelysins target a range of ECM proteins, and include MMPs-3, -10 and -11. The membrane-type MMPs (MT-MMPs; including MMP-14, -15, -16, -17, -24, and -25) are characterized by their attachment to the cell membrane, and can degrade a variety of ECM components, including gelatin, fibronectin, and laminin.[157] The gelatinases (MMP-2 and -9) are selective for type IV collagen and gelatin (denatured collagen).[158] MMP-12, also known as metalloelastase or macrophage elastase, is expressed primarily in macrophages, is essential for macrophage migration, and is capable of digesting several ECM molecules.[159]

Table 1.1: Matrix Metalloproteinases[160,161, 162]

Type	MMP Designation	Common Name
Collagenase	MMP-1	Collagenase-1
	MMP-8	Collagenase-2
	MMP-13	Collagenase-3
Gelatinase	MMP-2	Gelatinase-A
	MMP-9	Gelatinase-B
Stromelysin	MMP-3	Stromelysin-1
	MMP-10	Stromelysin-2
	MMP-11	Stromelysin-3
	MMP-19	Stromelysin-4
Matrilysin	MMP-7	Matrilysin-1
	MMP-26	Matrilysin-2
Membrane Type	MMP-14	MT1-MMP
	MMP-15	MT2-MMP
	MMP-16	MT3-MMP
	MMP-17	MT4-MMP
	MMP-24	MT5-MMP
	MMP-25	MT6-MMP
Other	MMP-12	Metalloelastase
	MMP-20	Enamelysin
	MMP-23	Cysteine-Array MMP
	MMP-27	
	MMP-28	Epilysin

1.4.3 MMPs: Physiological vs. pathological

Physiologically, MMPs play an important role in embryogenesis by controlling cell migration and tissue remodeling, the two fundamental processes of embryogenesis and wound healing.[121-132] In addition, MMPs contribute to cardiac development by orchestrating the direction of cardiac looping during fetal development, which involves ventral closure of the heart and gut tubes, and

asymmetric cell proliferation in the dorsal mesocardium, to drive the looping direction.[163] On the other hand, MMPs have been shown to also play a critical role in various diseases, such as chronic obstructive pulmonary disease,[164] asthma,[164] rheumatoid arthritis,[165] cancer,[166] and cardiomyopathy.[167, 168,169,170]

The MMPs play a significant role in extracellular remodeling, and studies have demonstrated that increased MMP expression and activity takes place in chronic heart failure.[167, 168] MMPs cause alterations in collagen structure[47, 171] and composition[91] within the LV myocardium in several cardiac disease states, which in turn influences LV geometry.[172, 173] Increased MMP-2 activity was detected in spontaneously hypertensive rats and found to mediate cardiac hypertrophy, and systolic and diastolic dysfunction.[169] Studies using MMP-deficient mice have illuminated the crucial role of MMPs, not only in tissue homeostasis, but also in disease progression. MMP-2 and MMP-9 play significant roles in cardiac rupture after myocardial infarction[174] and in aortic aneurysm formation.[175] MMP-9 and MMP-14 are associated with ischemia and repefusion.[176] Studies of atherosclerotic plaque formation indicate that MMP-12 promotes the expansion of atherosclerotic lesions.[177] In clinical studies, MMP-2 and MMP-9 levels were increased in the plasma of patients with unstable angina or acute myocardial infarction.[170] Some of the MMPs that have been reported to be involved in myocardial remodeling are as follows: collagenases MMP-1, MMP-8, and MMP-13; gelatinases MMP-2 and MMP-9; metalloelastase MMP-12; and the membrane-type MMP, MMP-14 (MT1-MMP).[139, 148]

1.4.4 Regulation of MMPs

The regulation of MMPs is complex and occurs at several levels. Inflammatory cytokines, including TNF and IL-1ß along with several growth factors trigger intracellular signaling cascades that result in MMP transcriptional induction. For example, the MAP kinase cascades, stimulated by IL-1ß and TNF, result in activation of AP-1 transcription factors, which bind to several MMP promoters.[178] Pathways that activate NF-κB are also involved in upregulating the transcription of MMPs. Conversely, transcription of several MMPs is suppressed by glucocorticoids, retinoic acid, and anti-inflammatory cytokines such as TGF-ß1 and IFN-ß.[159] TGF-ß1 and IFN-ß stimulate activation of the Smad and STAT transcription factor families, respectively, which bind to, and inhibit the transcription of MMPs containing the appropriate DNA binding sites, such as MMP-1 and MMP-7.[178] Cell-cell or cell-matrix interactions, mediated by adhesion molecules and integrins, can also lead to the transcriptional regulation of MMPs.[159] The transcriptional upregulation of MMPs does not translate into an increase in MMP activity; however, unless activation mechanisms are already in place. Disruption of the cysteine switch, by proteolytic or non-proteolytic mechanisms, results in prodomain removal and activation.[179] MMPs are secreted as inactive zymogens with a pro-peptide domain that must be removed or unfolded to expose the active binding site, hence, triggering the catalytic activity of the metalloproteinases,[133] and an active MMP has the ability to induce proteolytic activation of other MMPs.[180] The prodomain of MMP zymogens contains a cysteine residue (Cys73) that stabilizes the pro-MMP in its inactive

form by forming a bond between its thiol group and the Zn^{2+} in the catalytic domain. Moreover, the intact Cys73 thiol-Zn^{2+} bond sequesters the Zn^{2+} from the catalytic site, thereby rendering the MMP inactive. MMP activation thus requires disruption of this bond through a mechanism called the "cysteine switch,[181] which occurs when replacing the thiol group of the cysteine residue with water and the release of the propeptide. Activation of proMMP-2 appears to be a unique occurrence among the MMPs, where the binding of TIMP-2 to proMMP-2 is required for proMMP-2 activation by membrane-type MMPs.[159] Another MMP activation system is furin-dependent intracellular activation, with enzymes that are either secreted or act as cell surface-bound active enzymes.[182] Their activation is regulated by the tissue-specific location of the enzyme, and their inactivation is controlled by endogenous inhibitors or by proteolysis. Activation of MMPs can also be mediated by reactive oxygen and nitrogen species through a pathway not necessarily involving the proteolytic removal of the propeptide domain.[119] Oxidation of the cysteine72 prodomain thiol breaks the thiol-Zn^{2+} bond (flipping the cysteine switch), an event that is followed by autolytic cleavage and loss of the zymogen prodomain.[183] Once activated, several mechanisms exist to suppress the proteolytic activity of MMPs. The TIMPs are a family of four proteins that serve as the major endogenous inhibitors of MMPs, binding to MMPs in a 1:1 ratio.[159]

1.5 Oxidative Stress

1.5.1 Overview

Reactive oxygen species (ROS) include superoxide ($O_2^{\bullet -}$), hydroxyl ($OH^{\bullet}$) as well as hydrogen peroxide (H_2O_2), while reactive nitrogen species (RNS) include peroxynitrite. Antioxidant systems encompass a host of enzymes (e.g., superoxide dismutase, catalase, or glutathione peroxidase) and vitamins (e.g., C and E).[184] Oxidative stress in living organisms occurs when an imbalance exists between free radical production and endogenous antioxidant defense, provoking tissue damage through oxidative modification of essential cellular biomolecules. Although toxic in high levels, low levels of ROS are essential in many biochemical processes. These include intracellular messaging during cell differentiation and cell cycle progression, growth arrest, apoptosis,[185] and immune cell activation.[186]

1.5.2 Reactive oxygen species (ROS), reactive nitrogen species (RNS), and antioxidants

ROS are oxygen-containing molecules that can readily donate or extract electrons from other molecules, and are divided into free radicals and non-radical-reactive species.[187] Free radicals are species that contain one or more unpaired electron allowing them to react with other molecules. Molecular diatomic oxygen (O_2) is considered as a free radical species because it has two unpaired electrons (di-radical); however it has restricted reactivity. The addition of one electron to O_2 forms the superoxide anion radical ($O_2^{\bullet -}$), which is considered the “primary” ROS

and can generate “secondary” ROS by interacting with other molecules directly or via enzyme- or metal-catalyzed processes.[188] Superoxide is normally dismutated to H_2O_2 and singlet oxygen. While H_2O_2 is not a free radical, it is still a common ROS albeit less reactive than hydroxyl radicals. Additional single electron reductions of H_2O_2 form $OH^{\bullet}$.[189] The $OH^{\bullet}$ radical can also be produced through the Fenton reaction ($Fe^{2+} + H_2O_2 \rightarrow Fe^{3+} + OH^{\bullet} + OH^-$) or by the Haber-Weiss reaction ($O_2^{\bullet-} + H_2O_2 \rightarrow O_2 + OH^{\bullet} + OH^-$).[190] On the other hand, nitric oxide ($NO^{\bullet}$) is a nitrogen radical synthesized from L-arginine and O_2 by the action of nitric oxide synthase (NOS).[191] The peroxynitrite ($ONOO^-$) anion is a short-lived oxidant species that is produced by the reaction of nitric oxide ($NO^{\bullet}$) and superoxide ($O_2^{\bullet-}$) radicals. Peroxynitrite ($ONOO^-$) can either react with carbon dioxide (in equilibrium with physiological levels of bicarbonate anion), which leads to the formation of carbonate ($CO_3^{\bullet-}$) and nitrogen dioxide ($NO_2^{\bullet}$) radicals, or can be protonated to form peroxynitrous acid, a highly unstable intermediate species with a very short half-life, which spontaneously undergoes either homolytic or heterolytic cleavage to form $NO_2^{\bullet}$ and $OH^{\bullet}$.[192]

Reactive species can be eliminated by a number of enzymatic and nonenzymatic antioxidant mechanisms. Superoxide dismutase (SOD) immediately converts $O_2^{\bullet-}$ to H_2O_2, which is then detoxified to water either by catalase in the lysosomes or by glutathione peroxidase in the mitochondria. Another important enzyme is glutathione reductase, which is a prolific glutathione regenerator used as a hydrogen donor by glutathione peroxidase during the detoxification of H_2O_2.

Glutathione (GSH) is another antioxidant that acts as a scavenger as well as a cosubstrate for GSH peroxidase, and it serves as a major intracellular redox system.

Normally, superoxide generated in the mitochondria can be degraded by Mn-SOD or by Cu/Zn-SOD in the cytosol. In the endoplasmic reticulum, NADPH-cytochrome P_{450} reductase can leak electrons onto O_2, to generate $O_2^{\bullet -}$. Reduced flavin adenine dinucleotide and cytochrome-b_5 can also contribute to this system. Within the peroxisomes, enzymes are present to produce H_2O_2 directly, and H_2O_2 can react with Fe^{2+} or Cu^{2+} to form hydroxyl radicals via the Fenton reaction.[193]

1.5.3 ROS in cardiovascular diseases

Potential sources of ROS generation in the myocardium during disease include the mitochondria[194] and cytosolic enzymes, such as xanthine oxidase,[195] cytochrome P_{450} oxidases, and uncoupled NO synthases (which generate superoxide instead of NO when deficient in tetrahydrobiopterin),[196] NADPH oxidase,[60] microsomes and peroxisomes, and transition metals such as Fe^{2+} and Cu^{2+}. Superoxide is also produced from both complexes I and III of the electron transport chain.[197] A significant number of *in vitro* and *in vivo* studies have demonstrated ROS activation in cardiovascular diseases such as cardiac hypertrophy[198] and in the failing heart.[199, 200] Genetically hypertensive rats show increased ROS production in venules and arterioles, in comparison to normotensive animals.[201] Moreover, plasma markers of free radical-induced lipid

peroxidation are positively correlated with the degree of HF severity.[202, 203] Interestingly, antioxidant therapy has been shown to attenuate the progression of cardiac failure in animal models,[204] and several experimental studies indicate that antioxidants can attenuate cardiac hypertrophy, fibrosis, matrix remodeling, and apoptosis in rodents with myocardial infarction.[204, 205] Clinical observations in patients with heart failure demonstrate elevated plasma levels of $O_2^{\bullet-}$ with concomitant decreases in ROS-scavenging enzymes, such as SOD, catalase, and glutathione peroxidase.[206, 207] Increased oxidative stress has been demonstrated in several experimental models of chronic heart failure including myocardial infarction-induced heart failure, tachycardia-induced cardiomyopathy, and volume overload cardiac dysfunction.[208] Furthermore, a correlation between ROS production and angiogenesis has been documented *in vivo,*[209] in injured arteries,[210] and in the ischemic myocardium.[211]

ROS can contribute to cardiac remodeling processes via activating MMPs and can also act as signaling molecules in the development of compensatory hypertrophy,[212-215] and play important roles in cell signaling[198] and inflammation through NF-κB.[216] For example, a primary mechanism by which angiotensin II influences blood pressure is via activation of the ROS signaling pathways.[217, 218] Experimental evidence suggest that ROS contribute to cardiomyocyte loss via apoptosis or other cell death mechanisms.[219, 220] Their damaging effect is conducted through lipid peroxidation,[221] protein modification,[222] DNA mutagenesis,[223] cardiomyocyte apoptosis,[215] and impairment of non-enzymatic

antioxidant cellular defenses. Addition of a free radical electron to a fatty acid residue of phospholipids causes fragmentation of the lipid or alteration of its chemical structure, a process referred to as lipid peroxidation. In addition to affecting the structure of the cellular membranes, lipid peroxidation products such as malondialdehyde, can act as mutagenic and carcinogenic agents.[224] DNA bases can also be modified by oxidation, resulting in single- and double-strand breaks or mispairing of purine and pyrimidine during DNA replication. Finally, free radicals can damage proteins and cause cross-linking, carbonyl formation, and protein denaturation.[225]

1.5.4 NADPH oxidase: A major source of ROS

NADPH oxidase (nicotinamide adenosine dinucleotide phosphate oxidase) was first identified in neutrophils, where it is involved in non-specific host defense against microbes during phagocytosis.[184] The enzyme catalyzes electron transfer from NADPH (reduced nicotinamide adenine dinucleotide phosphate) to molecular oxygen, to produce superoxide. NADPH oxidase is considered as a major source of ROS in the heart and is especially important in modulating of the signal transduction pathways.[184, 226] Studies from several laboratories have addressed the potential involvement of NADPH oxidase in the pathophysiology of left ventricular cardiac hypertrophy[227-229] and heart failure.[230-232] Increased NADPH oxidase activation has also been shown in perivascular fibrosis.[233]

NADPH oxidase is an enzyme complex comprised of six subunits: $p91^{phox}$, $p22^{phox}$, $p47^{phox}$, $p40^{phox}$, $p67^{phox}$ and the small guanosine triphosphatase Rac as a

regulatory subunit (Figure 1.3).[234] Activation of this oxidase requires the assembly of at least four cytosolic proteins ($p67^{phox}$, $p47^{phox}$, $p40^{phox}$, and the small guanosine triphosphatase Rac) with the $p22^{phox}$ and $p91^{phox}$ to form an active enzyme complex.[235] The $Gp91^{phox}$ subunit was discovered to be a member of a family of five homologues: NoXl, NOX2, NOX3, NOX4, and NOX5. The NOX family can be classified into three groups based on predicted domain structures: (i) NOX1-NOX4 have up to 60% homology and are predicted to contain six transmembrane α-helices and an NADPH-binding domain towards the C-terminus; (ii) NOX5 has the same basic structure as NOX1-NOX4 but with an additional N-terminal calmodulin-like Ca^{2+}-binding domain; (iii) DUOX1 (Dual oxidase 1) and DUOX2 (Dual oxidase 2) are similar to NOX5 but include an additional N-terminal peroxidase homology domain. Expression of the NOX isoform varies in a cell-specific manner. NOX1 is expressed in epithelia (e.g., colon) as well as in vascular smooth muscle cells. NOX2 is expressed in endothelial cells, cardiomyocytes, and fibroblasts, in addition to its classical expression in phagocytes. NOX3 is primarily expressed in fetal tissues and in adult inner ear. NOX4 was first identified in kidney but is in fact widely expressed in many tissues, including placenta, endothelial cells, vascular smooth muscle cells, cardiomyocytes, fibroblasts, ovaries, testis, and skeletal muscle. NOX5 is expressed in fetal tissues and adult testis, spleen, ovaries, placenta, and pancreas. Several cell types can co-express more than one NOX subunit. For example, cultured vascular smooth muscle cells express both NOX1 and NOX4, while endothelial cells and cardiomyocytes co-express NOX2 and NOX4.[236]

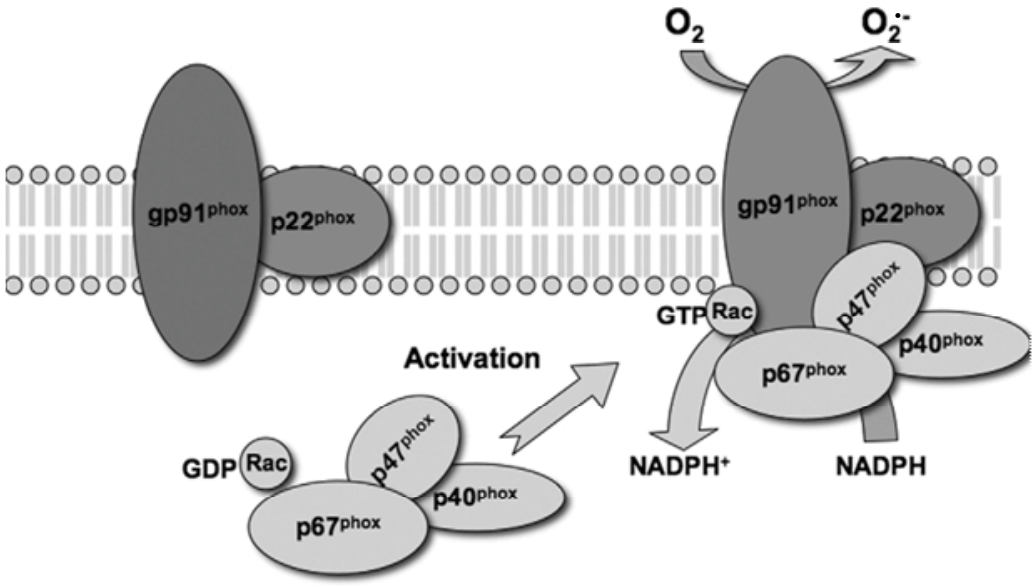

Figure 1.3: Structure and activation of NADPH oxidase.

A number of stimuli can activate NADPH oxidase during cardiac remodeling, including: (1) G-protein-coupled receptor agonists, e.g., angiotensin II and ß-adrenergic receptor agonists;[237] (2) growth factors, e.g., vascular endothelial growth factor;[238] (3) cytokines, e.g., tumor necrosis factor alpha;[239] and (4) mechanical stress.[240,241] The activation of the enzyme; however, requires the recruitment of cytoplasmic subunits $p47^{phox}$, $p67^{phox}$, and Rac to the membrane after having gone through posttranscriptional modifications (for $p47^{phox}$) and conformational changes (for Rac) (Figure 1.3). Once activated, the NADPH oxidase will produce superoxide according to the following equation:

$$NADPH + 2O_2 \rightarrow NADP+ + 2O_2^{\bullet}- + H^+$$

NADPH oxidase in non-phagocytic cells is made up of six subunits, and recruitment of the cytosolic subunits to the membrane subunits is required for enzyme activation. Activation of the oxidase involves the stimulus-induced

translocation of the cytosolic subunits p47 ^{phox}, p67 ^{phox}, and p40^{phox} and GTP-bound Rac to cytochrome b_{558}, which is composed of gp91^{phox} and p22^{phox}. The assembled oxidase can then use NADPH as a substrate for the reduction of molecular oxygen to $O_2^{\cdot -}$ (Figure 1.3).[242]

1.6 Thesis Hypothesis and Objectives

1.6.1 Hypothesis:

TNF triggers the expression and activation of MMPs through NADPH-dependent superoxide production.

1.6.2 Objectives:

1. Does TNF play a key role in pressure-overload cardiomyopathy? Does TNF have an impact on MMPs expression and activation in pressure-overload mediated cardiac remodeling?
2. Can TNF directly induce the expression and activation of MMPs?
3. Which cardiac cell type is responsible for induction and activation of MMPs in response to TNF?
4. Does TNF-mediated MMP induction and activation in cardiomyocytes and cardiofibroblasts occur through NADPH-dependent superoxide production?

Chapter 2. Materials and Methods

2.1 Aortic Banding in Mice: Transverse Aortic Constriction (TAC)

Wild-type (WT) and $TNF^{-/-}$ mice were purchased from Jackson laboratories. All experiments were conducted in accordance with the guidelines of the University of Alberta Animal Care Committee and the Canadian Council of Animal Care.

Eight- to ten-week old male C57BL/6 WT and $TNF^{-/-}$ mice (20-25 g) were used in these experiments. Mice were anesthetized with 1.5 mg ketamine/xylazine (100 mg/kg, and 10 mg/kg, respectively) by one intraperitoneal (i.p.) injection. A topical depilatory agent was applied to the neck and chest area to remove fur at and around the area of incision. The skin was cleaned with Germex (antibacterial), and Betadine (topical antiseptic). One dose of penicillin (10 mg/Kg, 0.1 mL, i.p.) was administered prior to the start of surgery. Mice were placed in supine position and body temperature was maintained at $37^{o}C$ with a heating pad. Once the animal was in surgical plane of anesthesia (lack of reflex or response to toe-pinching), a horizontal incision of 1 cm in length was made at the level of second intercostal space. A 6-0 silk suture was passed under the aortic arch. A bent 26-gauge needle was then placed next to the aortic arch and the suture was snugly tied around the needle and aorta between the left common carotid artery and brachiocephalic trunk. The needle was quickly removed

allowing the suture to constrict the aorta. The incision was closed in layers and the mice were allowed to recover on a warming pad until fully awake. Immediately after the surgery, mice received one dose of buprenorphine (0.02 mg/Kg, 0.1 mL i.p.) and a dose of penicillin (10 mg/Kg, 0.1 mL, i.p.). Buprenorphine was administered every 8 hours for the first 24 hours after surgery. The sham-operated animals underwent the same procedure without the aortic constriction. Aortic constriction was confirmed in all TAC mice by measuring the pressure gradient in the aortic arc across the constriction using Doppler imaging (echocardiography) and a supersternal notch view. The TAC procedure generated a pressure gradient of 50-60 mmHg. Animals were sacrificed at 2-weeks and at 10-weeks, post-surgery. The chest cavity was opened and the heart was cut. Hearts were excised and washed in PBS (+4°C). Sham-operated mice were used as controls. The atria and the right ventricle were separated and discarded. The left ventricle was weighed, flash-frozen in liquid nitrogen, and kept at -80 ^{o}C until used for experiments.

2.2 Echocardiography

Transthoracic echocardiography was performed in WT and TNF-/- mice at 10-weeks post-surgery using a Vevo®770 high resolution imaging system (VisualSonics) under isoflurane (1%) anesthesia. Heart rates are generally maintained at more than 400 beats per minute with these regimens. Excess hair was removed with chemical treatment (Nair, Church & Dwight Co, Inc) to minimize signal attenuation. Cardiac ventricular dimensions, including left

ventricular end-diastolic dimension (LVEDD) and left ventricular endsystolic dimension (LVESD), and LV wall thickness were measured by M-mode recordings. The measurements for each mouse were performed from three different images. Fractional shortening (FS) was calculated as 100 x (LVEDD-LVESD)/LVEDD. Echocardiographic imaging was performed by Donna Beker in the Cardiovascular Core Facility at the University of Alberta.

2.3 Primary Culture of Neonatal Mouse Cardiomyocytes and Cardiofibroblasts

Neonatal (1-2 day old) WT and $TNF^{-/-}$ mice were obtained from corresponding breeding pairs maintained in our animal facility at the University of Alberta. Calcium and bicarbonate-free Hanks with HEPES (CBFHH) solution was prepared (as described in Tables 2.1 and 2.2) and the pH was adjusted to 7.5 with NaOH, before being filter-sterilized in a culture hood using a 0.22 µm filter (Millipore, Billerica, MA). Fifty mL of CBFHH solution was set aside to collect and wash the hearts. The digestion solution was prepared by adding trypsin (200 g) (Gibco, Burlington, ON) and 200 µL gentamicin (50 µg/mL) (Santa Cruz Biotechnology, Inc., Santa Cruz, CA) to 200 mL CBFHH. The cell isolation protocol was performed at room temperature.

Table 2.1: 100X stock for making calcium and bicarbonate-free Hanks with HEPES (CBFHH).

Compound	g/50 mL
NaCl (Fisher)	10.0
KCl (Fisher)	2.0
$MgSO_4.7H_2O$ (EMD)	1.0
D-glucose (EMD)	5.0
KH_2PO_4 (EMD)	0.3
$NaH_2PO_4.H_2O$ (Anachemia)	0.23
HEPES (Fisher)	2.38

Table 2.2: 1X Calcium and bicarbonate-free Hanks with HEPES (CBFHH) from 100X stock; total volume = 250 mL.

Compound	mL of 100X stock	Final concentration (mM)
NaCl (Fisher)	10.0	137.0
KCl (Fisher)	2.5	5.36
$MgSO_4.7H_2O$ (EMD)	2.5	0.81
D-glucose (EMD)	2.5	5.55
KH_2PO_4 (EMD)	2.5	0.44
$NaH_2PO_4.H_2O$ (Anachemia)	2.5	0.34
HEPES (Fisher)	25.0	20.06
ddH_2O	202.5	--

Wild-type neonatal mice (1-2 day old) were sacrificed by cervical dislocation, the chest was opened using a pair of small straight scissors, and the heart was excised and transferred to a falcon tube containing 20 mL CBFHH. After all the hearts were collected, the lungs, vessels, and atria were removed. The ventricles were transferred to a clean petri dish containing CBFHH and cut into very small pieces, before being transferred to a sterile 50 mL falcon tube. Using a sterile pipette and an automatic pipetter, 10 mL of the digestion solution

(CBFHH+trypsin+gentamycin) was added to the hearts, and a small stirring bar (0.3 cm long) was placed in a Falcon tube which was then placed in a beaker and on a magnetic stirrer. The hearts were slowly stirred for 10 minutes. The solution from the first digestion was discarded. Another 10 mL of fresh digestion solution was added to the hearts and stirred for 10 minutes. The serial digestion of the hearts was continued with three repetitions of 10 -minute stirrings in 10 mL fresh buffer, followed by 5-minute stirrings in 5 mL fresh buffer until the hearts were completely digested. The digested cells were collected in four 50 mL Falcon tubes containing 7.5 mL fetal bovine serum (FBS)/tube to inhibit trypsin and any further digestion of the isolated cells. The collected aliquots containing the isolated cells were centrifuged at 200 ×*g* for 5 minutes. The supernatant was discarded and the pellet was gently resuspended in 10 mL culture medium (DMEM/F12 + 15% FBS + 1% Penicillin/Streptomycin). The resuspended cells were pooled together and centrifuged at 200 ×*g* for 5 minutes. The supernatant was discarded and the pellet was suspended in 10-15 mL of culture medium. Cardiofibroblasts were separated from cardiomyocytes by differential adhesion. The collected cells were plated in two 100-mm culture plates (polysterene-coated, Falcon), and incubated at 37^{o}C in 5% CO_2 + 95% O_2 for 35 minutes to allow for adhesion of the cardiofibroblasts. The culture plates were brought to the tissue culture hood and myocytes were displaced by physical agitation of the plates. The media containing the cardiomyocytes were collected in a 50 mL falcon tube, and fresh media was added to the fibroblasts that remained attached to the plate. The culture plates containing the fibroblasts were then placed in an incubator (37^{o}C in 5% CO_2 +

95% O_2) and allowed to proliferate. The media containing the cardiomyocytes were filtered through a cell strainer (70 μm pore size, BD Falcon) to remove cell clumps. Cardiomyocytes were counted by diluting 0.2 mL of the cell solution in 0.3 mL of CBFHH, and 500 μL trypan blue (0.4%) (Gibco, Burlington, ON). Trypan blue stains the dead cells blue while the viable cells remain colorless. A hemocytometer (Figure 2.1) was used to count the viable cardiomyocytes. The number of cells/mL was calculated as follows: Average cell count per area x 5 (dilution factor) x 10,000. Bromodeoxyuridine (BrdU, 0.1 mM) was added to the culture media, and the cardiomyocytes were plated in 24-well Primeria culture plates (Falcon) at a plating density of 700,000 cells/well. Cardiomyocytes were incubated at 37 ^{o}C, 5% CO_2 and 95% O_2 for 24 hours. After 24 hours, cardiomyocytes were inspected under a light microscope, then washed with serum-free media, and the culture media was replaced with serum-free DMEM/F12 + ITS supplement (insulin, transferrin, selenium) (Cellgro, Manassas, VA). After 24 hours of serum-starvation, cardiomyocytes were treated as follows: i) Control (PBS), ii) rTNF (20ng/ml) (Peprotech Inc., Mississauga, ON) or iii) rTNF (20ng/ml) + apocynin (1mM) (Sigma-Aldrich Canada Ltd., Oakville, Ontario). The treated cells were incubated at 37^{o}C, and 5% CO_2 + 95% O_2 for 1 hour or 24 hours. Cardiomyocytes were harvested for protein or RNA analyses as described in Sections 2.6.2 and 2.13, and kept in a -80 °C freezer until used in experiments.

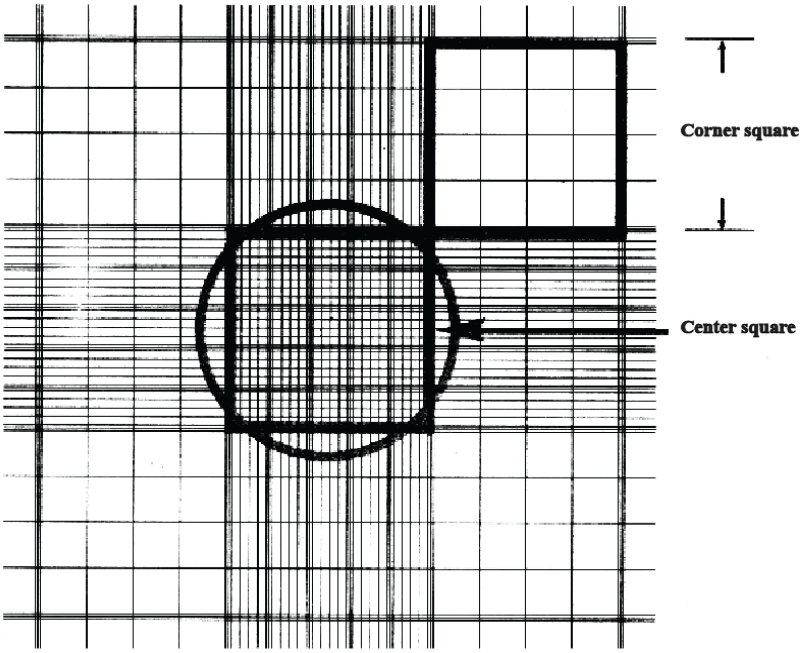

Figure 2.1: The hemocytometer was used to count cardiomyocytes and cardiofibroblasts. It consists of a thick glass microscope slide with a rectangular indentation that creates a chamber. The area of the hemocytometer consists of 9, large, 1 x 1 mm (1 mm^2) squares. The depth of the counting chamber is 0.1 mm. The center square is divided into 25 smaller squares (0.2 mm x 0.2 mm = 0.04 mm^2).

Cardiofibroblasts were allowed to proliferate in serum-containing culture medium (DMEM-F12 + 15% FBS + penicillin/streptomysin). When the fibroblasts reached 90% confluency, cells were split and re-seeded in 24-well Primeria plates (BD Biosciences, Mississauga, ON) as follows: culture medium was removed and cells were washed with warm, sterile PBS solution, and then trypsinized with 0.05% trypsin (Gibco, Burlington, ON) for 10-12 minutes. Fibroblasts were collected and transferred to a 50 mL falcon tube, containing 15% FBS (to stop the action of trypsin). The fibroblast solution was centrifuged at 200 ×*g*, at 4 °C for 5 minutes. The pellet was resuspended in medium (DMEM-F12 + 1% ITS + 1% BrdU). Cells were counted and re-plated in 24-well Primeria plates

(surface area = 2 cm^2/well) at a density of 700,000 cells/well, and then incubated at 37 ^oC, 5% CO_2 and 95% O_2 for 24 hours. Cultured cardiofibroblasts were treated for 1 hour or 24 hours as follows: control (PBS), rTNF (20 ng/ml) or rTNF (20 ng/ml) + apocynin (1 mM). Cells were harvested for RNA and protein analyses, and stored in a -80 °C freezer until used in experiments (Sections 2.6.2 and 2.13). Conditioned medium was also collected and stored at -80°C.

The hemocytometer (Figure 2.1) was used to count cardiomyocytes and cardiofibroblasts. The cell density was calculated based on the following formula: average cell count per area x 5 (dilution factor) x 10,000 (volume of the counting chamber) = cells/mL.

2.4 Immunofluorescent Staining

Culture plates containing cardiomyocytes or cardiofibroblasts were washed with PBS, and the cells were fixed with 4% paraformaldehyde, permeabilized with 1% Triton X-100 for 20 minutes, and blocked with blocking solution (1% bovine serum albumin in PBS) for 1 hour at room temperature. Primary antibodies (α-sarcomeric actin [1:800 dilution; Sigma-Aldrich Canada Ltd., Oakville, Ontario] as a marker for cardiomyocytes, and vimentin [1:800 dilution, Thermo Scientific, Waltham, MA] as a marker for cardiofibroblasts) were diluted in PBS (room temperature), added to the cells, and incubated at 4 ^oC overnight. The next day, cells were washed three times with PBS, and incubated in Alexa fluor-conjugated secondary antibodies (FITC-conjugated secondary

antibody for cardiomyocytes and CY3-conjugated antibody for cardiofibroblasts, 1:500 dilution, Molecular Probes, Burlington, ON), with DAPI nuclear staining (1:800 dilution, Molecular Probes, Burlington, ON). Cells were then washed three times with PBS (room temperature), and visualized under an Olympus IX81 fluorescent microscope (Carson Scientific Imaging Group, Ontario, Canada) using Slidebook 2D, 3D Timelapse Imaging Software (Intelligent Imaging Innovations Inc., Santa Monica, CA).

2.5 LDH (lactate dehydrogenase) assay

LDH levels were measured using a CytoTox 96® Non-Radioactive Cytotoxicity Assay kit (Promega, Nepean, ON). LDH is a stable cytosolic enzyme released upon cell lysis into the cell culture medium. The amount of LDH released is measured using a 30 min coupled enzymatic assay based on the conversion of a tetrazolium salt INT (2-*p*-iodophenyl-3-*p*-nitrophenyl-5-phenyltetrazolium chloride), forming a red formazin product, with the amount of colour formed being proportional to the number of lysed cells. A 50 µl portion of the cell culture medium from each sample was transferred to a 96-well plate (Helena Biosciences, Sunderland, UK). A 50 µl portion of Substrate Mix (1 vial of substrate plus 12 ml of assay buffer; Promega, Nepean, ON) was added to each well and the plate was covered in a foil to prevent exposure to light. Samples were then incubated at room temperature for 30 minutes after which the reaction was stopped by the addition of 50 µl of stop solution (1 M acetic acid). Absorbance

was measured in arbitrary units at 450 nm using a spectrophotometer (Molecular Devices, Sunnyvale, CA).

2.6 Protein Extraction

2.6.1 Mouse hearts

i) Protein extraction in RIPA buffer: RIPA buffer (100 μl) (Tables 2.3 and 2.4) was added to the LV tissue (~100 mg) in an Eppendorff tube. Using a mini mortar and pestle (VWR, Mississauga, ON), heart tissue was homogenized so that no lumps of tissue were present. The tissue homogenate was then placed on ice for 15 minutes, and then vortexed for 5-10 seconds. This was repeated 4 times, and the tissue homogenate was then centrifuged at 12,000 ×*g* at 4 °C for 10 minutes. Pellets were discarded and the protein-containing supernatant was stored at -80°C.

Table 2.3: RIPA buffer without EDTA for gelatin zymography and MMP activity assays.

Compound	Concentration
Tris (pH 7.4) (Calbiochem)	50.0 mM
NaCl (Fisher)	150.0 mM
Sodium dodecyl sulfate (SDS) (BioRad)	0.1%
Nonidet-P40 (NP40) (Sigma)	1.0%
Deoxycholate-N4 (Sigma)	1.0%

Table 2.4: RIPA extraction buffer.

Reagent	Volume
RIPA buffer (Table 2.3)	980.0 µl
Phosphatase inhibitor (Calbiochem) (Catalogue No. 539134)	10.00 µl
Protease inhibitor (Calbiochem) (Catalogue No. 539134)	10.0 µl

ii) Protein extraction in PBS: A piece (~ 100 mg) of frozen heart tissue was cut on dry ice to minimize the tissue freeze-thawing effect. PBS buffer (100 µl) (Tables 2.5 and 2.6) was added to each sample. Heart tissues were gently homogenized using a mini mortar and pestle (VWR, Mississauga, ON), and the tissue homogenate was placed on ice for 15 minutes. Homogenization and chilling was repeated three times. Tubes containing tissue homogenate were centrifuged at 4 °C and 1,000 ×*g* for 10 minutes. The supernatant was transferred to Eppendorff tubes and stored at -80°C.

Table 2.5: PBS extraction buffer.

Reagent	Volume
PBS buffer (Table 2.5)	980.0 µl
Phosphatase inhibitor (Calbiochem) (Catalogue No. 539134)	10.0 µl
Protease inhibitor (Calbiochem) (Catalogue No. 539134)	10.0 µl

Table 2.6: Phosphate-buffered solution (PBS) (1x).

Compound	Weight (g)
NaCl (Fisher)	8.0
KCl (Fisher)	0.2
Na_2HPO_4 (EMD)	1.44
KH_2PO_4 (EMD)	0.24

The pH of the solution was adjusted to 7.4 using HCl, and measured using a pH meter.

iii) Protein extraction in cytobuster buffer: Cytobuster buffer (100 µl) (Table 2.7) was added to heart tissue (100 mg). Using a pestle, the heart tissue was homogenized for one minute, and then placed on ice for 15 minutes. This was repeated 4 times. The tissue homogenate was then centrifuged at 4 °C and 12,000 ×g for 10 minutes. The supernatant was kept at -80°C and the pellets were discarded.

Table 2.7: Cytobuster extraction buffer.

Reagent	Volume
Cytobuster buffer (Novagen) (Catalogue No. 71009-4)	980.0 µl
Phosphatase inhibitor cocktail (Calbiochem) (Catalogue No. 539134)	10.0 µl
Protease inhibitor cocktail (Calbiochem) (Catalogue No. 539134)	10.0 µl

2.6.2 Cultured cardiomyocytes and cardiofibroblasts

i) Extraction in RIPA buffer: Cultured cells were scraped with RIPA buffer (100 µl) (Tables 2.3 and 2.4). Cells were subjected to three, freeze/thaw

cycles to rupture the cell membrane and release the protein contents of the cells. Cell homogenates were centrifuged at 12,000 ×*g* at 4 °C for 10 minutes. Pellets were discarded and the supernatant was stored at -80°C until used for experiments.

ii) Extraction in PBS: Cultured cells were harvested using PBS buffer (Tables 2.5 and 2.6). Cells were kept on ice and vortexed every 15 minutes, and then centrifuged at 1,000 ×*g* and 4 °C for 10 minutes. Supernatant was transferred to a sterile Eppendorff tube, and stored at -80°C.

iii) Extraction in Cytobuster buffer: Cardiomyocytes and cardiofibroblasts were lysed in Cytobuster buffer (Table 2.7), subjected to 3 cycles of freeze/thaw, and centrifuged at 12,000 ×*g* and 4 °C for 10 minutes. The supernatant was transferred to a new Eppendorff tube and stored at -80°C.

2.7 Protein Quantification

Protein concentration was determined using the BioRad colorimetric assay according to the manufacturer's instructions (BioRad, Hercules, CA) (Table 2.8). This assay is based on the reaction of the protein with an alkaline copper tartrate solution and a Folin reagent. Two steps are followed to create the color development: 1) the reaction between protein and copper in an alkaline medium, and 2) the subsequent reduction of the Folin reagent by the copper-treated protein. Color development is primarily due to the amino acids tyrosine and tryptophan, and to a lesser extent, cystine and histidine. Proteins reduce the Folin reagent by

the loss of one, two, or three oxygen atoms, thereby producing one or more of several possible reduced species which have a characteristic blue color with maximum absorbance at 750 nm and minimum absorbance at 405 nm.

Table 2.8: Reagent package in the BioRad DC protein assay kit.

Reagent	Volume
Reagent A (an alkaline copper tartrate solution)	250.0 mL
Reagent B (a dilute Folin Reagent)	2000.0 mL
Reagent S	5.0 mL

Reagent A' was prepared by adding 20 μl of reagent S to each mL of reagent A. Reagent A, reagent A', reagent B, and reagent C were stored away from direct sunlight at RT (25 °C). Reagent A' was prepared fresh each time.

Protein standards (BSA) and experimental samples (5 μl) were pipetted into a 96-well plate (Eppendorff). Reagent A' (reagent A + reagent S, 25 μl) was added to each well, followed by Reagent B (200 μl). The plate was gently agitated on a rocker for 15 minutes at room temperature. Absorbance was recorded at 750 nm using a microplate reader (Molecular Devices, Sunnyvale, CA). Protein concentrations of the experimental samples were calculated based on the recorded absorbance for the standards.

The protein standards were composed of a series of concentrations: 2.0, 1.5, 1.0, 0.8, 0.6, 0.4, 0.2, 0.1, and 0 (blank) (BSA, mg/mL).

2.8 Lucigenin Chemiluminescence

The lucigenin chemiluminescence assay was used to measure NADPH oxidase activity.[243] Heart tissue and cardiac cell proteins were extracted using PBS and quantified (as described in Sections 2.6 and 2.7). Nicotinamide adenine dinucleotide phosphate (NADPH) (EMD Chemicals, Gibbstown, NJ) was dissolved in PBS (1 mM), added to 100 μg protein extracted in PBS, and incubated at 37 °C for 10 minutes. Diphenyleneiodonium sulfate (DPI), an NADPH oxidase inhibitor, was dissolved in dimethyl sulfoxide (DMSO) (100 μM) (Sigma-Aldrich Canada Ltd., Oakville, Ontario), and added to selected samples to ensure that the recorded luminescent signals were NADPH-driven. Lucigenin (Sigma-Aldrich Canada Ltd., Oakville, Ontario) (50 μM) (dissolved in DMSO ≥ 99.9%) was added to the samples. Chemiluminescent signals were recorded using a FB-12 luminometer at 37 °C. Readings between 4-6 minutes after the start of the reaction were averaged, and after subtracting background signals, recorded in a tube contained PBS, NADPH (100 μM), and lucigenin. Data was expressed as relative light unit/second.

2.9 Dihydroethidium Fluorescence Staining

Superoxide levels were measured in cultured cardiomyocytes and cardiofibroblasts using the oxidant sensitive dye, dihydroethidium (DHE). Ethidium bromide, an oxidant sensitive fluorophore, derived from the oxidation of DHE was used to measure superoxide production.[244] Cultured cardiomyocytes

and cardiofibroblasts were washed once with 0.5 mL of DMEM/F12 culture medium. Cells were incubated in 20 μM DHE (dissolved in DMSO ≥ 99.9%) at room temperature. Cells incubated in PBS were used to record the background signals. Since DHE is light-sensitive, the plates were covered with aluminum foil to minimize exposure to light. After 30 minutes of incubation, cells were washed with a phenol-free clear DMEM-F12 medium (Gibco, Burlington, ON) for three times. Fluorescence signals were recorded from three different fields per well with fluorescence detection equipment that included a fluorescence microscope equipped with a camera, coupled with imaging software for data acquisition and analysis. Background signals recorded from the cells treated with PBS were subtracted from the readings. Fluorescence intensity/cell was calculated as follows:

$$\text{Fluorescence intensity/cell} = \frac{\text{Fluorescence intensity/field}}{\text{number of cells}}$$

2.10 Anti-Nitrotryosine Immunofluorescence Staining

Peroxynitrite is a product of nitric oxide and superoxide, and leads to the nitration of tyrosine residues in proteins.[245] The extent of nitrotyrosine formation is used as a measure of reactive nitrogen species. Cultured cells were washed with warm PBS, and fixed with 250 μl of 4% formaldehyde for 20 minutes at room temperature. Cells were then washed with PBS, and permeabilized with 250 μl of permeabilizing buffer (0.1% Triton-X 100 in PBS) for 5 minutes at room

temperature. Cells were then washed with PBS, and blocked with 250 μl of blocking buffer (1% BSA in PBS) for 40 minutes at room temperature. Blocking buffer was removed and cells were washed once with PBS. Anti-nitrotyrosine primary antibody solution (250 μl) (in 0.1% BSA in PBS) was added to each well (Millipore, Billerica, MA) (1:600 dilution). Culture plates were sealed with Parafilm (Pechiney, Chicago, IL) to prevent evaporation of the antibody and incubated overnight at 4 °C. The next day, primary antibody was pipetted out and cells were washed three times with warm PBS. The secondary antibody solution (250 μl of Alexa Fluor 488 donkey anti-rabbit, 1:600 dilution in 0.1% BSA in PBS) was added to each well for 60 minutes at room temperature. The culture plates were covered with aluminum foil to protect them from exposure to light. After one hour, the secondary antibody was removed and cells were washed three times with warm PBS.

Cell nuclei were counter-stained with 250 μl of nuclear stain solution [DAPI (4',6-diamidino-2-phenylindole) (Molecular Probes, at 1:20,000 dilution in 0.1% BSA in PBS] for 5 minutes at room temperature, then washed 3 times with warm PBS. Finally, cells were covered with warm PBS, and visualized under an Olympus IX81 fluorescent microscope (Carson Scientific Imaging Group, Ontario, Canada) using Slidebook 2D, 3D Timelapse Imaging Software (Intelligent Imaging Innovations Inc., Santa Monica, CA)

2.11 Griess Reaction

The Griess reaction was used to measure nitrite levels (a stable product of peroxynitrite).[246] Peroxynitrite is a highly unstable RNS, which decomposes to nitrite (NO_2^-) and nitrate (NO_3^-).[247] In the Griess reaction, nitrate is converted to nitrite by nitrate reductase. Spectrophotometric quantification of nitrite was performed according to the manufacturer's instructions with triplicates of each sample (Sigma-Aldrich, Oakville, ON). Sodium nitrite was provided in the kit as the standard. Conditioned media was added to an equal volume of Griess reagent in triplicates, in a 96-well plate and incubated at room temperature for 15 minutes. Absorbance at 540 nm was measured and nitrite concentrations were calculated based on the standard curve. Data was represented as mean micromoles of nitrite.

2.12 Gelatin Zymography

Gelatin zymography was used to demonstrate the activity of gelatin-degrading proteinases, MMP-2 and MMP-9.[248] Spacers and glass plates were made perfectly aligned to avoid leakage. The electrophoresis unit was assembled (BioRaD, Hercules, CA). The separating gel was prepared by mixing ingredients (Table 2.9), which was loaded into the chamber between glass plates, and topped with ddH_2O to make the edge of the gel smooth and even. Gels were allowed to polymerize (~30 minutes). Meanwhile, the stacking gel was prepared by mixing ingredients (Table 2.10). The H_2O on top of the gel was poured out, and the stacking gel was loaded on top of the separating gel and a 10-well comb was placed into the chamber between glass plates. The stacking gel was allowed to

polymerize (~20 minutes). Running buffer (Table 2.11) was poured into the BioRad tank and between the gels to submerge the wells. The comb was removed and wells were cleaned with running buffer. Samples were mixed with loading buffer (Table 2.12) and loaded into the wells. Electrodes were properly connected and the gels were run at a fixed current (30 mA/gel) for an hour.

Table 2.9: Separating gel solution (8% gel).

Compound	**Volume (mL)**
Gelatin type-A (from porcine skin) dissolved in ddH_2O (Final conc.=2 mg/mL) (Sigma)	6.9
1.5 M Tris-HCl (pH 8.8) (Calbiochem)	3.8
10% SDS (BioRad)	0.15
30% acrylamide (BioRad)	6.9
10% ammonium persulfate (BioRad)	0.15
TEMED (100%) (J.T. Baker)	0.06

Gelatin stock was prepared by dissolving 163.9 mg gelatin in 40 mL dd H_2O at 55°C for an hour, and vortexed every 10 minutes until gelatin was completely dissolved.

Table 2.10: Stacking gel solution (5% acrylamide).

Compound	**Volume (mL)**
dd H_2O	2.7
1 M Tris-HCl (pH 8.8) (Calbiochem)	0.5
10% SDS (BioRad)	0.04
30% acrylamide (BioRad)	0.67
10% (w/v) ammonium persulfate (APS) (BioRad)	0.04
TEMED (100%) (J.T. Baker)	0.004

Table 2.11: SDS running buffer (1x).

Compound	Concentration
Tris (pH 8.3) (Calbiochem)	25.0 mM
Glycine (EMD)	192.0 mM
SDS (BioRad)	1%

Table 2.12: Protein loading buffer (4X).

Compound	
30% glycerol (Sigma)	3.0 mL
8% SDS (BioRad)	0.8 g
250 mM Tris-HCl (pH 6.7) (Calbiochem)	5.0 mL of 500.0 mM Tris-HCl stock
0.02% bromophenol blue (EMD)	2.0 mL of 0.1% stock
1 μM DTT (Thermo Scientific)	40.0 μL of 1 mL stock

After electrophoresis, the gel apparatus was disassembled. The gel was washed for 1 hour with 2.5% Triton X-100 solution at room temperature (3 times for 20 minutes, each) to remove sodium dodecyl sulfate (SDS). The washing solution (2.5% Triton-X 100) was prepared by adding 12.5 mL Triton-X 100 into 487.5 mL ddH_2O, and stirred for 20 minutes. Gels were rinsed with incubation buffer (Table 2.13) and incubated in fresh incubation buffer at 37 °C for 48 hours. At the end of the incubation period, gels were stained with staining buffer (Table 2.14), and rocked gently overnight at room temperature. Gels were destained with a destaining buffer (Table 2.15) until the MMP-2 and MMP-9 bands appeared as clear bands against a dark blue background. Zymograms were scanned using a

calibrated densitometer GS 800 (BioRad) and the band intensities were analyzed by densitometry using the ImageJ software program (NIH, USA).

Table 2.13: Substrate/Incubation buffer.

Compound	
50 mM Tris-Cl (Calbiochem)	15.0 mL of 2M stock
5 mM $CaCl_2$ (Fisher)	1.5 mL of 2M stock
150 mM NaCl (Fisher)	5.25 g
0.05% NaN_3 (EMD)	6.0 mL of 5.0% stock
dd H_2O	572.25 mL

Incubation buffer was prepared and kept at 4°C.

Table 2.14: Staining solution.

Compound	**Volume**
2% Coomassie blue (EMD)	4.0 mL
25% methanol (Fisher)	50.0 mL
10% acetic acid (VWR)	20.0 mL
dd H_2O	126.0 mL

Table 2.15: Destaining solution.

Compound	**in 500.0 mL**
2% methanol (Fisher)	10.0 mL
4% acetic acid (VWR)	20.0 mL
dd H_2O	470.0 mL

2.13 RNA Extraction

RNA extraction was performed using the TRIzol reagent (Invitrogen, Burlington, ON) according to the manufacturer's instructions. Cells or heart tissue were homogenized in 1 mL TRIzol and incubated at room temperature for 4

minutes. Filter-tips were used throughout the procedure of RNA extraction to reduce the chance of sample contamination. Chloroform was added (0.2 ml/tube) using 1 mL glass pipettes; the tube was vigorously shaken for 15 seconds and incubated at room temperature for 2 to 3 minutes. Samples were centrifuged at 12,000 $\times g$ for 15 minutes at 4 °C. Following centrifugation, three layers were formed in each tube: 1) an upper colorless layer containing RNA, 2) a middle white layer containing protein, and 3) a lower pink fraction containing DNA. The upper clear fraction was transferred to a new Eppindorff tube. The RNA was precipitated by adding isopropyl alcohol (0.5 mL/tube) and incubated at -20 °C for 2-3 days to maximize the yield of RNA. Samples were then centrifuged at 12,000 $\times g$ for 15 minutes at 4 °C. The supernatant was discarded and the RNA pellet was washed once with 75% ethanol (prepared using RNase-free water), and centrifuged at 7,500 $\times g$ for 5 minutes at 4°C. The supernatant was discarded and the resulting RNA pellet was air-dried for 10 minutes. RNA pellets were re-dissolved in RNase-free water by repeat-pipetting. Finally, RNA was quantified using a Nanodrop-1000 spectrophotometer (ThermoFisher Scientific, Nepean, ON). Measurements were taken at a wavelength of 280 nm. RNA was then stored in -80°C.

2.14 Complementary DNA (cDNA) Preparation

cDNA was prepared from RNA samples (as extracted according to Section 2.13). Filter-tips were used to reduce the chance of sample contamination. RNA (1 µg) was added to PCR H_2O to make a total volume of 9 µl. Random hexamers

(2 µl/sample) (Amersham Pharmacia, Piscataway, NJ) were added to the solution. Samples were incubated at 70 ^{o}C for 10 minutes. cDNA stock solution (9 µL/sample) (Table 2.16) was added to samples, and incubated at 4 ^{o}C for 5 minutes. The incubated samples were briefly centrifuged at 4 ^{o}C at 2,000 *g* for 1 minute, and then placed on ice. Finally, samples were incubated at 40 ^{o}C for 1 hour to obtain the cDNA as the final product. cDNA was stored at -20^{o}C until used.

Table 2.16: cDNA stock solution.

Reagent	**Volume (µl)**
Buffer (5 X) (Invitrogen)	4.0
Dithiothreitol (0.1 M stock) (Invitrogen)	2.0
Deoxynucleotide Triphosphate (dNTP) (25.0 mM stock) (Invitrogen)	1.0
Superscript II (Invitrogen)	1.0
RNase inhibitor (40.0 U/µl stock) (Invitrogen)	1.0

Ingredients were mixed, which was enough for 1 µg RNA (one sample). The cDNA stock solution was kept on ice.

2.15 TaqMan Real-Time Polymerase Chain Reaction (RT-PCR)

Changes in gene expression were measured using quantitative TaqMan RT-PCR. cDNA from each sample was diluted 100X in PCR H_2O (Fisher Scientific, Nepean, ON). The standard curve was prepared using cDNA from mouse brain tissue, as it abundantly expresses all genes (Table 2.17). Diluted cDNA (5 ng for experimental samples and 1 ng for ribosomal RNA, 18S) was added to the reaction mix (Tables 2.18 and 2.19) in a 384-well plate (Applied

Biosystems, Streetsville, ON). Plates were covered with an adhesive cover. Samples were subjected to the following thermal cycling on the ABI Prism 7900 sequence detector: 2 minutes at 50 °C to activate uracil-DNA glycosylase (UNG), 10 minutes at 95 °C (activation), 40 cycles of denaturation at 97 °C for 30 seconds, and annealing and extension at 60 °C for 1 minute. When the 40 cycles of amplification were completed, cycle threshold (CT) values for gene of interest and standards were recorded. A standard curve was generated and RNA levels for each gene was calculated based on the corresponding standard curve.

Table 2.17: Standard (STD) samples used in RT-PCR.

STD curve was prepared using cDNA from mouse brain tissue. Serial dilutions were made as follows:		
STD	**Concentration**	**Ingredients**
STD1	20.0 ng/10.0 µL	12 µl of RT product + 288 µl PCR H_2O
STD2	10.0 ng/10.0 µL	150 µL of STD1 + 150 µL PCR H_2O
STD3	5.0 ng/10.0 µL	150 µL of STD2 + 150 µL PCR H_2O
STD4	2.5 ng/10.0 µL	150 µL of STD3 + 150 µL PCR H_2O
STD5	1.25 ng/10.0 µL	150 µL of STD4 + 150 µL PCR H_2O
STD6	0.607 ng/10.0 µL	150 µL of STD4 + 150 µL PCR H_2O

Table 2.18: TaqMan reaction mix for one sample to detect the genes of interest was made by mixing the following ingredients.

Reagent	**Concentration**	**Volume/sample (µl)**
Mastermix (applied Biosystems)	33% of the final volume of reaction	8.33
Forward Primer	200.0 nM	0.5
Reverse Primer	200.0 nM	0.5
Probe	100.0 nM	0.5
PCR H_2O		5.17

Table 2.19: TaqMan Reaction mix for one sample to detect18S was made by mixing the following ingredients.

Reagent	Concentration	Volume/STD (µl)
Mastermix (Applied Biosystems)	33% of the final volume of reaction	8.33
Forward Primer	100.0 nM	0.125
Reverse Primer	100.0 nM	0.125
Probe	50.0 nM	0.125
PCR H_2O		14.295

2.16 Collagenase Activity Assay

Collagenase activity was measured using EnzChek Collagenase assay (Molecular Probes, Burlington, ON) The reaction buffer (10X), used in the collagenase activity assay (EnzCheck collagenase assay), was made as follows: 0.5 M Tris-HCl (pH 7.6); 1.5 M NaCl; 50 mM $CaCl_2$; and 2 mM sodium azide. The reaction buffer (1X) was prepared by diluting 2 mL of the 10X reaction buffer in 18 mL ddH2O.

DQ fluorescent-tagged collagen type I (Molecular Probes D-12054, Burlington, ON) was dissolved in water (1 mg/mL). In a black 96-well plate, 20 µL of the collagen solution and 80 µL of 1X reaction buffer were added to each well. Protein homogenates from experimental samples (100 µg) were then added to the wells in duplicates. The samples were incubated with the collagen mixture at room temperature, protected from light for two hours. Fluorescence intensity was measured with a microplate reader fluorometer equipped with standard fluorescein filters for excitation at 485 ± 12 nm and emission detection at 530 ±

12 nm. All values were corrected for background fluorescence. An increase in fluorescence is proportional to proteolytic activity of the samples. The collagenase activity was reported as relative change compared to the control group.

2.17 Statistical Analysis

The averaged data are reported as mean ± SEM. Comparisons between two groups were performed using an unpaired Student's t-test. Comparisons among multiple groups or between two groups at multiple timepoints were performed by either one-way or two-way ANOVA, as appropriate, followed by the Newman-Keuls correction for multiple comparisons using the GraphPad Prism software program. P value of ≤ 0.05 was considered significant. Prism software was used for statistical analysis (GraphPad Software, Inc., La Jolla, CA).

Chapter 3. Results

3.1 TNF$^{-/-}$ Mice Exhibit Less Ventricular Hypertrophy, Oxidative Stress and MMP Activation Compared to WT Mice Following Pressure Overload

This study examined how TNF-deficiency affects pressure overload-induced cardiac failure *in vivo*. WT and TNF$^{-/-}$ mice were subjected to transverse aortic constriction (TAC), and cardiac function was assessed by trans-thoracic echocardiography. Animals were sacrificed at 2-weeks and 10-weeks post-surgery. At 10-weeks post-TAC, TNF$^{-/-}$ mice exhibited attenuated cardiac hypertrophy (as shown by the heart weight-to-tibial length ratio, LVW/TL), less LV dilation (as shown by the left ventricular end diastolic diameter, LVEDD), and preserved cardiac function (as shown by the fractional shortening, FS), in comparison to WT mice (Table 3.1 and Figure 3.1).

Table 3.1: Echocardiographic and hemodynamic parameters at 10-weeks post-TAC.

	WT – Sham	**WT-TAC**	**TNF$^{-/-}$ - Sham**	**TNF$^{-/-}$ - TAC**
n	6	8	6	8
HR (bpm)	548.0±7.0	564.0±11.0	561±8.0	551.0±9.0
LVEDD (mm)	3.99±0.07	5.63±0.11*,#	3.97±0.05	4.42±0.13.0*
LVESD (mm)	1.89±0.03	4.54±0.09*,#	1.88±0.04	2.62±0.28*
FS (%)	52.8±1.5	18.9±2.50*,#	53.6±1.2	40.2±3.7*
PAV_c (cm/s)	109.8±1.8	76.2±2.70*	115.4±1.5	91.1±2.8*
E-wave (cm/s)	87.1±2.1	74.4±3.10*,#	87.7±1.3	83.1±2.0
$+dP/dt_{max}$ (mmHg/sec)	11371.0±316.0	5721.0±312.0*,#	10982.0±302.0	8827.0±439.0
$-dP/dt_{max}$ (mmHg/sec)	11037.0±292.0	5478.0±307.0*,#	10781.0±319.0	8618.0±625.0
LVEDP (mmHg)	3.33±0.43	15.1±1.44*,#	2.92±0.35.0	7.62±1.97*

HR=heart rate; LVAWT=LV anterior wall thickness; LVEDD, LVESD=LV end diastolic and systolic dimension, respectively; FS=fractional shortening=(LVEDD-LVESD)/LVEDD x 100%; PAV_C=peak aortic velocity corrected for HR; E-wave=early-filling transmitral diastolic wave; HW/TL=heart weight/tibial length ratio; $+dP/dt_{max}$, $-dP/dt_{max}$=maximum and minimum first derivative of the LV pressure, respectively. LVEDP=LV end diastolic pressure; values are mean±SEM; $^{*}P<0.05$ compared to the corresponding sham group; # $P<0.05$ compared to all other groups. Echocardiography was done by Donna Beker.

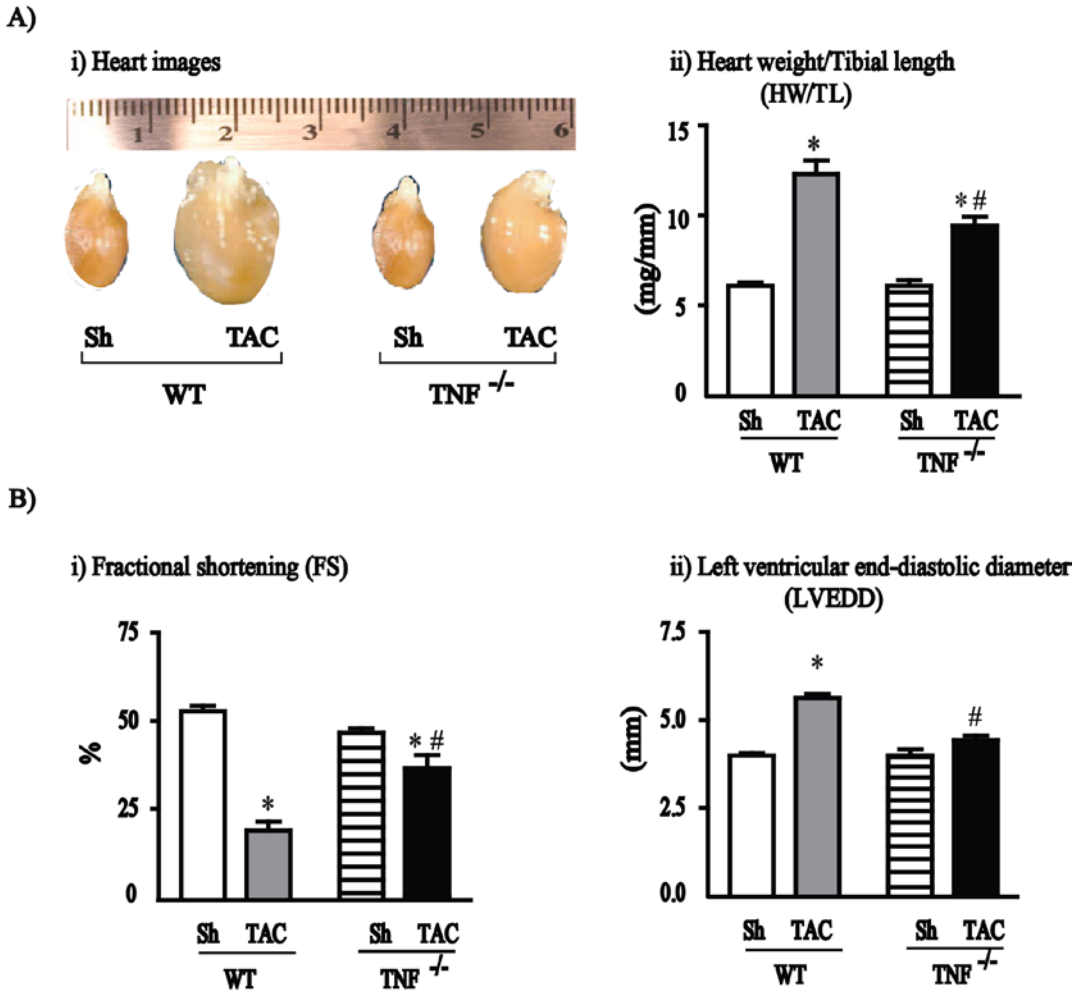

Figure 3.1: Adult TNF$^{-/-}$ mice subjected to cardiac pressure overload (TAC) exhibited attenuated cardiomyopathy compared to parallel WT mice.

(A) Representative heart images (i) and heart weight-to-tibial length ratio (HW/TL) (ii). (B) Echocardiographic parameters, Fractional shortening (FS) (i), and left ventricular end-diastolic diameter (LVEDD) (ii) in WT and TNF-deficient (TNF$^{-/-}$) mice, at 10-weeks following sham (Sh) or transverse aortic constriction (TAC) (n=6/sham and n=8/TAC). Statistical analysis was obtained using two-way ANOVA. *$P < 0.05$ compared to the corresponding sham, #$P < 0.05$ compared to the parallel WT-TAC. The TAC surgery was performed by Sandra Kelly and echocardiographic analysis was done by Donna Beker.

This study investigated whether the attenuated cardiac remodeling and dysfunction was linked to MMP activation and/or ROS production. Following surgery, MMP-2 and MMP-9 exhibited a different pattern of upregulation (Figure 3.3). At 2-weeks post-TAC, MMP-2 activity (as detected by gelatin zymography at 72 and 64 kDa) was significantly upregulated in WT-TAC myocardium, and to a less extent in $TNF^{-/-}$ TAC hearts (Figure 3.3i). Nevertheless, MMP-9 activity was detected at 10-weeks post-TAC at a greater magnitude in WT mice than MMP-9 activity in TNF KO mice at 10-weeks post-surgery (Figure 3.3ii). Total collagenase activity was markedly enhanced in WT but not in $TNF^{-/-}$ myocardium at 2- and 10-weeks post-TAC (Figure 3.4). Concomitant with the increased MMP proteolytic activity, superoxide production was significantly elevated in WT but not in $TNF^{-/-}$ myocardium, at 2-weeks post-TAC (Figure 3.2A). At 10-weeks post-TAC, NADPH-dependent superoxide production subsided as the myocardial hypertrophy progressed to a dilated cardiomyopathy, but remained significantly elevated compared to the sham-operated mice at 10-weeks post-TAC (Figure 3.2B).

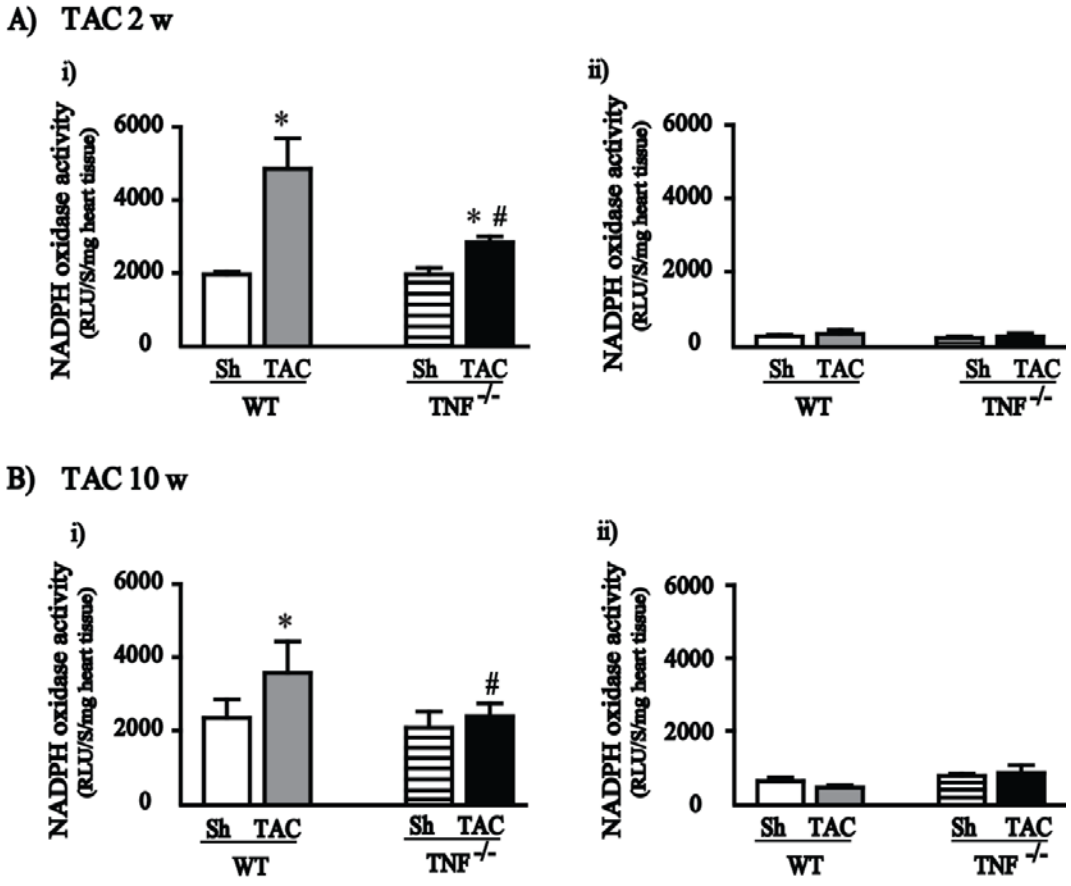

Figure 3.2: Cardiac pressure overload triggered a stronger NADPH-dependent superoxide production in WT than in $TNF^{-/-}$ myocardium post-TAC.

(A) Superoxide production was detected in heart tissue homogenate at 2-weeks post-surgery by lucigenin chemiluminescence (i) and signals were abolished with diphenyleneiodonium sulfate (ii). (B) Lucigenin chemiluminescence showed superoxide production in heart tissue at 10-weeks post-surgery (i). Luminescence signals were completely ablated with DPI (ii). (n=5/group). Statistical analysis was obtained by two-way ANOVA $*P < 0.05$ compared to the corresponding sham, $\#P < 0.05$ compared to the parallel WT-TAC. RLU/S=relative light unit/second/mg heart tissue homogenate. Graphs were plotted using GraphPad Prism. Statistical analysis was done by two-way ANOVA. Experiments were performed by Ahmed Awad.

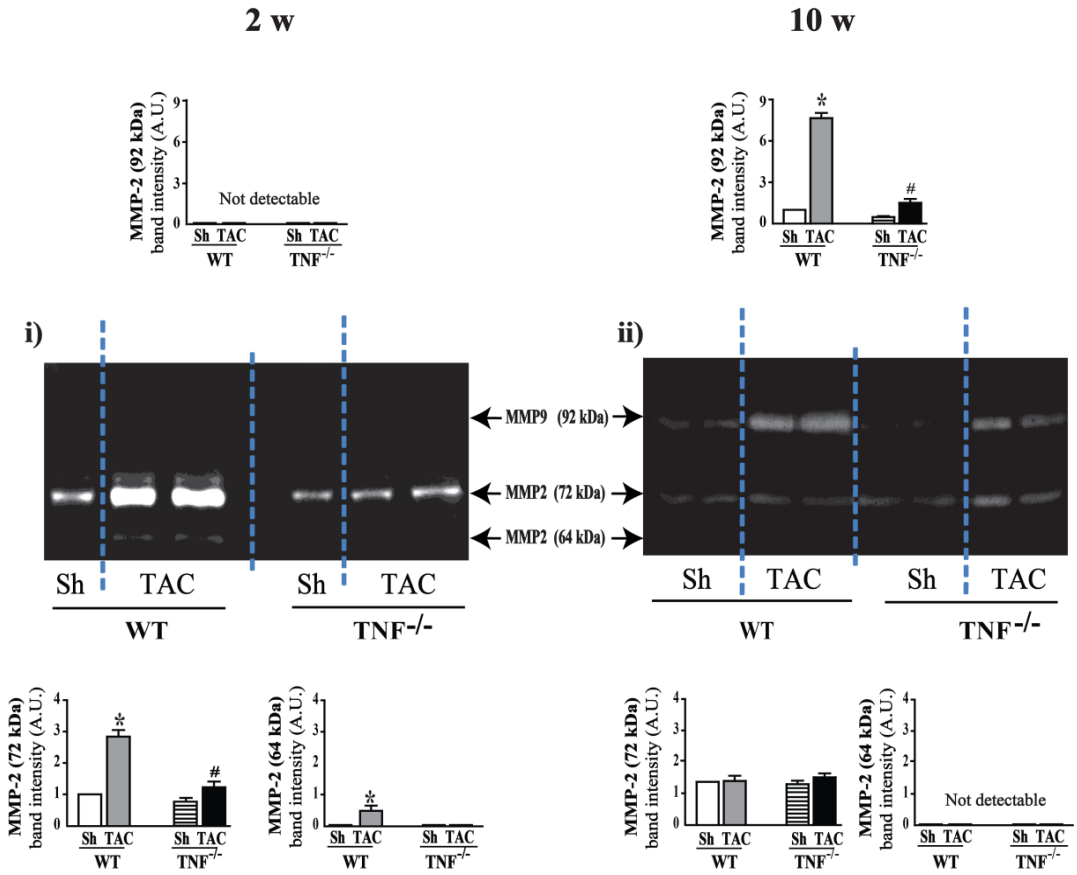

Figure 3.3: Alterations in MMP2 and MMP9 levels at 2-weeks and 10-weeks post-sham or post-TAC in WT and $TNF^{-/-}$ mice.

(i) Pro- and active MMP-2, but not MMP-9, at 72 and 64 kDa were upregulated in WT mice at 2-weeks post-TAC compared to $TNF^{-/-}$-TAC mice (n=3/sham group and n=4/TAC group). (ii) At 10-weeks post-TAC, MMP-9 activity was elevated in WT-TAC mice in comparison to $TNF^{-/-}$-TAC mice (n=4/group). $*P < 0.05$ compared to the corresponding sham, $\#P < 0.05$ compared to the parallel WT-TAC A.U. = Arbitrary Unit. MMP-2 and MMP-9 band intensities were analyzed using Image J software (NIH, USA). Statistical analyses were obtained by two-way ANOVA. Experiments were performed by Ahmed Awad.

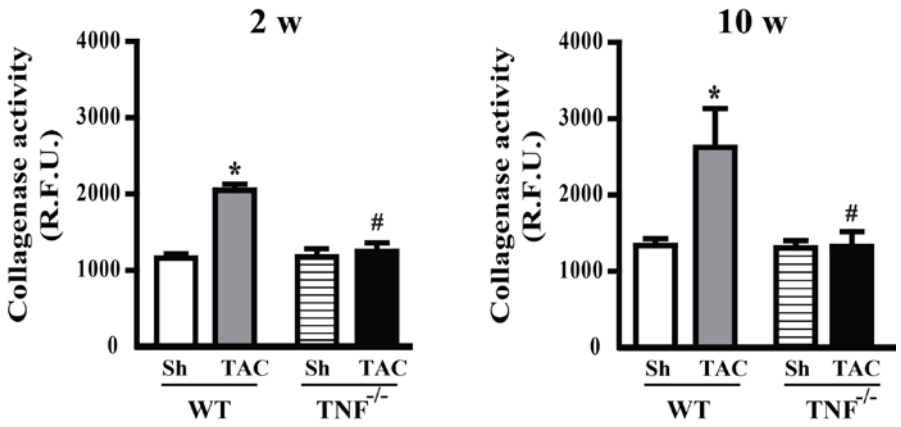

Figure 3.4: Collagenase activity at 2-weeks and 10 weeks post-sham or post-TAC in WT and $TNF^{-/-}$ mice.

Total collagenase activity was enhanced in WT but not in $TNF^{-/-}$ myocardium at 2- and 10-weeks post-TAC (n=5/group). $*P < 0.05$ compared to the corresponding sham, $\#P < 0.05$ compared to the parallel WT-TAC. R.F.U= Relative Fluorescent Unit. Statistical analysis was obtained by two-way ANOVA. Experiments were performed by Ahmed Awad and Wanling Pan.

3.2 TNF Triggers the Production of Superoxide and Peroxynitrite in Cardiomyocytes and Cardiofibroblasts with the Latter Cell Type showing a Slower and Less Severe Response

In vivo findings suggested that TNF-deficiency is associated with less superoxide production and MMP activities in response to pressure overload. To examine whether or not TNF plays a causal role in triggering superoxide and/or proteolytic activities in the myocardium, an *in vitro* culture system of cardiomyocytes and cardiofibroblasts isolated from neonatal WT mice was used. The differential contribution of cardiomyocytes and cardiofibroblasts to this process was also examined. The purity of the cultured cells was examined with immunofluorescent staining (α-sarcomertic actin for cardiomyocytes and vimentin for cardiofibroblasts (Figure 3.5A). Relative expressions of different markers for cardiac cell: α-sarcomeric actin (marker of cardiomyocytes),[249] vimentin (a marker for cardiofibroblasts),[250] CD31 (a marker of endothelial cells),[251] and calponin-1 (a marker for smooth muscle cells)[252] were compared to confirm the purity of the cultured cells (Figure 3.5B).

Treatment of cultured cardiomyocytes and cardiofibroblasts with rTNF (20 ng/mL) revealed a temporally and quantitatively different pattern of superoxide production in the two cell types (as measured by DHE fluorescence) (Figure 3.7). LDH assay was used to confirm absence of necrosis in cultured cells upon treatment with rTNF alone or when combined with apocynin (Figure 3.6). DAPI nuclear staining was used to control for number of cultured cardiomyocytes and cardiofibroblasts. TNF treatment triggered the production of superoxide in

cardiomyocytes within 1 hour, which rose 3-fold by 24 hours of rTNF treatment (Figure 3.7A). In cardiofibroblasts; however, superoxide production occurred only after 24 hours of rTNF treatment (Figure 3.7B). In addition, rTNF triggered an increase in NADPH oxidase activity, measured by lucigenin assay, which mirrored the pattern of increase in superoxide production with an accelerated and greater increase in cardiomyocytes compared to cardiofibroblasts. Furthermore, the TNF-induced NADPH oxidase activity was completely blocked by 100 μM apocynin in both cell types (Figure 3.8).

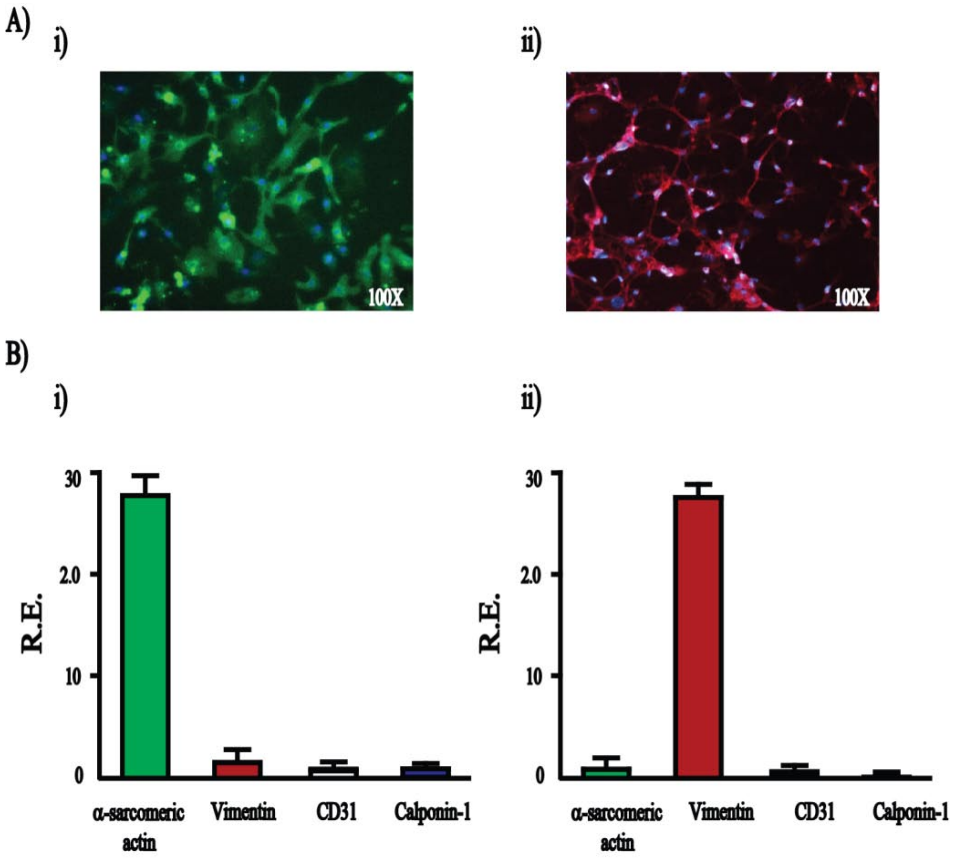

Figure 3.5: Immunofluorescent staining and relative expression of markers for different cardiac cell types to ensure the purity of the cultured cells.

(A) Representative immunofluorescent images for isolated cardiomyocytes (i) and cardiofibroblasts (ii) stained for specific markers. Cardiomyocytes were stained for α-sarcomeric actin (Fetci-labeled) (i), whereas vimentin (Cy3-labeled) was used as a marker for cardiofibroblasts (ii). (B) mRNA expression of markers: α-sarcomeric actin (cardiomyocytes), vimentin (cardiofibroblasts), CD31 (endothelial cells), and calponin-1 (smooth muscle cells) for different cardiac cells in isolated cardiomyocytes (i) and cardiofibroblasts (ii). (n=4-5/group). *P< 0.05 compared to all groups. R.E. = Relative expression. Experiments were done by Ahmed Awad and Xiuhua Wang.

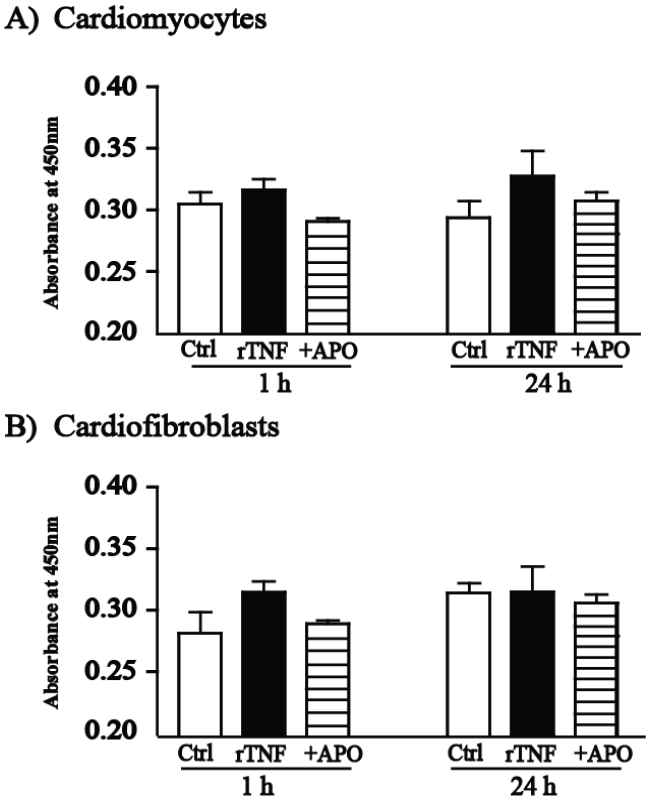

Figure 3.6: LDH assay test performed on media of cultured cells shows that the dose of rTNF used to treat the cells did not induce apoptosis.

LDH release was examined to investigate potential cell damage upon rTNF-treatment or rTNF+apocynin treatment in cardiomyocytes (A) and cardiofibroblasts (B). LDH release was measured in arbitrary units at 450 nm wavelength. Results are means±S.E.M. (n=5). When statistical analysis (using two-way ANOVA) was carried out on the levels of LDH release, no significant difference (P>0.05) was seen between any of the samples.

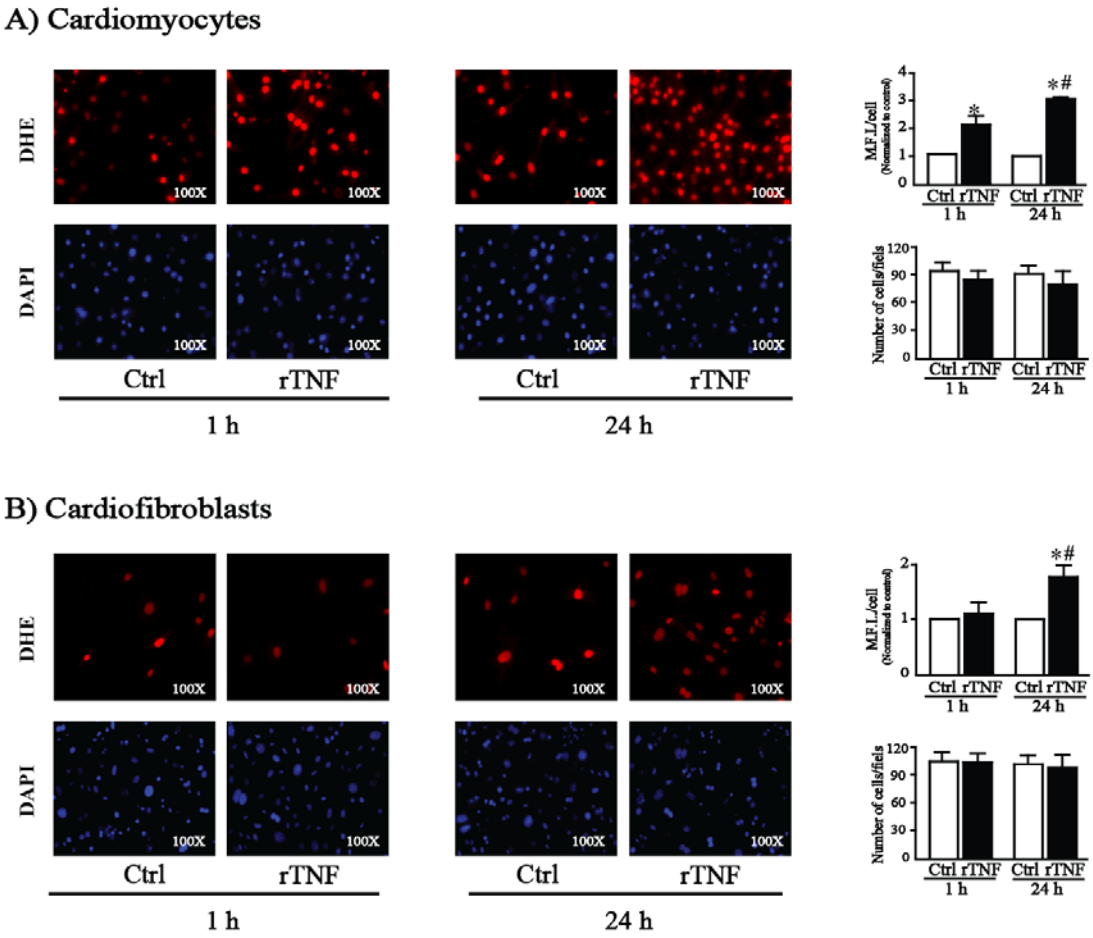

Figure 3.7: Dihydroethedium (DHE) fluorescent staining showing that TNF triggered an accelerated and stronger superoxide production in cardiomyocytes compared to cardiofibroblasts.

Superoxide levels were measured by dihydroethidium (DHE) staining of cardiomyocytes (A-i) and cardiofibroblasts (B-i). DAPI staining was used to control for the number of cells/field for cardiomyocytes (A-ii) and cardiofibroblasts (B-ii). Averaged quantified signal intensity and number of cells/field (n=12 fields/group) are shown as bar graphs, PBS (white) and rTNF for 1 hour or 24 hours (black). Reported values (mean ± SEM) were normalized to the control within each group. *$P < 0.05$ compared to control, # $P< 0.05$ compared to 1 hour treatment. Ctrl = control, rTNF = recombinant TNF. MFI=Mean Fluorescent Intensity. Statistical analyses were done using one-way ANOVA followed by Newman-Keuls test. Experiment was performed by Ahmed Awad.

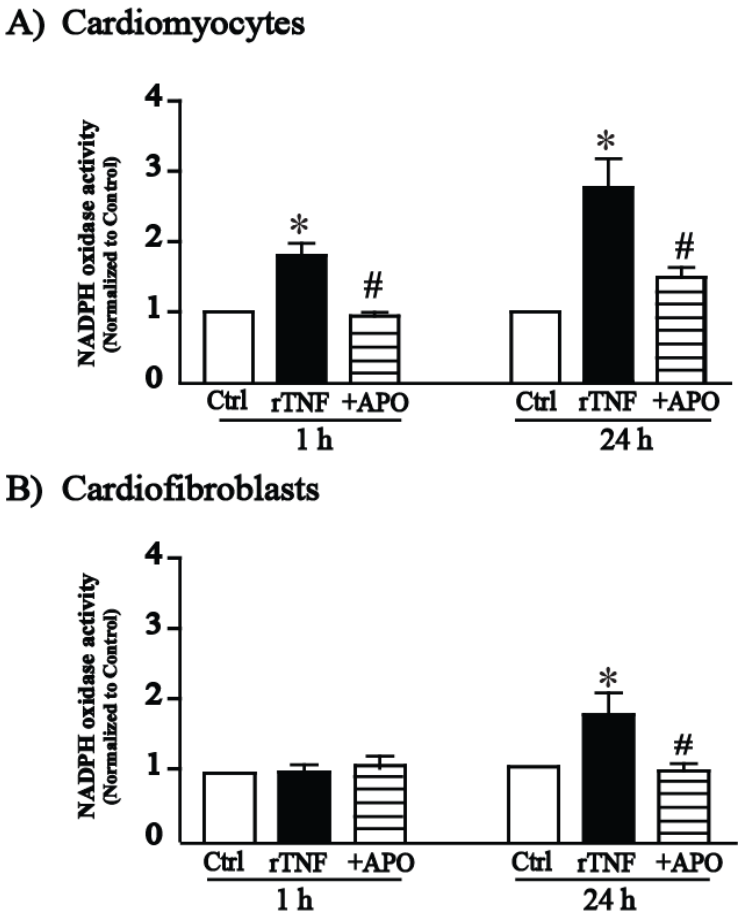

Figure 3.8: TNF treatment triggered a faster and stronger NADPH oxidase activity in wild-type cultured neonatal mouse cardiomyocytes than in cardiofibroblasts.

(A) rTNF initiated NADPH-dependant superoxide production in cardiomyocytes cell types at 1 and 24 hours post-treatment. Chemiluminescent signals were abolished upon using apocynin (an NADPH oxidase inhibitor). (B) In cardiofibroblasts, rTNF mediated NADPH-dependant superoxide production only after 24 hours of treatment. Averaged data are shown as bar graphs, PBS (white), rTNF for 1 hour or 24 hours (black), and rTNF+Apocyin (hatched). (n=5-7/group). Reported values were normalized to the control within each group, and are reported as mean ± SEM. *$P < 0.05$ compared to control, # $P< 0.05$ compared to 1 hour treatment. Ctrl = control, rTNF = recombinant TNF, and +APO = rTNF+ apocynin. Statistical analyses were done using one-way ANOVA followed by Newman-Keuls test. Experiments were performed by Ahmed Awad.

TNF treatment also triggered a marked and significant expression of nitric oxide synthase (iNOS) mRNA in cardiomyocytes and cardiofibroblasts after 24 hours (Figure 3.9A). Concomitantly, a rise in nitrite anion was detected in conditioned media of both cardiac cell types, as measured by the Griess reaction assay (Figure 3.9B). This was associated with a rapid and significant increase in nitrotyrosine staining intensity, a marker of peroxynitrite production, after 1 hour and 24 hours in cardiomyocytes, but only after 24 hours of rTNF treatment in cardiofibroblasts (Figure 3.9C). DAPI nuclear staining was used to ensure a relative number of cells per culture.

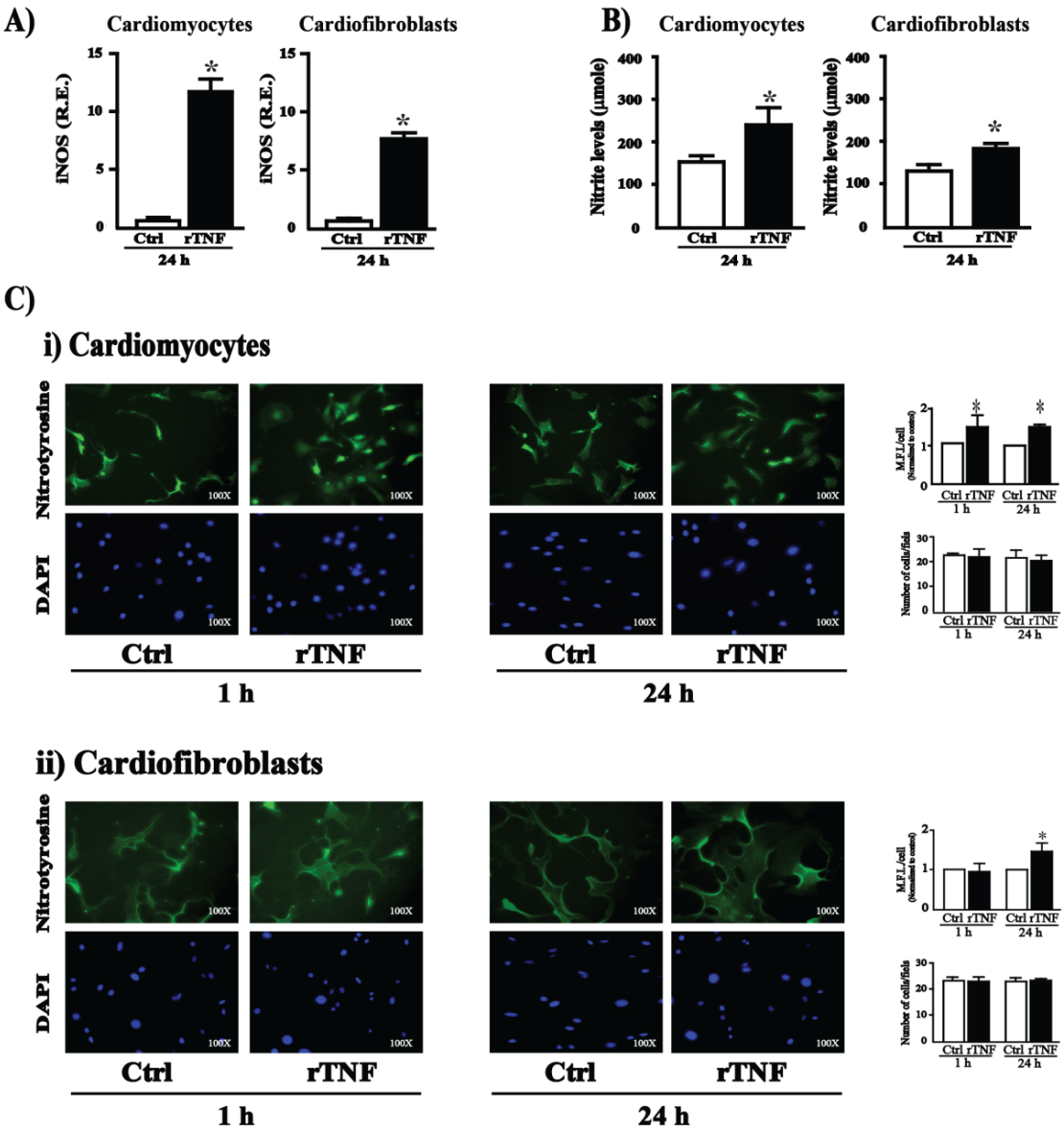

Figure 3.9: TNF-treatment results in nitrotyrosine formation (an indicator of peroxynitrite formation) in wild-type mouse cardiomyocytes and cardiofibroblasts.

(A) mRNA expression of iNOS in cardiomyocytes and cardiofibroblasts after 24 hours of rTNF-treatment. (B) Nitrate/nitrite levels in conditioned media of cardiomyocytes and cardiofibroblasts were measured by the Greiss reaction assay in control and in TNF-treated cardiomyocytes and cardiofibroblasts. (C) Representative images of nitrotyrosine-stained cardiomyocytes (i) and cardiofibroblasts (ii) after 1 hour or 24 hours of treatment with rTNF. Quantification of the signal intensity (n=12 fields/group) is presented as bar graphs normalized to the control group. *P< 0.05 compared to control. #P<0.05 compared to 1 hour treatment. Ctrl = control, rTNF = recombinant TNF. R.E. = rRelative expression, M.F.I. = mean fluorescent intensity. Experiments were performed by Ahmed Awad.

3.3 TNF Induces MMP Expression and Activation Primarily via Superoxide Production

Since cardiomyocytes were found to contribute to TNF-mediated oxidative stress more than were cardiofibroblasts, we investigated whether or not TNF mediates MMP induction and activation through ROS production. We first examined whether or not TNF can induce expression and/or activation of MMPs. Expression analyses of gelatinases, MMP-2, and MMP-9 mRNA levels, showed a different pattern of induction by TNF. Gelatin zymography showed a significant increase in MMP-9 levels after 24 hours of TNF stimulation in both cell types, and to a greater degree in the conditioned media rather than in the cell homogenate (Figure 3.12). MMP-2 levels; however, were not affected by TNF stimulation in either cell type. Examining the mRNA expression profile of MMP-9, in response to TNF, revealed a significant increase (40-fold) at 24 hour in cardiomyocytes, compared to a 10-fold increase in cardiofibroblasts (Figure 3.10). Hence, TNF is a strong inducer of MMP-9 but not of MMP-2 in cardiomyocytes and cardiofibroblasts *in vitro*. We further found that blockade of superoxide by apocynin, an NADPH oxidase inhibitor, significantly suppressed the TNF-induced increase in MMP-9 mRNA and protein levels in cardiomyocytes, and protein levels in cardiofibroblasts (Figures 3.10 and 3.12). Interestingly, NADPH oxidase inhibitor exerted no inhibition on MMP-9 mRNA levels in cardiofibroblasts, indicating a differential mechanism of rTNF-mediated MMP-9 mRNA expression in cardiomyocytes vs. cardiofibroblasts.

Next, we examined the influence of rTNF on collagenases such as MMP-8, MMP-13, and MMP-14/MT1-MMP and elastase MMP-12 (Figure 3.10), which influence the remodeling of the myocardial extracellular matrix and further contribute to the progression of cardiomyopathy. In cardiomyocytes, rTNF treatment significantly induced expression of MMP-8 (3-fold), MMP-12 (3-fold), and MMP-13 (3-fold), which were suppressed by apocynin treatment (Figure 3.10A). TNF did not induce mRNA levels of MMP-14/MT1-MMP (Figure 3.10 A-ii). In cardiofibroblasts, rTNF caused a significant increase in expression of MMP-8 (8-fold), MMP-13 (2.5-fold), and MMP-14 (2-fold) (Figure 3.10 B-ii), which were reduced upon superoxide inhibition. The increase in MMP-14; however, was only partially suppressed (by 45%) with apocynin. rTNF did not increase mRNA levels of MMP-12 in the cardiofibroblasts (Figure 3.10 B-iii).

We investigated the effect of rTNF on TIMPs. TNF significantly inhibit TIMP-3 expression (mRNA) in both cardiomyocytes and cardiofibroblasts. rTNF treatment did not affect mRNA levels of TIMP-2 and TIMP-4. Interestingly, TIMP-1 mRNA levels were found to be highly induced upon rTNF-treatment.

We further demonstrated that these TNF-mediated changes in MMP expression levels are well reflected in the MMP activities of the culture systems. Total collagenase activity increased significantly in the conditioned media from cardiomyocyte and cardiofibroblast cultures following rTNF-treatment (Figure 3.13), and was suppressed by apocynin treatment with a pattern that was similar to the TNF-dependent expression profile of MMPs

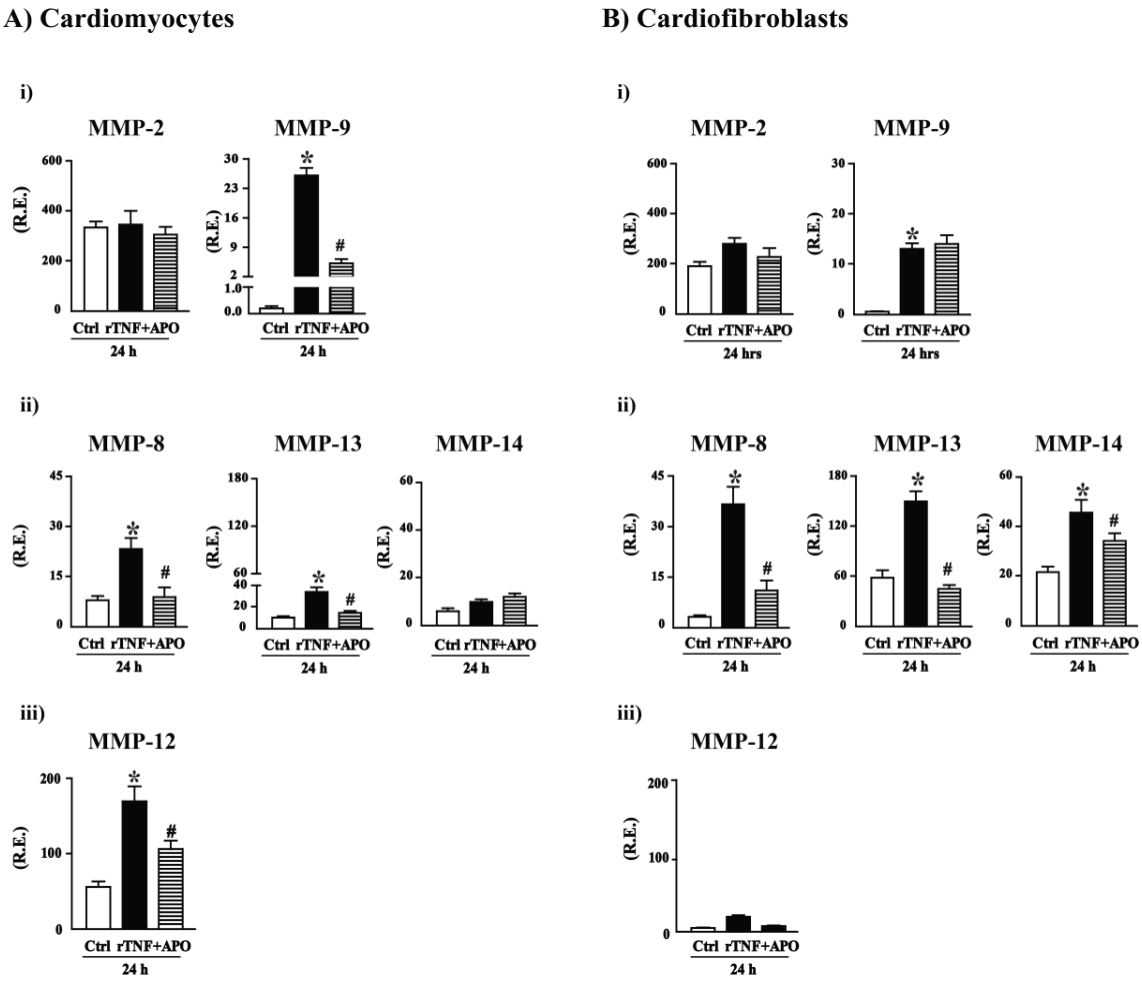

Figure 3.10: TNF can induce expression and activation of a number of gelatinases, collagenases, and metalloelastase differently according to cardiac cell types.

mRNA expression of MMP-2 and MMP-9 (i), MMP-8, MMP-13 and MMP-14 (ii), MMP-12 (iii) in cardiomyocytes (A) and cardiofibroblasts (B). rTNF induced MMP-9 and MMP-12 more in cardiomyocytes, and MMP-8, MMP-13 and MMP-14 more in cardiofibroblasts. These inductions were concomitant with superoxide production and were inhibited with apocynin (an NADPH oxidase inhibitor). **P*< 0.05 compared to control, #*P* < 0.05 compared to rTNF group. R.E.= Relative expression. Ctrl = control, rTNF = recombinant TNF, and +APO = rTNF+ apocynin. Statistical analyses were done using one-way ANOVA followed by Newman-Keuls test. The cells were cultured and treated by Ahmed Awad. TaqMan RT-PCR was done by Xiuhua Wang.

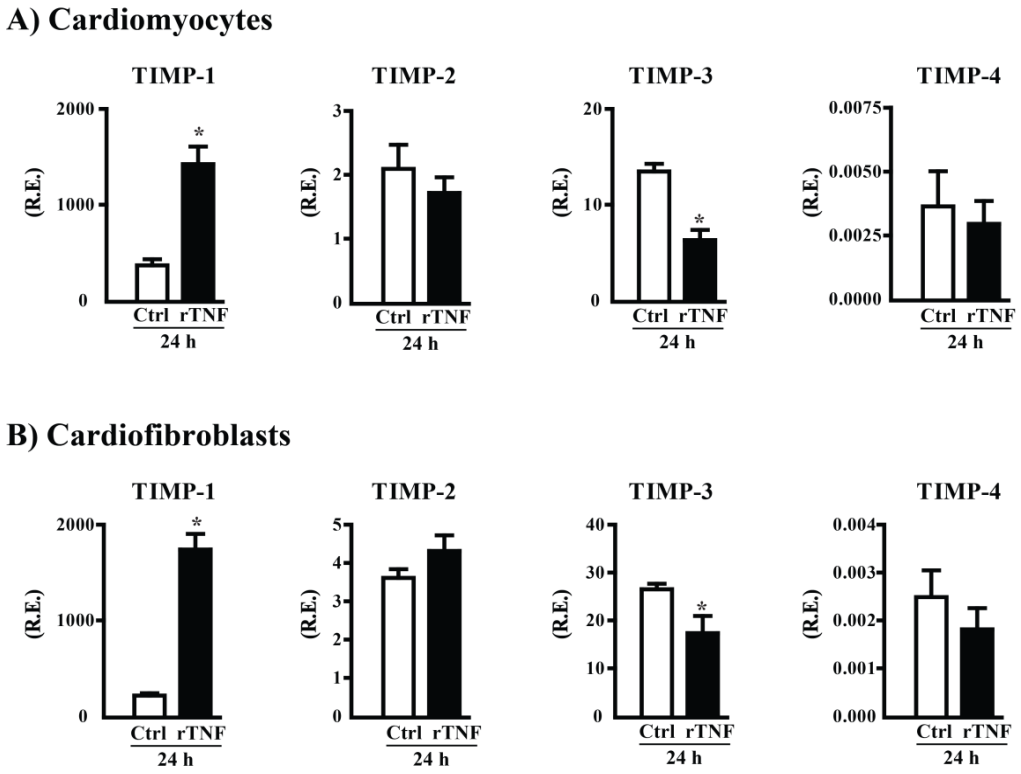

Figure 3.11: TIMP profile: mRNA expression of TIMP-1, TIMP-2, TIMP-3, and TIMP-4 in cardiomyocytes (A) and cardiofibroblasts (B).

TNF significantly inhibited TIMP-3 expression (mRNA) in both cardiomyocytes and cardiofibroblasts. rTNF treatment did not affect mRNA levels of TIMP-2 and TIMP-4. Interestingly, TIMP-1 mRNA levels were found to be highly induced upon rTNF-treatment. *P< 0.05 compared to control. R.E.= Relative expression. Ctrl = control, and rTNF = recombinant TNF. Statistical analyses were done using student's t-test. The cells were cultured and treated by Ahmed Awad. TaqMan RT-PCR was done by Xiuhua Wang.

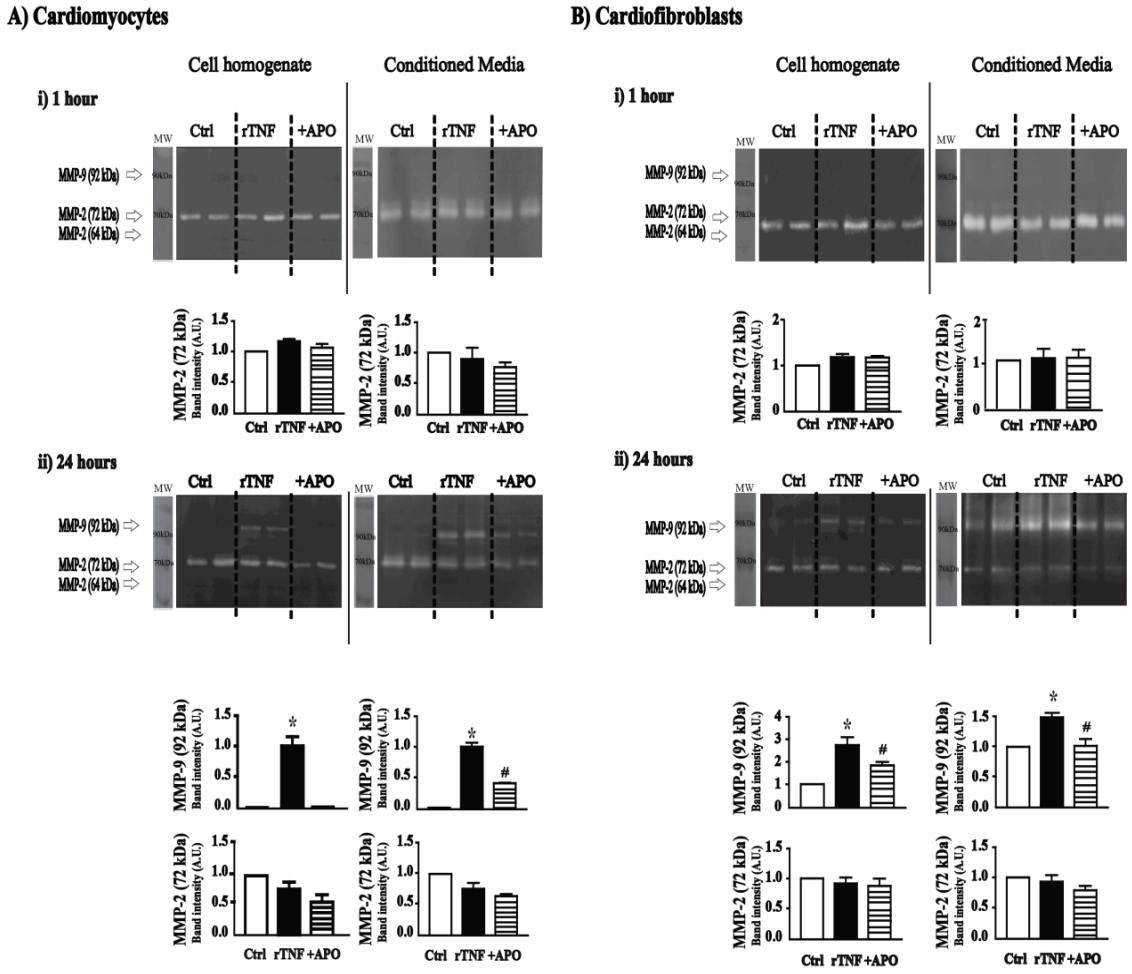

Figure 3.12: In cultured cardiomyocytes and cardiofibroblasts, rTNF induces the activity of MMP-9, but not MMP-2, in a superoxide-dependent fashion.

Gelatin zymography on cell homogenate and conditioned media from wild-type cardiomyocyte (A) and cardiofibroblast (B) control, rTNF- or rTNF+apocynin-treated groups after 1 hour (i) or 24 hours (ii) of treatment. Averaged band intensity for MMP-2 and MMP-9 are presented as bar graphs, control (white), rTNF (black), rTNF+apocynin (horizontal hatch). (n=4/group). *$P< 0.05$ compared to all other groups. #$P< 0.05$ compared to rTNF-treated group. Ctrl = control, rTNF = recombinant TNF, APO = apocynin, MW = molecular weight. R.E. = Relative expression. Statistical analysis was performed by one-way ANOVA followed by Student-Newman-Keuls test. The experiments were done by Ahmed Awad

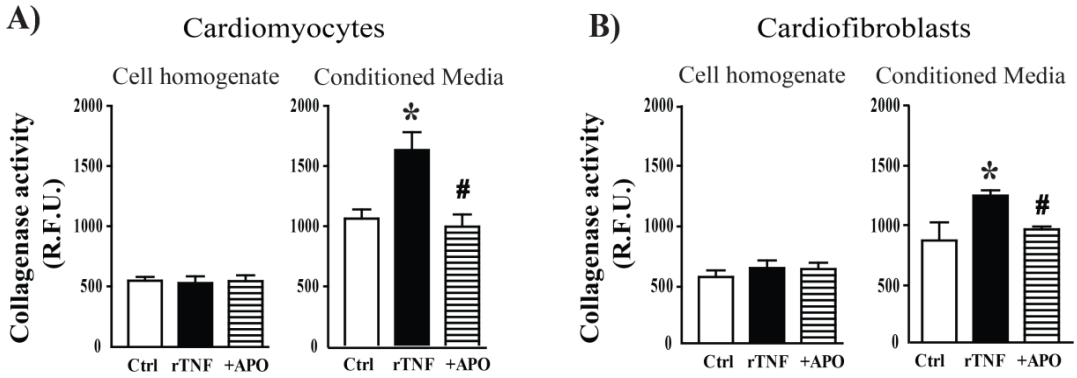

Figure 3.13: rTNF stimulates collagenase activity in the conditioned media but not in the cell homogenate of cultured cardiomyocytes and cardiofibroblasts.

Collagenase activity of cell homogenate and conditioned media from wild-type cardiomyocyte (A) and cardiofibroblast (B), control, rTNF- or rTNF+apocynin-treated groups after 24 hours (n=3/group; 5 wells were pooled together to get one sample). rTNF treatment induced a greater increase in collagenase activity in the conditioned media of cardiomyocytes compared to cardiofibroblasts after 24 hours of treatment. *$P< 0.05$ compared to all other groups. #$P< 0.05$ compared to rTNF-treated group. Ctrl = control, rTNF = recombinant TNF, APO = apocynin. R.F.U. = Relative fluorescent unit. Statistical analyses were performed using one-way ANOVA. The cells were cultured, treated and harvested by Ahmed Awad. Collagenase activity was done by Xiuhua Wang.

Chapter 4. Discussion

4.1 Summary of Findings

This study led to five main findings:

(1) $TNF^{-/-}$ mice exhibit attenuated cardiomyopathy with significantly less cardiac hypertrophy and left ventricular dilation following transverse aortic-constriction (TAC), compared to that of WT mice. This improvement in cardiac structure and function in $TNF^{-/-}$ mice was associated with reduced superoxide production and collagenase activity, less MMP-2 activation, at an early time, and reduced MMP-9 activation at later stages of the disease.

(2) *In vitro,* TNF stimulation triggered an accelerated and stronger NADPH-dependant superoxide production in cultured neonatal mouse cardiomyocytes, compared to that of cardiofibroblasts. Cardiomyocytes showed a significant increase in superoxide production in a time-dependant fashion, while in cardiofibroblasts, superoxide production occurred only after 24 hours post-rTNF treatment.

(3) TNF induced induction and activation of MMPs differently in cardiomyocytes compared to cardiofibroblasts. rTNF-treatment induced a significantly greater mRNA expression of MMP-9 and MMP-12 in cardiomyocytes, compared to that of cardiofibroblasts; whereas the expression of

MMP-8, MMP-13 and MMP-14/MT1-MMP were higher in cardiofibroblasts, compared to cardiomyocytes. Nevertheless, MMP-2 mRNA levels were not affected by TNF stimulation in either cell type.

(4) Total collagenase activity after 24 hours of TNF stimulation was greater in the conditioned media of cultured cardiomyocytes compared to cardiofibroblasts.

(5) TNF-induced MMP expression and activation occurred via NADPH-dependant superoxide production in both cardiac cell types.

4.2 *In Vivo* Model of Left Ventricular Pressure Overload

Aortic constriction is a commonly used experimental model of cardiac pressure overload to study the effects of mechanical stress on the LV and to evaluate the cellular and molecular mechanisms underlying LV hypertrophy and heart failure in response to hemodynamic stress. LV pressure overload can be created in animal models by constricting the ascending,[253] transverse,[254] descending[255] or abdominal aorta.[256] Constriction of the ascending aorta is more likely to cause an excessive and abrupt overload on the LV in mice, which may lead to ventricular arrhythmias, while constriction of the abdominal aorta, a significant part of the circulation system serving as a reactive vascular bed, may delay the myocardial response to the increased pressure overload. Transverse aortic constriction (TAC) generates a gradual and progressive LV hypertrophy in mice, hence, is often the most suitable technique for inducing experimental

pressure overload.[257] Therefore, we used the TAC model in WT and TNF$^{-/-}$ mice to determine the role of TNF in pressure overload cardiomyopathy and to characterize the secondary effectors that mediate the TNF effects. At 4 weeks post-TAC, animals develop concentric hypertrophy characterized by an increase in LV posterior wall thickness with a small change in LV internal dimension and no change in LV function,[258] while heart failure occurs at 12-weeks post-surgery.[259] We chose two different time points of 2-weeks and 10-weeks post-surgery to study the early molecular alterations and the transition from dilated cardiomyopathy to heart failure.

4.3 The Improved Cardiomyopathy in TNF$^{-/-}$ Mice following Pressure Overload is Associated with Reduced Superoxide Production and MMP Activities

The objective of this study was to assess the role of TNF in progression of LV pressure overload cardiomyopathy and to determine the downstream effectors of TNF in cardiac disease. We found that at 10-weeks post-TAC, TNF$^{-/-}$ mice exhibited attenuated cardiomyopathy with significantly less cardiac hypertrophy and LV dilation as well as relative preservation of systolic function, compared to WT mice. It has been reported that TNF mRNA and TNF protein levels are rapidly elevated in the hearts of animal models subjected to pressure overload and mechanical stress.[59, 113] Serum TNF levels were found to be significantly elevated in patients with aortic stenoses compared to control subjects.[58] Overexpression of TNF in the heart has been reported to lead to cardiac hypertrophy, progressive LV remodeling[114] and LV dysfunction in transgenic mice,[116] while its deficiency

results in improved cardiac function and survival in experimental models of heart disease.[48, 260] *In vitro* studies have shown that TNF leads to disparate effects, including augmentation of myocyte contractility and myocyte hypertrophy,[173] depression of myocyte contractility,[172] myocyte apoptosis,[57] or myocyte hypertrophy.[115] These findings indicate that TNF plays a complex role in a variety of cardiac diseases. In this study, a reduction in superoxide production and proteolytic activities was seen in TNF-deficient myocardium, compared to that in the wild-type heart, in response to pressure overload. These findings could explain the attenuated cardiac remodeling and dysfunction in $TNF^{-/-}$ mice compared to wild-type mice.

This study also investigated the early molecular events that may lead to the functional improvement in TNF-deficient mice. Adverse cardiac remodeling during disease is associated with aberrant remodeling of the extracellular matrix through elevated and uncontrolled activity of MMPs.[59, 148, 261, 262] In this study, at 2-weeks post-TAC, MMP-2 (72 and 64 kDa) was significantly upregulated in WT myocardium, while MMP-9 (92 kDa) rose by 10-weeks post-TAC. In the $TNF^{-/-}$-TAC myocardium; however, MMP-2 levels, as detected by gelatin zymography, did not increase, while the increase in MMP-9 at 10-weeks was smaller than that seen in the WT-TAC myocardium. Furthermore, total collagenase activity, was enhanced in WT but not in the $TNF^{-/-}$ myocardium at 2- and 10-weeks post-TAC. This data suggests the possibility that TNF activates cardiac gelatinases and collagenases to mediate the ECM remodeling and deterioration in cardiac

function, in response to pressure overload. These findings are in agreement with an earlier study demonstrating that cardiac MMP-9 levels were upregulated to a greater extent in WT, compared to $TNF^{-/-}$ mice, in response to pressure overload.[48] Increased MMP-2 and MMP-9 levels have been reported in mice overexpression of TNF that developed left ventricular hypertrophy and dilation,[263] and in the pharmacological inhibition of MMPs that prevented ventricular remodeling and dysfunction in these mice.[264] Thus, TNF may be upregulating cardiac MMP activity.

NADPH-dependent superoxide production was significantly elevated in WT-TAC, but not in $TNF^{-/-}$-TAC myocardium, at 2-weeks post-TAC. The production of NADPH-dependant superoxide in the myocardium gradually subsided over time, as the myocardial hypertrophy progressed to a dilated cardiomyopathy, but the production was still significantly elevated compared to the sham-operated group at 10-weeks post-TAC. The superoxide production was strongly inhibited by diphenylene iodonium, a NADPH oxidase inhibitor,[265, 266] suggesting that the produced superoxide, in response to cardiac pressure overload, is mediated by NADPH oxidase.[265] Oxidative stress has been reported in the myocardium of patients with chronic systolic LV failure,[203] as well as in the myocardium of animal models of myocardial infarction[267, 268] and in pressure overload-induced heart failure.[199, 269,270] In addition, administration of Vitamin E, an antioxidant, prevented the transition from compensated hypertrophy to heart failure in pressure overload cardiomyopathy.[271] These findings indicate the

participation of oxidative stress in cardiac remodeling, but do not identify the link between TNF and oxidative stress in the myocardium. This link has been identified in endothelial cells where TNF mediates endothelial dysfunction[272-274] through the generation of oxidative stress.[274-277] In any case, little is known about the direct role of TNF in generating oxidative stress in the myocardium. Our *in vivo* study demonstrates that TNF-deficiency in the myocardium plays a role in minimizing the superoxide production in the hearts in response to LV pressure overload.

Given the biological complexity of the factors contributing to pressure overload-induced cardiac remodeling, it would be misleading to propose a single molecule as being responsible for cardiac decompensation. Nevertheless, the *in vivo* findings provide evidence that TNF triggers a cascade of events, including NADPH-dependent superoxide production and MMP activation that contribute to adverse cardiac remodeling and dysfunction in heart disease. Due to the systemic complications associated with *in vivo* studies; however, it is difficult to decipher a direct connection between cardiac TNF, ROS, and MMPs in disease. To determine the direct effects of TNF on NADPH-superoxide production and proteolytic activation, leading to the progression of cardiomyopathy, we used more controlled experimental settings, with an *in vitro* system of cultured neonatal cardiomyocytes and cardiofibroblasts.

4.4 TNF Triggers an Accelerated and Stronger Production of NADPH-Dependent Superoxide in Cardiomyocytes compared to Cardiofibroblasts

As previously discussed, the finding from our *in vivo* study indicates that TNF is involved in the production of NADPH-dependant superoxide following pressure overload. The question that we asked was which cardiac cell type contributes more to cardiac remodeling in response to stress such as LV pressure overload. We examined the effects of TNF on cardiomyocytes and cardiofibroblasts, since cardiomyocytes are the contractile unit in the heart[278] and their coordinated contractions cause the blood to move through the heart.[279] In addition, cardiomyocytes serve as a major source of cardiac TNF in response to stimuli such as lipopolysaccharides.[280] Production of TNF by cardiomyocytes *in vivo* is sufficient to cause severe cardiac disease in mice overexpressing TNF.[114] On the other hand, cardiofibroblasts play an essential role in the process of fibrotic myocardial remodeling in the injured and failing heart.[281, 282] Cardiofibroblasts produce most of the fibrillar collagen in the heart.[283,284] TNF was found to be elevated in the myocardium within the infarcted myocardium , and it was found to be localized to the cardiac fibroblasts.[285, 286] Cardiofibroblasts have been shown to proliferate in response to hypertrophic stimuli such as phenylepinephrine.[287] Cultured cardiomyocytes and cardiofibroblasts provide a useful system for examining the direct effects of different factors, such as cytokines, on each cardiac cell type.

In this study, we used a sub-apoptotic dose of rTNF to stimulate cultured neonatal cardiomyocytes and cardiofibroblasts. Absence of apoptosis was confirmed with the lactate dehydrogenase assay and with DAPI (Hoechst) nuclear staining. Cardiomyocytes showed a 1.8-fold increase in $O_2^{\bullet-}$ production within 1 hour, which rose to 3-fold by 24 hours of rTNF treatment. In cardiofibroblasts, in contrast, $O_2^{\bullet-}$ production occurred only after 24 hours and only by 1.7-fold, according to the lucigenin chemiluminescence. The delayed TNF-mediated NADPH oxidase activity and subsequent $O_2^{\bullet-}$ production in cardiofibroblasts could be explained by the fact that the cellular mechanisms leading to the activation of NADPH oxidase and production of $O_2^{\bullet-}$ require translocation of cytosolic subunits of NADPH to the membrane and their assembly, as well as the phosphorylation of another subunit, P47. Disruption of any of these processes would inhibit the production of NADPH-dependent $O_2^{\bullet-}$.

Our data identifies the participation of each cell type in cardiomyopathies associated with increased cardiac TNF levels. In cardiomyopathy, TNF triggers $O_2^{\bullet-}$ production beyond the cells capacity to neutralize the harmful effect of oxidative stress. Disturbing the balance between oxidants and antioxidants towards increased oxidative stress subsequently triggers a number of cardiomyopathic processes, as observed in ischemia-reperfusion injury, myocardial infarction, and heart failure.[288] In this study, the TNF-triggered NADPH oxidase activity and $O_2^{\bullet-}$ production in cardiomyocytes and cardiofibroblasts is amplified in both cell types, though at different rates and

magnitudes, and in a time-dependent fashion. Cardiomyocytes show stronger and faster production of NADPH-dependant $O_2^{\bullet-}$ in response to the increase of TNF, compared to the production in cardiofibroblasts. Much of the toxicity from $O_2^{\bullet-}$ is mediated by the formation of even more reactive species such as the extremely reactive peroxynitrite. $O_2^{\bullet-}$ can react with nitric oxide to produce the highly reactive peroxynitrite, which has been implicated in damage within the mitochondria.[289] At low levels of peroxynitrite, the S-glutathiolation of the cysteine residue of the cysteine switch in the propeptide exposes the catalytic zinc atom and frees the catalytic site thereby activating MMPs.[290, 291]

4.5 TNF Mediates MMP Induction and Activation in an NADPH Oxidase-Dependent Manner

In cultured cardiomyocytes, TNF triggered a rapid and significant increase in MMP-9 mRNA expression, which was followed by a delayed increase in protein levels. This lag is not surprising since most MMPs have been shown to respond to stimuli at the transcriptional level with delayed kinetics, over a time-frame of several hours.[292] The increase in MMP-9 levels was significantly blocked by apocynin in cardiomyocytes, but not blocked in cardiofibroblasts, suggesting an involvement of different molecular mechanisms in these two cell types. Among the collagenases, TNF triggered a significant increase in expression of MMP-8, MMP-12, MMP-13, and to a lesser degree, MMP-14, with a significant rise in total collagenase activity in the conditioned media of both cell types, which was blocked by apocynin (a NADPH oxidase inhibitor).

Consistently, ROS and inflammatory cytokines have been reported to regulate matrix metalloproteinase activity in cardiomyocytes and cardiofibroblasts.[293] Hydrogen peroxide and xanthine/xanthine oxidase have been shown to cause direct activation of latent MMPs in conditioned media from cardiac fibroblasts *in vitro*.[294,295] Based on their promoter structures, MMPs have been classified into three groups: 1) those containing TATA boxes with proximal AP-1 (activator protein-1) (e.g., MMP-9, MMP-12, and MMP-13), which are often induced by TNF or interleukin-1;[296] 2) those containing TATA boxes, but no promoter proximal AP-1 site (e.g., MMP-8); and 3) those with no TATA box or proximal AP-1 (e.g., MMP-2, MMP-14).[297] Hence, the promoter structure of each MMP could be a critical determinant for its induction by different stimuli. MMP-2 and MMP-14, which showed minimal responses to TNF, fall into the last category with a similar promoter structure. A number of signaling pathways are activated during cardiac hypertrophy and heart failure,[298-300] which can target the MMP-2 promoter.[301-305] TNF significantly induced TIMP-1 in both cardiac cell-types. TIMP-3 expression was significantly downregulated in cardiomyocytes and cardiofibroblasts following rTNF treatment, while no difference was seen in mRNA levels for TIMP-2 or TIMP-4. The lack of effect of TNF on TIMP-2 mRNA expression in both cardiac cell types could explain the lack of change in MMP-2 activity in cardiomyocytes and cardiofibroblasts, examined by gelain zymography. Activation of MMP-2 is unique among the MMPs, where the binding of TIMP-2 to MMP-2 is required for MMP-2 activation by membrane-type MMPs.[151] rTNF treatment did not increase MMP-2 protein levels *in vitro*,

whereas, *in vivo*, TNF-deficiency suppressed MMP-2 elevation following pressure overload. The lack of MMP-2 activation in the $TNF^{-/-}$-TAC hearts *in vivo* is likely secondary to the less progressive cardiac dilation and failure in TNF-deficient mice.

In patients with aortic stenosis, TIMP-1 levels were significantly elevated in the LV myocardium, directly correlating with the degree of fibrosis.[306] TIMP-1 has also been shown to be significantly elevated in the myocardium of patients with progressive heart failure[307] and in idiopathic dilated cardiomyopathy.[308] Elevated plasma TIMP-1 levels have been correlated with myocardial hypertrophy,[309] fibrosis, and diastolic dysfunction in hypertensive.[310] TIMP-1 has also been proposed to promote fibrosis by inducing collagen synthesis.[310, 311] TIMP-3 is an effective inhibitor of a number of ADAMs and is the only physiological inhibitor of ADAM-17/TACE.[312] The reduction in TIMP-3 protein levels following rTNF treatment could be a protective mechanism to reduce the TNF-mediated signaling. TIMP-3 deficiency in mice led to dilated cardiomyopathy and heart failure.[313] TIMP-4 is the only TIMP with a proposed intracellular localization in cardiomyocytes, based on *ex vivo* ischemia-reperfusion studies where a rapid enhanced release of TIMP-4 upon reperfusion of the ischemic heart was concomitant with increased net myocardial MMP activity contributing to acute myocardial stunning injury.[314]

TNF-induced $O_2^{\bullet -}$ production most likely occurs through MAPK activation that activates AP-1 and NF-κb. Ischemia has been reported to activate ERK and

JNK, members of the MAPK signaling cascade, as well as transcription factors, NF-, κB, and API, via NADPH oxidase-derived ROS production.[315] Reduction of ROS can suppress inflammatory signaling by inhibiting the NF-κB cascade.[316] MAPKs are key signaling molecules in many cell types, and the phosphorylation of the components of AP-1 by MAPKs mediates rapid activation of AP-1.[317, 318] When activated, the AP-1 complex binds to a palindromic binding sequence (5´-TGACGTCA-3´) in the regulatory region of its target genes.[319] In adult rabbit cardiomyocytes, activation of protein kinase C epsilon type (PKCε) increases AP-1 DNA binding activity, which is completely abolished by inhibition of the ERK and JNK pathways.[320] Within 30 minutes of pressure overload in the rat heart, increased activities of JNK and p38 MAPK, enhanced phosphorylation of c-Jun, and increased ventricular AP-1 DNA binding activity was detected.[321] Angiotensin II infusion induced the activation of JNK, which was followed by the induction of left ventricular AP-1 DNA binding activity *in vivo*.[322] Taken together, this data suggests that MAPK pathways can mediate the AP-1 DNA binding activity in response to hypertrophic stimuli.

In our *in vitro* studies, the direct effects of TNF where demonstrated in the induction of MMPs under controlled conditions and in the absence of systemic complications of *in vivo* studies. We found that TNF can trigger expression and activation of matrix metalloproteinases which are key determinants of myocardial remodeling. Furthermore, the induction occurs in a NADPH-dependent manner,

differentially in cardiomyocytes and cardiofibroblasts, with temporal differences in magnitude.

4.6 Conclusions

In conclusion, TNF-mediated $O_2^{\bullet-}$ production and MMPs activation underlie the progression of cardiac hypertrophy and dysfunction in LV pressure overload cardiac disease. Cardiomyocytes exhibit a faster and stronger $O_2^{\bullet-}$ production in response to TNF, compared to that of cardiofibroblasts, and TNF-mediated MMP induction and activation occur primarily in a NADPH oxidase-dependant manner. Our *in vivo* and *in vitro* findings demonstrate a causal role for TNF in NADPH-dependant $O_2^{\bullet-}$ production and MMPs activation, leading to the deterioration of cardiac function in pressure overload cardiomyopathy. These findings provide further insight into the mechanism by which TNF can adversely affect cardiac structure and function in disease in response to stress.

4.7 Limitations of the Study

The research presented in this thesis is part of an ongoing investigation to expand our understanding of the molecular basis of cardiac remodeling in response to pressure overload. In this study, we used small animal models to study the molecular mechanisms that underlie cardiac remodeling in pressure overload cardiac disease. Small rodents are less expensive and allow for larger sample sizes to be examined. Given the complexity of heart disease and the differences

between species, our findings need to be confirmed in larger mammals, such as dogs, pigs, and monkeys.

The signaling mechanism, by which TNF induces MMP expression and activation, and the contribution of NADPH-dependent $O_2^{\bullet-}$ should be investigated in depth. In the future, we may use TNF-receptor-deficient mice (TNF-R1$^{-/-}$ and TNF-R2$^{-/-}$) to investigate which TNF receptor is involved in the TNF-mediated adverse effects on the myocardium.

We did not measure circulating levels of TNF in WT-sham and WT-TAC mice to demonstrate TNF elevation and to confirm previous reports. In addition to cardiomyocytes and fibroblasts, TNF can be secreted by other cardiac cells such as smooth muscle cells or endothelial cells. Our *in vitro* studies did not include these cell types, though our *in vivo* findings may still reflect their contributions.

MMP-1 is an important collagenase in the human heart.[159] In our study, however, we could not examine the impact of TNF on this collagenase since small rodents (mice and rats) do not express MMP-1.[134] Other collagenases, such as MMP-8 and MMP-13 are the key collagenases found in rodent hearts.

4.8 Future Directions

Our aim is to examine the molecular mechanisms underlying cardiac hypertrophy, which is a major step in cardiac remodeling. Hypertrophy has been recapitulated *in vitro,* using primary isolated cardiomyocytes. In these models, hypertrophy is induced by stretch, or by Gq-protein-coupled receptor agonists,

such as angiotensin-ll, endothelin-1, or phenylephrine. Isolated cardiomyocytes, that are subjected to stretch, exhibit hypertrophic characteristics including increased protein synthesis and fetal gene expression by 48 hours.[323] This *in vitro* model could be used to simulate the TAC-induced alterations *in vivo.*

Likely, mechanical stress affects ion channels in the heart, but it remains to be determined whether or not the stretch-activated ion channels are the initial mechanosensors in stretch-induced cardiac remodeling in response to pressure overload. Stretch-activated ion channels have been suggested to directly interact with the cytoskeleton, thus, may intrinsically sense the cell stretch.[324] Opening of stretch-activated ion channels causes an increase in intracellular Ca^{2+}, since some of the channels are permeable to Ca^{2+}, and the influx causes Ca^{2+}-induced Ca^{2+} release.[325]

Preliminary data from our lab suggests enhanced fibrosis in wild-type TAC hearts and this fibrosis was partially inhibited in TNF knockout hearts in response to TAC. Fibrosis, which is the disproportionate accumulation of fibrillar collagen, is an integral feature of the remodeling seen in the failing heart. Accumulation of type I collagen, the main fibrillar collagen found in cardiac fibrosis, stiffens the ventricles and impedes both contraction and relaxation.[326] Fibrosis can also impair the electrical coupling of cardiomyocytes by separating cardiomyocytes from the ECM proteins.[327] Future studies could examine how increased pressure overload affects electric conduction in the heart.

Mechanical stress can also lead to hypertrophy, independently of neural or hormonal factors. For example, isolated hearts, in which the aortic pressure was elevated by perfusion, demonstrate increased protein synthesis.[328] Several candidates have been proposed as the sensors of these mechanical signals, including integrins and stretch-activated channels/ion exchangers.[329] Integrins, the primary mechanical sensors involved in hypertrophy, are heterodimeric transmembrane proteins that link the ECM to the actin cytoskeleton within the cell. In cardiomyocytes, these connections are made at the costameres, where z-discs are connected to the integrins. The costameres are rich in signaling molecules and are likely sites of mechanical sensing.[330] These signaling pathways could be explored in pressure overloaded cardiomyopathy, along with the role of TNF in these processes.

Other cardiac cell types that could contribute to cardiac remodeling in pressure overload cardiac disease need to be studied. Since peripheral vascular function is disturbed in patients with advanced heart failure,[331] the participation of endothelial cells in cardiac remodeling should also be investigated.

We intend to further study the participation of cells of the immune system in the process of cardiac remodeling. A modest increase in myocardial neutrophil density was noted after three days of TAC, though it did not reach statistical significance, and the density was markedly increased after seven days of TAC.[332] Cardiac mast cell degranulation has been shown to initiate MMP activation and subsequent myocardial fibrillar collagen degradation.[333] Further studies should be

conducted to investigate the participation of mast cells and other inflammatory cells in the progression of cardiac remodeling in a pressure overload cardiac disease and consider the involvement of TNF.

Other sources of $O_2^{\bullet-}$, such as xanthine oxidase, could contribute to cardiac remodeling, post-TAC. Xanthine oxidase results in the generation of $O_2^{\bullet-}$. Moreover, increased xanthine oxidase activity has been reported in congestive heart failure leading to increased oxidative stress and depressed myocardial contractile performance.[334] Several studies have reported that xanthine oxidase inhibition with allopurinol or oxypurinol can improve LV function in the failing heart,[335] prevent myocardial infarct-induced LV remodeling,[336] and reverse LV remodeling in animals with dilated cardiomyopathy.[337] The role of TNF in xanthine oxidase activation needs to be determined.

This study has clarified the downstream pathway of TNF in cardiomyopathies such as cardiac pressure overload and shown the different cardiac cellular contributions to TNF, NADPH-dependant $O_2^{\bullet-}$, and the MMP axis. Future studies should investigate the therapeutic effect of anti-TNF therapy, either alone or in combination with MMP inhibitors and anti-oxidants, in pressure overload-induced cardiac hypertrophy and failure. Etanercept is a soluble TNF receptor fusion protein,[338] and infliximab is a chimeric compound that recognizes human TNF.[339] Both of these agents block TNF activity by binding to circulating soluble TNF, to prevent it from interacting with its membrane-bound receptors to trigger a cellular response. The impact of anti-TNF therapy at an early time point

(2-weeks post-TAC) can be compared to later time points (10-weeks post-TAC). These results can also be compared to a combination therapy in which anti-TNF, anti-MMP (MMPi), and anti-oxidants are used. N-acteyl cysteine is a sulfhydryl group-containing amino acid believed to serve as a glutathione precursor, which can increase or sustain the production of this ROS scavenger. Furthermore, the administration of cysteine was shown to increase tissue levels of GSH[340], thus, possibly reducing ROS levels.[341] These approaches may be useful in reducing $O_2^{\bullet-}$ production in response to disease.

Chapter 5. References

1. Daviglus ML, Lloyd-Jones DM, Pirzada A. Preventing cardiovascular disease in the 21st century: therapeutic and preventive implications of current evidence. *Am J Cardiovasc Drugs.* 2006;6:87-101.

2. http://www.who.int/mediacentre/news/releases/pr72/en/index.html.

3. Lopez AD, Mathers CD, Ezzati M, Jamison DT, Murray CJ. Global and regional burden of disease and risk factors, 2001: systematic analysis of population health data. *Lancet.* 2006;367:1747-1757.

4. Pearson TA. Cardiovascular disease in developing countries: myths, realities, and opportunities. *Cardiovasc Drugs Ther.* 1999;13:95-104.

5. Kahn R, Robertson RM, Smith R, Eddy D. The impact of prevention on reducing the burden of cardiovascular disease. *Diabetes Care.* 2008;31:1686-1696.

6. http://www.cihr-irsc.gc.ca/e/28901.html.

7. Nabel EG. Cardiovascular disease. *N Engl J Med.* 2003;349:60-72.

8. Armstrong PW, Moe GW. Medical advances in the treatment of congestive heart failure. *Circulation.* 1993;88:2941-2952.

9. Jessup M, Brozena S. Heart failure. *N Engl J Med.* 2003;348:2007-2018.

10. Cohn JN, Ferrari R, Sharpe N. Cardiac remodeling--concepts and clinical implications: a consensus paper from an international forum on cardiac remodeling. *J Am Coll Cardiol.* 2000;35:569-582.

11. Ganau A, Devereux RB, Pickering TG, Roman MJ, Schnall PL, Santucci S, Spitzer MC, Laragh JH. Relation of left ventricular hemodynamic load and contractile performance to left ventricular mass in hypertension. *Circulation.* 1990;81:25-36.

12. Remme WJ. Pharmacological modulation of cardiovascular remodeling: a guide to heart failure therapy. *Cardiovasc Drugs Ther.* 2003;17:349-360.

13. Tang WH, Francis GS. Evolving concepts in left ventricular systolic and diastolic remodeling: implications for therapy. *Curr Cardiol Rep.* 2004;6:200-204.

14. Mann DL, Bristow MR. Mechanisms and models in heart failure: the biomechanical model and beyond. *Circulation.* 2005;111:2837-2849.

15. Hunter JJ, Chien KR. Signaling pathways for cardiac hypertrophy and failure. *N Engl J Med.* 1999;341:1276-1283.

16. Tardiff JC. Cardiac hypertrophy: stressing out the heart. *J Clin Invest.* 2006;116:1467-1470.

17. Heineke J, Molkentin JD. Regulation of cardiac hypertrophy by intracellular signalling pathways. *Nat Rev Mol Cell Biol.* 2006;7:589-600.

18. Lips DJ, deWindt LJ, van Kraaij DJ, Doevendans PA. Molecular determinants of myocardial hypertrophy and failure: alternative pathways for beneficial and maladaptive hypertrophy. *Eur Heart J.* 2003;24:883-896.

19. Russell B, Motlagh D, Ashley WW. Form follows function: how muscle shape is regulated by work. *J Appl Physiol.* 2000;88:1127-1132.

20. Mihl C, Dassen WR, Kuipers H. Cardiac remodelling: concentric versus eccentric hypertrophy in strength and endurance athletes. *Neth Heart J.* 2008;16:129-133.

21. Holycross BJ, Radin MJ. Cytokines in heart failure: potential interactions with angiotensin II and leptin. *Mol Interv.* 2002;2:424-427.

22. Gottdiener JS, Gay JA, Maron BJ, Fletcher RD. Increased right ventricular wall thickness in left ventricular pressure overload: echocardiographic determination of hypertrophic response of the "nonstressed" ventricle. *J Am Coll Cardiol.* 1985;6:550-555.

23. Chandrashekhar Y, Westaby S, Narula J. Mitral stenosis. *Lancet.* 2009;374:1271-1283.

24. Loya YS, Mashru MR, Patil RB, Karbhase JN, Sharma S. Isolated tricuspid stenosis: a case report with review of literature. *Indian Heart J.* 1989;41:270-273.

25. Bogaard HJ, Abe K, Vonk Noordegraaf A, Voelkel NF. The right ventricle under pressure: cellular and molecular mechanisms of right-heart failure in pulmonary hypertension. *Chest.* 2009;135:794-804.

26. Guilbert JJ. The world health report 2002 - reducing risks, promoting healthy life. *Educ Health (Abingdon).* 2003;16:230.

27. Kearney PM, Whelton M, Reynolds K, Muntner P, Whelton PK, He J. Global burden of hypertension: analysis of worldwide data. *Lancet.* 2005;365:217-223.

28. Phillips D. Aortic stenosis: A review. *American Association of Nurse Anesthetists Journal (AANA) J.* 2006;74:309-315.

29. Otto CM. Aortic stenosis. Clinical evaluation and optimal timing of surgery. *Cardiol Clin.* 1998;16:353-373, vii.

30. Chambers JB. Aortic stenosis. *Eur J Echocardiogr.* 2009;10:i11-19.

31. Frey N, Katus HA, Olson EN, Hill JA. Hypertrophy of the heart: a new therapeutic target? *Circulation.* 2004;109:1580-1589.

32. Omens JH, Miller TR, Covell JW. Relationship between passive tissue strain and collagen uncoiling during healing of infarcted myocardium. *Cardiovasc Res.* 1997;33:351-358.

33. Lee AA, Delhaas T, McCulloch AD, Villarreal FJ. Differential responses of adult cardiac fibroblasts to in vitro biaxial strain patterns. *J Mol Cell Cardiol.* 1999;31:1833-1843.

34. Sasayama S, Ross J, Jr., Franklin D, Bloor CM, Bishop S, Dilley RB. Adaptations of the left ventricle to chronic pressure overload. *Circ Res.* 1976;38:172-178.

35. Wikman-Coffelt J, Parmley WW, Mason DT. The cardiac hypertrophy process. Analyses of factors determining pathological vs. physiological development. *Circ Res.* 1979;45:697-707.

36. Briest W, Homagk L, Rassler B, Ziegelhoffer-Mihalovicova B, Meier H, Tannapfel A, Leiblein S, Saalbach A, Deten A, Zimmer HG. Norepinephrine-induced changes in cardiac transforming growth factor-beta isoform expression pattern of female and male rats. *Hypertension.* 2004;44:410-418.

37. Lim JY, Park SJ, Hwang HY, Park EJ, Nam JH, Kim J, Park SI. TGF-beta1 induces cardiac hypertrophic responses via PKC-dependent ATF-2 activation. *J Mol Cell Cardiol.* 2005;39:627-636.

38. Waeber B, Brunner HR. Cardiovascular hypertrophy: role of angiotensin II and bradykinin. *J Cardiovasc Pharmacol.* 1996;27 Suppl 2:S36-40.

39. Dhalla NS WJ. Role of protein kinase C and protein kinase A in heart function in health and disease. *Exp Clin Cardiol.* 1999;4:7–19.

40. Zhang W EV, Nijjar MS, Gupta SK, Dhalla NS. Role of mitogenactivated protein kinase in cardiac hypertrophy and heart failure. *Exp Clin Cardiol.* 2003;8:173–183.

41. Clerk A, Kemp TJ, Harrison JG, Pham FH, Sugden PH. Integration of protein kinase signaling pathways in cardiac myocytes: signaling to and from the extracellular signal-regulated kinases. *Adv Enzyme Regul.* 2004;44:233-248.

42. Clerk A, Sugden PH. Untangling the Web: specific signaling from PKC isoforms to MAPK cascades. *Circ Res.* 2001;89:847-849.

43. Bueno OF, De Windt LJ, Tymitz KM, Witt SA, Kimball TR, Klevitsky R, Hewett TE, Jones SP, Lefer DJ, Peng CF, Kitsis RN, Molkentin JD. The MEK1-ERK1/2 signaling pathway promotes compensated cardiac hypertrophy in transgenic mice. *EMBO J.* 2000;19:6341-6350.

44. Behr TM, Nerurkar SS, Nelson AH, Coatney RW, Woods TN, Sulpizio A, Chandra S, Brooks DP, Kumar S, Lee JC, Ohlstein EH, Angermann CE, Adams JL, Sisko J, Sackner-Bernstein JD, Willette RN. Hypertensive end-organ damage and premature mortality are p38 mitogen-activated protein kinase-dependent in a rat model of cardiac hypertrophy and dysfunction. *Circulation.* 2001;104:1292-1298.

45. Dhalla NS, Alto LE, Heyliger CE, Pierce GN, Panagia V, Singal PK. Sarcoplasmic reticular Ca2+-pump adaptation in cardiac hypertrophy due to pressure overload in pigs. *Eur Heart J.* 1984;5 Suppl F:323-328.

46. Mochly-Rosen D, Henrich CJ, Cheever L, Khaner H, Simpson PC. A protein kinase C isozyme is translocated to cytoskeletal elements on activation. *Cell Regul.* 1990;1:693-706.

47. Weber KT, Janicki JS, Shroff SG, Pick R, Chen RM, Bashey RI. Collagen remodeling of the pressure-overloaded, hypertrophied nonhuman primate myocardium. *Circ Res.* 1988;62:757-765.

48. Sun M, Chen M, Dawood F, Zurawska U, Li JY, Parker T, Kassiri Z, Kirshenbaum LA, Arnold M, Khokha R, Liu PP. Tumor necrosis factor-alpha mediates cardiac remodeling and ventricular dysfunction after pressure overload state. *Circulation.* 2007;115:1398-1407.

49. Lainchbury JG, Espiner EA, Frampton CM, Richards AM, Yandle TG, Nicholls MG. Cardiac natriuretic peptides as predictors of mortality. *J Intern Med.* 1997;241:257-259.

50. Anker SD, von Haehling S. Inflammatory mediators in chronic heart failure: an overview. *Heart.* 2004;90:464-470.

51. Biasucci LM, Vitelli A, Liuzzo G, Altamura S, Caligiuri G, Monaco C, Rebuzzi AG, Ciliberto G, Maseri A. Elevated levels of interleukin-6 in unstable angina. *Circulation.* 1996;94:874-877.

52. Latini R, Bianchi M, Correale E, Dinarello CA, Fantuzzi G, Fresco C, Maggioni AP, Mengozzi M, Romano S, Shapiro L, et al. Cytokines in acute myocardial infarction: selective increase in circulating tumor necrosis factor, its soluble receptor, and interleukin-1 receptor antagonist. *J Cardiovasc Pharmacol.* 1994;23:1-6.

53. Levine B, Kalman J, Mayer L, Fillit HM, Packer M. Elevated circulating levels of tumor necrosis factor in severe chronic heart failure. *N Engl J Med.* 1990;323:236-241.

54. Neumann FJ, Ott I, Gawaz M, Richardt G, Holzapfel H, Jochum M, Schomig A. Cardiac release of cytokines and inflammatory responses in acute myocardial infarction. *Circulation.* 1995;92:748-755.

55. Torre-Amione G, Kapadia S, Benedict C, Oral H, Young JB, Mann DL. Proinflammatory cytokine levels in patients with depressed left ventricular ejection fraction: a report from the Studies of Left Ventricular Dysfunction (SOLVD). *J Am Coll Cardiol.* 1996;27:1201-1206.

56. Torre-Amione G, Kapadia S, Lee J, Durand JB, Bies RD, Young JB, Mann DL. Tumor necrosis factor-alpha and tumor necrosis factor receptors in the failing human heart. *Circulation.* 1996;93:704-711.

57. Edmunds NJ, Lal H, Woodward B. Effects of tumour necrosis factor-alpha on left ventricular function in the rat isolated perfused heart: possible mechanisms for a decline in cardiac function. *Br J Pharmacol.* 1999;126:189-196.

58. Kapadia SR, Yakoob K, Nader S, Thomas JD, Mann DL, Griffin BP. Elevated circulating levels of serum tumor necrosis factor-alpha in patients with hemodynamically significant pressure and volume overload. *J Am Coll Cardiol.* 2000;36:208-212.

59. Kassiri Z, Oudit GY, Sanchez O, Dawood F, Mohammed FF, Nuttall RK, Edwards DR, Liu PP, Backx PH, Khokha R. Combination of tumor necrosis factor-alpha ablation and matrix metalloproteinase inhibition prevents heart failure after pressure overload in tissue inhibitor of metalloproteinase-3 knock-out mice. *Circ Res.* 2005;97:380-390.

60. Murdoch CE, Zhang M, Cave AC, Shah AM. NADPH oxidase-dependent redox signalling in cardiac hypertrophy, remodelling and failure. *Cardiovasc Res.* 2006;71:208-215.

61. Carswell EA, Old LJ, Kassel RL, Green S, Fiore N, Williamson B. An endotoxin-induced serum factor that causes necrosis of tumors. *Proc Natl Acad Sci U S A.* 1975;72:3666-3670.

62. Coelho AL, Hogaboam CM, Kunkel SL. Chemokines provide the sustained inflammatory bridge between innate and acquired immunity. *Cytokine Growth Factor Rev.* 2005;16:553-560.

63. Meldrum DR. Tumor necrosis factor in the heart. *Am J Physiol.* 1998;274:R577-595.

64. Ermert M, Pantazis C, Duncker HR, Grimminger F, Seeger W, Ermert L. In situ localization of TNFalpha/beta, TACE and TNF receptors TNF-R1 and TNF-R2 in control and LPS-treated lung tissue. *Cytokine.* 2003;22:89-100.

65. Jacobs M, Staufenberger S, Gergs U, Meuter K, Brandstatter K, Hafner M, Ertl G, Schorb W. Tumor necrosis factor-alpha at acute myocardial infarction in rats and effects on cardiac fibroblasts. *J Mol Cell Cardiol.* 1999;31:1949-1959.

66. Henriksen PA, Newby DE. Therapeutic inhibition of tumour necrosis factor alpha in patients with heart failure: cooling an inflamed heart. *Heart.* 2003;89:14-18.

67. Kapadia SR, Oral H, Lee J, Nakano M, Taffet GE, Mann DL. Hemodynamic regulation of tumor necrosis factor-alpha gene and protein expression in adult feline myocardium. *Circ Res.* 1997;81:187-195.

68. Kapadia S, Lee J, Torre-Amione G, Birdsall HH, Ma TS, Mann DL. Tumor necrosis factor-alpha gene and protein expression in adult feline myocardium after endotoxin administration. *J Clin Invest.* 1995;96:1042-1052.

69. Vassalli P, Grau GE, Piguet PF. TNF in autoimmune diseases, graft-versus-host reactions, and pulmonary fibrosis. *Immunol Ser.* 1992;56:409-430.

70. Black RA, Rauch CT, Kozlosky CJ, Peschon JJ, Slack JL, Wolfson MF, Castner BJ, Stocking KL, Reddy P, Srinivasan S, Nelson N, Boiani N, Schooley KA, Gerhart M, Davis R, Fitzner JN, Johnson RS, Paxton RJ,

March CJ, Cerretti DP. A metalloproteinase disintegrin that releases tumour-necrosis factor-alpha from cells. *Nature.* 1997;385:729-733.

71. Zheng Y, Saftig P, Hartmann D, Blobel C. Evaluation of the contribution of different ADAMs to tumor necrosis factor alpha (TNFalpha) shedding and of the function of the TNFalpha ectodomain in ensuring selective stimulated shedding by the TNFalpha convertase (TACE/ADAM17). *J Biol Chem.* 2004;279:42898-42906.

72. Mohammed FF, Smookler DS, Taylor SE, Fingleton B, Kassiri Z, Sanchez OH, English JL, Matrisian LM, Au B, Yeh WC, Khokha R. Abnormal TNF activity in Timp3-/- mice leads to chronic hepatic inflammation and failure of liver regeneration. *Nat Genet.* 2004;36:969-977.

73. Hurtado O, Cardenas A, Lizasoain I, Bosca L, Leza JC, Lorenzo P, Moro MA. Up-regulation of TNF-alpha convertase (TACE/ADAM17) after oxygen-glucose deprivation in rat forebrain slices. *Neuropharmacology.* 2001;40:1094-1102.

74. Goto T, Ishizaka A, Kobayashi F, Kohno M, Sawafuji M, Tasaka S, Ikeda E, Okada Y, Maruyama I, Kobayashi K. Importance of tumor necrosis factor-alpha cleavage process in post-transplantation lung injury in rats. *Am J Respir Crit Care Med.* 2004;170:1239-1246.

75. Reddy P, Slack JL, Davis R, Cerretti DP, Kozlosky CJ, Blanton RA, Shows D, Peschon JJ, Black RA. Functional analysis of the domain structure of tumor necrosis factor-alpha converting enzyme. *J Biol Chem.* 2000;275:14608-14614.

76. Peschon JJ, Slack JL, Reddy P, Stocking KL, Sunnarborg SW, Lee DC, Russell WE, Castner BJ, Johnson RS, Fitzner JN, Boyce RW, Nelson N, Kozlosky CJ, Wolfson MF, Rauch CT, Cerretti DP, Paxton RJ, March CJ, Black RA. An essential role for ectodomain shedding in mammalian development. *Science.* 1998;282:1281-1284.

77. Garton KJ, Gough PJ, Philalay J, Wille PT, Blobel CP, Whitehead RH, Dempsey PJ, Raines EW. Stimulated shedding of vascular cell adhesion molecule 1 (VCAM-1) is mediated by tumor necrosis factor-alpha-converting enzyme (ADAM 17). *J Biol Chem.* 2003;278:37459-37464.

78. Bolger AP, Anker SD. Tumour necrosis factor in chronic heart failure: a peripheral view on pathogenesis, clinical manifestations and therapeutic implications. *Drugs.* 2000;60:1245-1257.

79. Wang M, Crisostomo PR, Markel TA, Wang Y, Meldrum DR. Mechanisms of sex differences in TNFR2-mediated cardioprotection. *Circulation.* 2008;118:S38-45.

80. Grell M, Wajant H, Zimmermann G, Scheurich P. The type 1 receptor (CD120a) is the high-affinity receptor for soluble tumor necrosis factor. *Proc Natl Acad Sci U S A.* 1998;95:570-575.

81. Grell M, Douni E, Wajant H, Lohden M, Clauss M, Maxeiner B, Georgopoulos S, Lesslauer W, Kollias G, Pfizenmaier K, Scheurich P. The transmembrane form of tumor necrosis factor is the prime activating ligand of the 80 kDa tumor necrosis factor receptor. *Cell.* 1995;83:793-802.

82. Kawasaki H, Onuki R, Suyama E, Taira K. Identification of genes that function in the TNF-alpha-mediated apoptotic pathway using randomized hybrid ribozyme libraries. *Nat Biotechnol.* 2002;20:376-380.

83. Baud V, Karin M. Signal transduction by tumor necrosis factor and its relatives. *Trends Cell Biol.* 2001;11:372-377.

84. Hsu H, Xiong J, Goeddel DV. The TNF receptor 1-associated protein TRADD signals cell death and NF-kappa B activation. *Cell.* 1995;81:495-504.

85. Liu ZG, Hsu H, Goeddel DV, Karin M. Dissection of TNF receptor 1 effector functions: JNK activation is not linked to apoptosis while NF-kappaB activation prevents cell death. *Cell.* 1996;87:565-576.

86. Ben-Neriah Y. Regulatory functions of ubiquitination in the immune system. *Nat Immunol.* 2002;3:20-26.

87. Kuwano K, Hara N. Signal transduction pathways of apoptosis and inflammation induced by the tumor necrosis factor receptor family. *Am J Respir Cell Mol Biol.* 2000;22:147-149.

88. Xavier AM, Isowa N, Cai L, Dziak E, Opas M, McRitchie DI, Slutsky AS, Keshavjee SH, Liu M. Tumor necrosis factor-alpha mediates lipopolysaccharide-induced macrophage inflammatory protein-2 release from alveolar epithelial cells. Autoregulation in host defense. *Am J Respir Cell Mol Biol.* 1999;21:510-520.

89. Gaur U, Aggarwal BB. Regulation of proliferation, survival and apoptosis by members of the TNF superfamily. *Biochem Pharmacol.* 2003;66:1403-1408.

90. Chinnaiyan AM, Tepper CG, Seldin MF, O'Rourke K, Kischkel FC, Hellbardt S, Krammer PH, Peter ME, Dixit VM. FADD/MORT1 is a common mediator of CD95 (Fas/APO-1) and tumor necrosis factor receptor-induced apoptosis. *J Biol Chem.* 1996;271:4961-4965.

91. Lin Y, Devin A, Rodriguez Y, Liu ZG. Cleavage of the death domain kinase RIP by caspase-8 prompts TNF-induced apoptosis. *Genes Dev.* 1999;13:2514-2526.

92. Fesik SW. Insights into programmed cell death through structural biology. *Cell.* 2000;103:273-282.

93. Beltinger CP, White PS, Maris JM, Sulman EP, Jensen SJ, LePaslier D, Stallard BJ, Goeddel DV, de Sauvage FJ, Brodeur GM. Physical mapping and genomic structure of the human TNFR2 gene. *Genomics.* 1996;35:94-100.

94. von Haehling S, Jankowska EA, Anker SD. Tumour necrosis factor-alpha and the failing heart--pathophysiology and therapeutic implications. *Basic Res Cardiol.* 2004;99:18-28.

95. Millar AB, Foley NM, Singer M, Johnson NM, Meager A, Rook GA. Tumour necrosis factor in bronchopulmonary secretions of patients with adult respiratory distress syndrome. *Lancet.* 1989;2:712-714.

96. Krown KA, Page MT, Nguyen C, Zechner D, Gutierrez V, Comstock KL, Glembotski CC, Quintana PJ, Sabbadini RA. Tumor necrosis factor alpha-induced apoptosis in cardiac myocytes. Involvement of the sphingolipid signaling cascade in cardiac cell death. *J Clin Invest.* 1996;98:2854-2865.

97. Pagani FD, Baker LS, Hsi C, Knox M, Fink MP, Visner MS. Left ventricular systolic and diastolic dysfunction after infusion of tumor necrosis factor-alpha in conscious dogs. *J Clin Invest.* 1992;90:389-398.

98. Oliff A, Defeo-Jones D, Boyer M, Martinez D, Kiefer D, Vuocolo G, Wolfe A, Socher SH. Tumors secreting human TNF/cachectin induce cachexia in mice. *Cell.* 1987;50:555-563.

99. Chung IY, Benveniste EN. Tumor necrosis factor-alpha production by astrocytes. Induction by lipopolysaccharide, IFN-gamma, and IL-1 beta. *J Immunol.* 1990;144:2999-3007.

100. Pignatelli P, De Biase L, Lenti L, Tocci G, Brunelli A, Cangemi R, Riondino S, Grego S, Volpe M, Violi F. Tumor necrosis factor-alpha as trigger of platelet activation in patients with heart failure. *Blood.* 2005;106:1992-1994.

101. Karin M, Delhase M. The I kappa B kinase (IKK) and NF-kappa B: key elements of proinflammatory signalling. *Semin Immunol.* 2000;12:85-98.

102. Matsumori A, Yamada T, Suzuki H, Matoba Y, Sasayama S. Increased circulating cytokines in patients with myocarditis and cardiomyopathy. *Br Heart J.* 1994;72:561-566.

103. Herskowitz A, Choi S, Ansari AA, Wesselingh S. Cytokine mRNA expression in postischemic/reperfused myocardium. *Am J Pathol.* 1995;146:419-428.

104. Zhang M, Xu YJ, Saini HK, Turan B, Liu PP, Dhalla NS. TNF-alpha as a potential mediator of cardiac dysfunction due to intracellular Ca2+-overload. *Biochem Biophys Res Commun.* 2005;327:57-63.

105. Haudek SB, Taffet GE, Schneider MD, Mann DL. TNF provokes cardiomyocyte apoptosis and cardiac remodeling through activation of multiple cell death pathways. *J Clin Invest.* 2007;117:2692-2701.

106. Yao L, Huang K, Huang D, Wang J, Guo H, Liao Y. Acute myocardial infarction induced increases in plasma tumor necrosis factor-alpha and interleukin-10 are associated with the activation of poly(ADP-ribose) polymerase of circulating mononuclear cell. *Int J Cardiol.* 2008;123:366-368.

107. Berry MF, Woo YJ, Pirolli TJ, Bish LT, Moise MA, Burdick JW, Morine KJ, Jayasankar V, Gardner TJ, Sweeney HL. Administration of a tumor necrosis factor inhibitor at the time of myocardial infarction attenuates subsequent ventricular remodeling. *J Heart Lung Transplant.* 2004;23:1061-1068.

108. Petersen JW, Felker GM. Inflammatory biomarkers in heart failure. *Congest Heart Fail.* 2006;12:324-328.

109. Tracey D, Klareskog L, Sasso EH, Salfeld JG, Tak PP. Tumor necrosis factor antagonist mechanisms of action: a comprehensive review. *Pharmacol Ther.* 2008;117:244-279.

110. Chung ES, Packer M, Lo KH, Fasanmade AA, Willerson JT. Randomized, double-blind, placebo-controlled, pilot trial of infliximab, a chimeric monoclonal antibody to tumor necrosis factor-alpha, in patients with moderate-to-severe heart failure: results of the anti-TNF Therapy Against Congestive Heart Failure (ATTACH) trial. *Circulation.* 2003;107:3133-3140.

111. Mann DL, McMurray JJ, Packer M, Swedberg K, Borer JS, Colucci WS, Djian J, Drexler H, Feldman A, Kober L, Krum H, Liu P, Nieminen M, Tavazzi L, van Veldhuisen DJ, Waldenstrom A, Warren M, Westheim A, Zannad F, Fleming T. Targeted anticytokine therapy in patients with chronic heart failure: results of the Randomized Etanercept Worldwide Evaluation (RENEWAL). *Circulation.* 2004;109:1594-1602.

112. Jeron A, Hengstenberg C, Engel S, Lowel H, Riegger GA, Schunkert H, Holmer S. The D-allele of the ACE polymorphism is related to increased QT dispersion in 609 patients after myocardial infarction. *Eur Heart J.* 2001;22:663-668.

113. Wang BW, Hung HF, Chang H, Kuan P, Shyu KG. Mechanical stretch enhances the expression of resistin gene in cultured cardiomyocytes via tumor necrosis factor-alpha. *Am J Physiol Heart Circ Physiol.* 2007;293:H2305-2312.

114. Bryant D, Becker L, Richardson J, Shelton J, Franco F, Peshock R, Thompson M, Giroir B. Cardiac failure in transgenic mice with myocardial expression of tumor necrosis factor-alpha. *Circulation.* 1998;97:1375-1381.

115. Yokoyama T, Nakano M, Bednarczyk JL, McIntyre BW, Entman M, Mann DL. Tumor necrosis factor-alpha provokes a hypertrophic growth response in adult cardiac myocytes. *Circulation.* 1997;95:1247-1252.

116. Diwan A, Dibbs Z, Nemoto S, DeFreitas G, Carabello BA, Sivasubramanian N, Wilson EM, Spinale FG, Mann DL. Targeted overexpression of noncleavable and secreted forms of tumor necrosis factor provokes disparate cardiac phenotypes. *Circulation.* 2004;109:262-268.

117. Gross J, Lapiere CM. Collagenolytic activity in amphibian tissues: a tissue culture assay. *Proc Natl Acad Sci U S A.* 1962;48:1014-1022.

118. McCawley LJ, Matrisian LM. Matrix metalloproteinases: they're not just for matrix anymore! *Curr Opin Cell Biol.* 2001;13:534-540.

119. Schulz R. Intracellular targets of matrix metalloproteinase-2 in cardiac disease: rationale and therapeutic approaches. *Annu Rev Pharmacol Toxicol.* 2007;47:211-242.

120. Egeblad M, Werb Z. New functions for the matrix metalloproteinases in cancer progression. *Nat Rev Cancer.* 2002;2:161-174.

121. Del Bigio MR, Seyoum G. Effect of matrix metalloproteinase inhibitors on rat embryo development in vitro. *Cells Tissues Organs.* 1999;165:67-73.

122. Yoshimoto M, Itoh F, Yamamoto H, Hinoda Y, Imai K, Yachi A. Expression of MMP-7(PUMP-1) mRNA in human colorectal cancers. *Int J Cancer*. 1993;54:614-618.

123. Ozaki I, Mizuta T, Zhao G, Yotsumoto H, Hara T, Kajihara S, Hisatomi A, Sakai T, Yamamoto K. Involvement of the Ets-1 gene in overexpression of matrilysin in human hepatocellular carcinoma. *Cancer Res.* 2000;60:6519-6525.

124. Davies G, Jiang WG, Mason MD. Matrilysin mediates extracellular cleavage of E-cadherin from prostate cancer cells: a key mechanism in hepatocyte growth factor/scatter factor-induced cell-cell dissociation and in vitro invasion. *Clin Cancer Res.* 2001;7:3289-3297.

125. Masaki T, Matsuoka H, Sugiyama M, Abe N, Goto A, Sakamoto A, Atomi Y. Matrilysin (MMP-7) as a significant determinant of malignant potential of early invasive colorectal carcinomas. *Br J Cancer.* 2001;84:1317-1321.

126. Crawford HC, Scoggins CR, Washington MK, Matrisian LM, Leach SD. Matrix metalloproteinase-7 is expressed by pancreatic cancer precursors and regulates acinar-to-ductal metaplasia in exocrine pancreas. *J Clin Invest.* 2002;109:1437-1444.

127. Jiang WG, Davies G, Martin TA, Parr C, Watkins G, Mason MD, Mokbel K, Mansel RE. Targeting matrilysin and its impact on tumor growth in vivo: the potential implications in breast cancer therapy. *Clin Cancer Res.* 2005;11:6012-6019.

128. Agnihotri R, Crawford HC, Haro H, Matrisian LM, Havrda MC, Liaw L. Osteopontin, a novel substrate for matrix metalloproteinase-3 (stromelysin-1) and matrix metalloproteinase-7 (matrilysin). *J Biol Chem.* 2001;276:28261-28267.

129. McGuire JK, Li Q, Parks WC. Matrilysin (matrix metalloproteinase-7) mediates E-cadherin ectodomain shedding in injured lung epithelium. *Am J Pathol.* 2003;162:1831-1843.

130. Cheung PY, Sawicki G, Wozniak M, Wang W, Radomski MW, Schulz R. Matrix metalloproteinase-2 contributes to ischemia-reperfusion injury in the heart. *Circulation.* 2000;101:1833-1839.

131. Chua PK, Melish ME, Yu Q, Yanagihara R, Yamamoto KS, Nerurkar VR. Elevated levels of matrix metalloproteinase 9 and tissue inhibitor of metalloproteinase 1 during the acute phase of Kawasaki disease. *Clin Diagn Lab Immunol.* 2003;10:308-314.

132. Gavin PJ, Crawford SE, Shulman ST, Garcia FL, Rowley AH. Systemic arterial expression of matrix metalloproteinases 2 and 9 in acute Kawasaki disease. *Arterioscler Thromb Vasc Biol.* 2003;23:576-581.

133. Greene J, Wang M, Liu YE, Raymond LA, Rosen C, Shi YE. Molecular cloning and characterization of human tissue inhibitor of metalloproteinase 4. *J Biol Chem.* 1996;271:30375-30380.

134. Nuttall RK, Sampieri CL, Pennington CJ, Gill SE, Schultz GA, Edwards DR. Expression analysis of the entire MMP and TIMP gene families during mouse tissue development. *FEBS Lett.* 2004;563:129-134.

135. Young KA, Hennebold JD, Stouffer RL. Dynamic expression of mRNAs and proteins for matrix metalloproteinases and their tissue inhibitors in the primate corpus luteum during the menstrual cycle. *Mol Hum Reprod.* 2002;8:833-840.

136. Brew K, Dinakarpandian D, Nagase H. Tissue inhibitors of metalloproteinases: evolution, structure and function. *Biochim Biophys Acta.* 2000;1477:267-283.

137. Blavier L, Henriet P, Imren S, Declerck YA. Tissue inhibitors of matrix metalloproteinases in cancer. *Ann N Y Acad Sci.* 1999;878:108-119.

138. Goldberg GI, Strongin A, Collier IE, Genrich LT, Marmer BL. Interaction of 92-kDa type IV collagenase with the tissue inhibitor of metalloproteinases prevents dimerization, complex formation with interstitial collagenase, and activation of the proenzyme with stromelysin. *J Biol Chem.* 1992;267:4583-4591.

139. Gomez DE, Alonso DF, Yoshiji H, Thorgeirsson UP. Tissue inhibitors of metalloproteinases: structure, regulation and biological functions. *Eur J Cell Biol.* 1997;74:111-122.

140. Coghlan HC, Coghlan L. Cardiac architecture: Gothic versus Romanesque. A cardiologist's view. *Semin Thorac Cardiovasc Surg.* 2001;13:417-430.

141. Weber KT, Sun Y, Tyagi SC, Cleutjens JP. Collagen network of the myocardium: function, structural remodeling and regulatory mechanisms. *J Mol Cell Cardiol.* 1994;26:279-292.

142. Miner EC, Miller WL. A look between the cardiomyocytes: the extracellular matrix in heart failure. *Mayo Clin Proc.* 2006;81:71-76.

143. Chiquet M. Regulation of extracellular matrix gene expression by mechanical stress. *Matrix Biol.* 1999;18:417-426.

144. Burlew BS, Weber KT. Connective tissue and the heart. Functional significance and regulatory mechanisms. *Cardiol Clin.* 2000;18:435-442.

145. Weber KT, Sun Y, Katwa LC. Wound healing following myocardial infarction. *Clin Cardiol.* 1996;19:447-455.

146. Ross RS. Cardiac remodeling: is 8 the heart's lucky number? *J Mol Cell Cardiol.* 2004;36:323-326.

147. Cucoranu I, Clempus R, Dikalova A, Phelan PJ, Ariyan S, Dikalov S, Sorescu D. NAD(P)H oxidase 4 mediates transforming growth factor-beta1-induced differentiation of cardiac fibroblasts into myofibroblasts. *Circ Res.* 2005;97:900-907.

148. Spinale FG. Myocardial matrix remodeling and the matrix metalloproteinases: influence on cardiac form and function. *Physiol Rev.* 2007;87:1285-1342.

149. Powell WC, Matrisian LM. Complex roles of matrix metalloproteinases in tumor progression. *Curr Top Microbiol Immunol.* 1996;213 (Pt 1):1-21.

150. Visse R, Nagase H. Matrix metalloproteinases and tissue inhibitors of metalloproteinases: structure, function, and biochemistry. *Circ Res.* 2003;92:827-839.

151. Nagase H. Activation mechanisms of matrix metalloproteinases. *Biol Chem.* 1997;378:151-160.

152. Roeb E, Schleinkofer K, Kernebeck T, Potsch S, Jansen B, Behrmann I, Matern S, Grotzinger J. The matrix metalloproteinase 9 (mmp-9) hemopexin domain is a novel gelatin binding domain and acts as an antagonist. *J Biol Chem.* 2002;277:50326-50332.

153. Ohbayashi H. Matrix metalloproteinases in lung diseases. *Curr Protein Pept Sci.* 2002;3:409-421.

154. Pei D, Kang T, Qi H. Cysteine array matrix metalloproteinase (CA-MMP)/MMP-23 is a type II transmembrane matrix metalloproteinase regulated by a single cleavage for both secretion and activation. *J Biol Chem.* 2000;275:33988-33997.

155. Murphy G, Knauper V, Atkinson S, Butler G, English W, Hutton M, Stracke J, Clark I. Matrix metalloproteinases in arthritic disease. *Arthritis Res.* 2002;4 Suppl 3:S39-49.

156. Holmbeck K, Bianco P, Birkedal-Hansen H. MT1-mmp: a collagenase essential for tumor cell invasive growth. *Cancer Cell.* 2003;4:83-84.

157. Pei D, Weiss SJ. Transmembrane-deletion mutants of the membrane-type matrix metalloproteinase-1 process progelatinase A and express intrinsic matrix-degrading activity. *J Biol Chem.* 1996;271:9135-9140.

158. Steffensen B, Wallon UM, Overall CM. Extracellular matrix binding properties of recombinant fibronectin type II-like modules of human 72-kDa gelatinase/type IV collagenase. High affinity binding to native type I collagen but not native type IV collagen. *J Biol Chem.* 1995;270:11555-11566.

159. Nagase H, Woessner JF, Jr. Matrix metalloproteinases. *J Biol Chem.* 1999;274:21491-21494.

160. Armstrong AL, Barrach HJ, Ehrlich MG. Identification of the metalloproteinase stromelysin in the physis. *J Orthop Res.* 2002;20:289-294.

161. Reynolds JJ. Collagenases and tissue inhibitors of metalloproteinases: a functional balance in tissue degradation. *Oral Dis.* 1996;2:70-76.

162. Tomlinson ML, Garcia-Morales C, Abu-Elmagd M, Wheeler GN. Three matrix metalloproteinases are required in vivo for macrophage migration during embryonic development. *Mech Dev.* 2008;125:1059-1070.

163. Brauer PR. MMPs--role in cardiovascular development and disease. *Front Biosci.* 2006;11:447-478.

164. Tetley TD. Macrophages and the pathogenesis of COPD. *Chest.* 2002;121:156S-159S.

165. Finlay GA, O'Driscoll LR, Russell KJ, D'Arcy EM, Masterson JB, FitzGerald MX, O'Connor CM. Matrix metalloproteinase expression and production by alveolar macrophages in emphysema. *Am J Respir Crit Care Med.* 1997;156:240-247.

166. Shapiro SD, Senior RM. Matrix metalloproteinases. Matrix degradation and more. *Am J Respir Cell Mol Biol.* 1999;20:1100-1102.

167. Janicki JS, Brower GL, Henegar JR, Wang L. Ventricular remodeling in heart failure: the role of myocardial collagen. *Adv Exp Med Biol.* 1995;382:239-245.

168. Gunja-Smith Z, Morales AR, Romanelli R, Woessner JF, Jr. Remodeling of human myocardial collagen in idiopathic dilated cardiomyopathy. Role of metalloproteinases and pyridinoline cross-links. *Am J Pathol.* 1996;148:1639-1648.

169. Mujumdar VS, Smiley LM, Tyagi SC. Activation of matrix metalloproteinase dilates and decreases cardiac tensile strength. *Int J Cardiol.* 2001;79:277-286.

170. Kai H, Ikeda H, Yasukawa H, Kai M, Seki Y, Kuwahara F, Ueno T, Sugi K, Imaizumi T. Peripheral blood levels of matrix metalloproteases-2 and -9 are elevated in patients with acute coronary syndromes. *J Am Coll Cardiol.* 1998;32:368-372.

171. Weber KT, Pick R, Silver MA, Moe GW, Janicki JS, Zucker IH, Armstrong PW. Fibrillar collagen and remodeling of dilated canine left ventricle. *Circulation.* 1990;82:1387-1401.

172. Spinale FG, Coker ML, Thomas CV, Walker JD, Mukherjee R, Hebbar L. Time-dependent changes in matrix metalloproteinase activity and expression during the progression of congestive heart failure: relation to ventricular and myocyte function. *Circ Res.* 1998;82:482-495.

173. Coker ML, Thomas CV, Clair MJ, Hendrick JW, Krombach RS, Galis ZS, Spinale FG. Myocardial matrix metalloproteinase activity and abundance with congestive heart failure. *Am J Physiol.* 1998;274:H1516-1523.

174. Hayashidani S, Tsutsui H, Ikeuchi M, Shiomi T, Matsusaka H, Kubota T, Imanaka-Yoshida K, Itoh T, Takeshita A. Targeted deletion of MMP-2 attenuates early LV rupture and late remodeling after experimental myocardial infarction. *Am J Physiol.* 2003;285:H1229-1235.

175. Longo GM, Xiong W, Greiner TC, Zhao Y, Fiotti N, Baxter BT. Matrix metalloproteinases 2 and 9 work in concert to produce aortic aneurysms. *J Clin Invest.* 2002;110:625-632.

176. Romanic AM, Harrison SM, Bao W, Burns-Kurtis CL, Pickering S, Gu J, Grau E, Mao J, Sathe GM, Ohlstein EH, Yue TL. Myocardial protection from ischemia/reperfusion injury by targeted deletion of matrix metalloproteinase-9. *Cardiovasc Res.* 2002;54:549-558.

177. Johnson JL, George SJ, Newby AC, Jackson CL. Divergent effects of matrix metalloproteinases 3, 7, 9, and 12 on atherosclerotic plaque stability in mouse brachiocephalic arteries. *Proc Natl Acad Sci U S A.* 2005;102:15575-15580.

178. Deschamps AM, Spinale FG. Pathways of matrix metalloproteinase induction in heart failure: bioactive molecules and transcriptional regulation. *Cardiovasc Res.* 2006;69:666-676.

179. Van Wart HE, Birkedal-Hansen H. The cysteine switch: a principle of regulation of metalloproteinase activity with potential applicability to the entire matrix metalloproteinase gene family. *Proc Natl Acad Sci U S A.* 1990;87:5578-5582.

180. Woessner JF Jr NH. Activation of the zymogen forms of matrix metalloproteinases 2000.:72–86.

181. Ra HJ, Parks WC. Control of matrix metalloproteinase catalytic activity. *Matrix Biol.* 2007;26:587-596.

182. Nagase H, Visse R, Murphy G. Structure and function of matrix metalloproteinases and TIMPs. *Cardiovasc Res.* 2006;69:562-573.

183. Okamoto T, Akuta T, Tamura F, van Der Vliet A, Akaike T. Molecular mechanism for activation and regulation of matrix metalloproteinases during bacterial infections and respiratory inflammation. *Biol Chem.* 2004;385:997-1006.

184. Lambeth JD. NOX enzymes and the biology of reactive oxygen. *Nat Rev Immunol.* 2004;4:181-189.

185. Ghosh J, Myers CE. Inhibition of arachidonate 5-lipoxygenase triggers massive apoptosis in human prostate cancer cells. *Proc Natl Acad Sci U S A.* 1998;95:13182-13187.

186. Yin D, Yuan X, Brunk UT. Test-tube simulated lipofuscinogenesis. Effect of oxidative stress on autophagocytotic degradation. *Mech Ageing Dev.* 1995;81:37-50.

187. Juurlink BH. Response of glial cells to ischemia: roles of reactive oxygen species and glutathione. *Neurosci Biobehav Rev.* 1997;21:151-166.

188. Valko M, Morris H, Cronin MT. Metals, toxicity and oxidative stress. *Curr Med Chem.* 2005;12:1161-1208.

189. Pastor N, Weinstein H, Jamison E, Brenowitz M. A detailed interpretation of OH radical footprints in a TBP-DNA complex reveals the role of

dynamics in the mechanism of sequence-specific binding. *J Mol Biol.* 2000;304:55-68.

190. Valko M, Rhodes CJ, Moncol J, Izakovic M, Mazur M. Free radicals, metals and antioxidants in oxidative stress-induced cancer. *Chem Biol Interact.* 2006;160:1-40.

191. Moyna NM, Thompson PD. The effect of physical activity on endothelial function in man. *Acta Physiol Scand.* 2004;180:113-123.

192. Merenyi G, Lind J, Goldstein S, Czapski G. Peroxynitrous acid homolyzes into $OH^{\bullet}$ and $NO_2^{\bullet}$ radicals. *Chem Res Toxicol.* 1998;11:712-713.

193. Mates JM, Perez-Gomez C, Nunez de Castro I. Antioxidant enzymes and human diseases. *Clin Biochem.* 1999;32:595-603.

194. Ide T, Tsutsui H, Hayashidani S, Kang D, Suematsu N, Nakamura K, Utsumi H, Hamasaki N, Takeshita A. Mitochondrial DNA damage and dysfunction associated with oxidative stress in failing hearts after myocardial infarction. *Circ Res.* 2001;88:529-535.

195. Engberding N, Spiekermann S, Schaefer A, Heineke A, Wiencke A, Muller M, Fuchs M, Hilfiker-Kleiner D, Hornig B, Drexler H, Landmesser U. Allopurinol attenuates left ventricular remodeling and dysfunction after experimental myocardial infarction: a new action for an old drug? *Circulation.* 2004;110:2175-2179.

196. Landmesser U, Dikalov S, Price SR, McCann L, Fukai T, Holland SM, Mitch WE, Harrison DG. Oxidation of tetrahydrobiopterin leads to uncoupling of endothelial cell nitric oxide synthase in hypertension. *J Clin Invest.* 2003;111:1201-1209.

197. Turrens JF. Mitochondrial formation of reactive oxygen species. *J Physiol.* 2003;552:335-344.

198. Sawyer DB, Siwik DA, Xiao L, Pimentel DR, Singh K, Colucci WS. Role of oxidative stress in myocardial hypertrophy and failure. *J Mol Cell Cardiol.* 2002;34:379-388.

199. Ide T, Tsutsui H, Kinugawa S, Utsumi H, Kang D, Hattori N, Uchida K, Arimura K, Egashira K, Takeshita A. Mitochondrial electron transport complex I is a potential source of oxygen free radicals in the failing myocardium. *Circ Res.* 1999;85:357-363.

200. Suematsu N, Tsutsui H, Wen J, Kang D, Ikeuchi M, Ide T, Hayashidani S, Shiomi T, Kubota T, Hamasaki N, Takeshita A. Oxidative stress mediates

tumor necrosis factor-alpha-induced mitochondrial DNA damage and dysfunction in cardiac myocytes. *Circulation.* 2003;107:1418-1423.

201. Lehoux S. Redox signalling in vascular responses to shear and stretch. *Cardiovasc Res.* 2006;71:269-279.

202. McMurray J, Chopra M, Abdullah I, Smith WE, Dargie HJ. Evidence of oxidative stress in chronic heart failure in humans. *Eur Heart J.* 1993;14:1493-1498.

203. Mallat Z, Philip I, Lebret M, Chatel D, Maclouf J, Tedgui A. Elevated levels of 8-iso-prostaglandin F2alpha in pericardial fluid of patients with heart failure: a potential role for in vivo oxidant stress in ventricular dilatation and progression to heart failure. *Circulation.* 1998;97:1536-1539.

204. Sia YT, Lapointe N, Parker TG, Tsoporis JN, Deschepper CF, Calderone A, Pourdjabbar A, Jasmin JF, Sarrazin JF, Liu P, Adam A, Butany J, Rouleau JL. Beneficial effects of long-term use of the antioxidant probucol in heart failure in the rat. *Circulation.* 2002;105:2549-2555.

205. Shiomi T, Tsutsui H, Matsusaka H, Murakami K, Hayashidani S, Ikeuchi M, Wen J, Kubota T, Utsumi H, Takeshita A. Overexpression of glutathione peroxidase prevents left ventricular remodeling and failure after myocardial infarction in mice. *Circulation.* 2004;109:544-549.

206. Keith M, Geranmayegan A, Sole MJ, Kurian R, Robinson A, Omran AS, Jeejeebhoy KN. Increased oxidative stress in patients with congestive heart failure. *J Am Coll Cardiol.* 1998;31:1352-1356.

207. Ghatak A, Brar MJ, Agarwal A, Goel N, Rastogi AK, Vaish AK, Sircar AR, Chandra M. Oxy free radical system in heart failure and therapeutic role of oral vitamin E. *Int J Cardiol.* 1996;57:119-127.

208. Korantzopoulos P, Galaris D, Papaioannides D, Siogas K. The possible role of oxidative stress in heart failure and the potential of antioxidant intervention. *Med Sci Monit.* 2003;9:RA120-125.

209. Ellis EA, Grant MB, Murray FT, Wachowski MB, Guberski DL, Kubilis PS, Lutty GA. Increased NADH oxidase activity in the retina of the BBZ/Wor diabetic rat. *Free Radic Biol Med.* 1998;24:111-120.

210. Ruef J, Hu ZY, Yin LY, Wu Y, Hanson SR, Kelly AB, Harker LA, Rao GN, Runge MS, Patterson C. Induction of vascular endothelial growth factor in balloon-injured baboon arteries. A novel role for reactive oxygen species in atherosclerosis. *Circ Res.* 1997;81:24-33.

211. Ushio-Fukai M, Alexander RW. Reactive oxygen species as mediators of angiogenesis signaling: role of NAD(P)H oxidase. *Mol Cell Biochem.* 2004;264:85-97.

212. Kwon SH, Pimentel DR, Remondino A, Sawyer DB, Colucci WS. H(2)O(2) regulates cardiac myocyte phenotype via concentration-dependent activation of distinct kinase pathways. *J Mol Cell Cardiol.* 2003;35:615-621.

213. Date MO, Morita T, Yamashita N, Nishida K, Yamaguchi O, Higuchi Y, Hirotani S, Matsumura Y, Hori M, Tada M, Otsu K. The antioxidant N-2-mercaptopropionyl glycine attenuates left ventricular hypertrophy in in vivo murine pressure-overload model. *J Am Coll Cardiol.* 2002;39:907-912.

214. Higuchi Y, Otsu K, Nishida K, Hirotani S, Nakayama H, Yamaguchi O, Matsumura Y, Ueno H, Tada M, Hori M. Involvement of reactive oxygen species-mediated NF-kappa B activation in TNF-alpha-induced cardiomyocyte hypertrophy. *J Mol Cell Cardiol.* 2002;34:233-240.

215. Pimentel DR, Amin JK, Xiao L, Miller T, Viereck J, Oliver-Krasinski J, Baliga R, Wang J, Siwik DA, Singh K, Pagano P, Colucci WS, Sawyer DB. Reactive oxygen species mediate amplitude-dependent hypertrophic and apoptotic responses to mechanical stretch in cardiac myocytes. *Circ Res.* 2001;89:453-460.

216. Hsu TC, Young MR, Cmarik J, Colburn NH. Activator protein 1 (AP-1)- and nuclear factor kappaB (NF-kappaB)-dependent transcriptional events in carcinogenesis. *Free Radic Biol Med.* 2000;28:1338-1348.

217. Bains JS, Potyok A, Ferguson AV. Angiotensin II actions in paraventricular nucleus: functional evidence for neurotransmitter role in efferents originating in subfornical organ. *Brain Res.* 1992;599:223-229.

218. Lassegue B, Sorescu D, Szocs K, Yin Q, Akers M, Zhang Y, Grant SL, Lambeth JD, Griendling KK. Novel gp91(phox) homologues in vascular smooth muscle cells : NOX1 mediates angiotensin II-induced superoxide formation and redox-sensitive signaling pathways. *Circ Res.* 2001;88:888-894.

219. von Harsdorf R, Li PF, Dietz R. Signaling pathways in reactive oxygen species-induced cardiomyocyte apoptosis. *Circulation.* 1999;99:2934-2941.

220. Sabri A, Hughie HH, Lucchesi PA. Regulation of hypertrophic and apoptotic signaling pathways by reactive oxygen species in cardiac myocytes. *Antioxid Redox Signal.* 2003;5:731-740.

221. Rathore N, John S, Kale M, Bhatnagar D. Lipid peroxidation and antioxidant enzymes in isoproterenol induced oxidative stress in rat tissues. *Pharmacol Res.* 1998;38:297-303.

222. Lockwood TD. Redox control of protein degradation. *Antioxid Redox Signal.* 2000;2:851-878.

223. Konat GW. H2O2-induced higher order chromatin degradation: a novel mechanism of oxidative genotoxicity. *J Biosci.* 2003;28:57-60.

224. Wang M, Dhingra K, Hittelman WN, Liehr JG, de Andrade M, Li D. Lipid peroxidation-induced putative malondialdehyde-DNA adducts in human breast tissues. *Cancer Epidemiol Biomarkers Prev.* 1996;5:705-710.

225. Stadtman ER. Protein oxidation and aging. *Free Radic Res.* 2006;40:1250-1258.

226. Cave AC, Brewer AC, Narayanapanicker A, Ray R, Grieve DJ, Walker S, Shah AM. NADPH oxidases in cardiovascular health and disease. *Antioxid Redox Signal.* 2006;8:691-728.

227. Xiao L, Pimentel DR, Wang J, Singh K, Colucci WS, Sawyer DB. Role of reactive oxygen species and NAD(P)H oxidase in alpha(1)-adrenoceptor signaling in adult rat cardiac myocytes. *Am J Physiol Cell Physiol.* 2002;282:C926-934.

228. Wenzel S, Taimor G, Piper HM, Schluter KD. Redox-sensitive intermediates mediate angiotensin II-induced p38 MAP kinase activation, AP-1 binding activity, and TGF-beta expression in adult ventricular cardiomyocytes. *FASEB J.* 2001;15:2291-2293.

229. Higuchi Y, Otsu K, Nishida K, Hirotani S, Nakayama H, Yamaguchi O, Hikoso S, Kashiwase K, Takeda T, Watanabe T, Mano T, Matsumura Y, Ueno H, Hori M. The small GTP-binding protein Rac1 induces cardiac myocyte hypertrophy through the activation of apoptosis signal-regulating kinase 1 and nuclear factor-kappa B. *J Biol Chem.* 2003;278:20770-20777.

230. Nadruz W, Jr., Lagosta VJ, Moreno H, Jr., Coelho OR, Franchini KG. Simvastatin prevents load-induced protein tyrosine nitration in overloaded hearts. *Hypertension.* 2004;43:1060-1066.

231. Heymes C, Bendall JK, Ratajczak P, Cave AC, Samuel JL, Hasenfuss G, Shah AM. Increased myocardial NADPH oxidase activity in human heart failure. *J Am Coll Cardiol.* 2003;41:2164-2171.

232. MacCarthy PA, Grieve DJ, Li JM, Dunster C, Kelly FJ, Shah AM. Impaired endothelial regulation of ventricular relaxation in cardiac hypertrophy: role of reactive oxygen species and NADPH oxidase. *Circulation.* 2001;104:2967-2974.

233. Rey FE, Pagano PJ. The reactive adventitia: fibroblast oxidase in vascular function. *Arterioscler Thromb Vasc Biol.* 2002;22:1962-1971.

234. Satoh M, Ogita H, Takeshita K, Mukai Y, Kwiatkowski DJ, Liao JK. Requirement of Rac1 in the development of cardiac hypertrophy. *Proc Natl Acad Sci U S A.* 2006;103:7432-7437.

235. Pagano PJ, Clark JK, Cifuentes-Pagano ME, Clark SM, Callis GM, Quinn MT. Localization of a constitutively active, phagocyte-like NADPH oxidase in rabbit aortic adventitia: enhancement by angiotensin II. *Proc Natl Acad Sci U S A.* 1997;94:14483-14488.

236. Dworakowski R, Anilkumar N, Zhang M, Shah AM. Redox signalling involving NADPH oxidase-derived reactive oxygen species. *Biochem Soc Trans.* 2006;34:960-964.

237. Li JM, Shah AM. Mechanism of endothelial cell NADPH oxidase activation by angiotensin II. Role of the p47phox subunit. *J Biol Chem.* 2003;278:12094-12100.

238. Ushio-Fukai M, Tang Y, Fukai T, Dikalov SI, Ma Y, Fujimoto M, Quinn MT, Pagano PJ, Johnson C, Alexander RW. Novel role of gp91(phox)-containing NAD(P)H oxidase in vascular endothelial growth factor-induced signaling and angiogenesis. *Circ Res.* 2002;91:1160-1167.

239. Frey RS, Rahman A, Kefer JC, Minshall RD, Malik AB. PKCzeta regulates TNF-alpha-induced activation of NADPH oxidase in endothelial cells. *Circ Res.* 2002;90:1012-1019.

240. Hwang J, Ing MH, Salazar A, Lassegue B, Griendling K, Navab M, Sevanian A, Hsiai TK. Pulsatile versus oscillatory shear stress regulates NADPH oxidase subunit expression: implication for native LDL oxidation. *Circ Res.* 2003;93:1225-1232.

241. Sumimoto H, Miyano K, Takeya R. Molecular composition and regulation of the Nox family NAD(P)H oxidases. *Biochem Biophys Res Commun.* 2005;338:677-686.

242. Bokoch GM, Diebold BA. Current molecular models for NADPH oxidase regulation by Rac GTPase. *Blood.* 2002;100:2692-2696.

243. Miller AA, Drummond GR, De Silva TM, Mast AE, Hickey H, Williams JP, Broughton BR, Sobey CG. NADPH oxidase activity is higher in cerebral versus systemic arteries of four animal species: role of Nox2. *Am J Physiol Heart Circ Physiol.* 2009;296:H220-225.

244. Al-Mehdi AB, Shuman H, Fisher AB. Intracellular generation of reactive oxygen species during nonhypoxic lung ischemia. *Am J Physiol.* 1997;272:L294-300.

245. Hall ED, Detloff MR, Johnson K, Kupina NC. Peroxynitrite-mediated protein nitration and lipid peroxidation in a mouse model of traumatic brain injury. *J Neurotrauma.* 2004;21:9-20.

246. Giustarini D, Dalle-Donne I, Colombo R, Milzani A, Rossi R. Adaptation of the Griess reaction for detection of nitrite in human plasma. *Free Radic Res.* 2004;38:1235-1240.

247. Pacher P, Beckman JS, Liaudet L. Nitric oxide and peroxynitrite in health and disease. *Physiol Rev.* 2007;87:315-424.

248. Takeda T, Nabae T, Kassab G, Liu J, Mittal RK. Oesophageal wall stretch: the stimulus for distension induced oesophageal sensation. *Neurogastroenterol Motil.* 2004;16:721-728.

249. Schimrosczyk K, Song YH, Vykoukal J, Vykoukal D, Bai X, Krohn A, Freyberg S, Alt EU. Liposome-mediated transfection with extract from neonatal rat cardiomyocytes induces transdifferentiation of human adipose-derived stem cells into cardiomyocytes. *Scand J Clin Lab Invest.* 2008;68:464-472.

250. van der Heide SM, Joosten BJ, Dragt BS, Everts ME, Klaren PH. A physiological role for glucuronidated thyroid hormones: preferential uptake by H9c2(2-1) myotubes. *Mol Cell Endocrinol.* 2007;264:109-117.

251. Ilan N, Cheung L, Pinter E, Madri JA. Platelet-endothelial cell adhesion molecule-1 (CD31), a scaffolding molecule for selected catenin family members whose binding is mediated by different tyrosine and serine/threonine phosphorylation. *J Biol Chem.* 2000;275:21435-21443.

252. Arakawa E, Hasegawa K, Irie J, Ide S, Ushiki J, Yamaguchi K, Oda S, Matsuda Y. L-ascorbic acid stimulates expression of smooth muscle-specific markers in smooth muscle cells both in vitro and in vivo. *J Cardiovasc Pharmacol.* 2003;42:745-751.

253. Hamawaki M, Coffman TM, Lashus A, Koide M, Zile MR, Oliverio MI, DeFreyte G, Cooper Gt, Carabello BA. Pressure-overload hypertrophy is unabated in mice devoid of AT1A receptors. *Am J Physiol.* 1998;274:H868-873.

254. Nakamura A, Rokosh DG, Paccanaro M, Yee RR, Simpson PC, Grossman W, Foster E. LV systolic performance improves with development of hypertrophy after transverse aortic constriction in mice. *Am J Physiol Heart Circ Physiol.* 2001;281:H1104-1112.

255. Sadoshima J, Montagne O, Wang Q, Yang G, Warden J, Liu J, Takagi G, Karoor V, Hong C, Johnson GL, Vatner DE, Vatner SF. The MEKK1-JNK pathway plays a protective role in pressure overload but does not mediate cardiac hypertrophy. *J Clin Invest.* 2002;110:271-279.

256. Henderson BC, Sen U, Reynolds C, Moshal KS, Ovechkin A, Tyagi N, Kartha GK, Rodriguez WE, Tyagi SC. Reversal of systemic hypertension-associated cardiac remodeling in chronic pressure overload myocardium by ciglitazone. *Int J Biol Sci.* 2007;3:385-392.

257. Rockman HA, Ross RS, Harris AN, Knowlton KU, Steinhelper ME, Field LJ, Ross J, Jr., Chien KR. Segregation of atrial-specific and inducible expression of an atrial natriuretic factor transgene in an in vivo murine model of cardiac hypertrophy. *Proc Natl Acad Sci U S A.* 1991;88:8277-8281.

258. Patten RD, Hall-Porter MR. Small animal models of heart failure: development of novel therapies, past and present. *Circ Heart Fail.* 2009;2:138-144.

259. Zemljic-Harpf AE, Ponrartana S, Avalos RT, Jordan MC, Roos KP, Dalton ND, Phan VQ, Adamson ED, Ross RS. Heterozygous inactivation of the vinculin gene predisposes to stress-induced cardiomyopathy. *Am J Pathol.* 2004;165:1033-1044.

260. Sun M, Dawood F, Wen WH, Chen M, Dixon I, Kirshenbaum LA, Liu PP. Excessive tumor necrosis factor activation after infarction contributes to susceptibility of myocardial rupture and left ventricular dysfunction. *Circulation.* 2004;110:3221-3228.

261. Graham HK, Horn M, Trafford AW. Extracellular matrix profiles in the progression to heart failure. European Young Physiologists Symposium Keynote Lecture-Bratislava 2007. *Acta Physiol (Oxf).* 2008;194:3-21.

262. Kassiri Z, Khokha R. Myocardial extra-cellular matrix and its regulation by metalloproteinases and their inhibitors. *Thromb Haemost.* 2005;93:212-219.

263. Li YY, Feng YQ, Kadokami T, McTiernan CF, Draviam R, Watkins SC, Feldman AM. Myocardial extracellular matrix remodeling in transgenic mice overexpressing tumor necrosis factor alpha can be modulated by anti-tumor necrosis factor alpha therapy. *Proc Natl Acad Sci U S A.* 2000;97:12746-12751.

264. Li YY, Kadokami T, Wang P, McTiernan CF, Feldman AM. MMP inhibition modulates TNF-alpha transgenic mouse phenotype early in the development of heart failure. *Am J Physiol Heart Circ Physiol.* 2002;282:H983-989.

265. Cross AR, Jones OT. The effect of the inhibitor diphenylene iodonium on the superoxide-generating system of neutrophils. Specific labelling of a component polypeptide of the oxidase. *Biochem J.* 1986;237:111-116.

266. Kono H, Rusyn I, Uesugi T, Yamashina S, Connor HD, Dikalova A, Mason RP, Thurman RG. Diphenyleneiodonium sulfate, an NADPH oxidase inhibitor, prevents early alcohol-induced liver injury in the rat. *Am J Physiol Gastrointest Liver Physiol.* 2001;280:G1005-1012.

267. Hill MF, Singal PK. Antioxidant and oxidative stress changes during heart failure subsequent to myocardial infarction in rats. *Am J Pathol.* 1996;148:291-300.

268. Olivetti G, Capasso JM, Sonnenblick EH, Anversa P. Side-to-side slippage of myocytes participates in ventricular wall remodeling acutely after myocardial infarction in rats. *Circ Res.* 1990;67:23-34.

269. Dhalla AK, Hill MF, Singal PK. Role of oxidative stress in transition of hypertrophy to heart failure. *J Am Coll Cardiol.* 1996;28:506-514.

270. Nakamura R, Egashira K, Machida Y, Hayashidani S, Takeya M, Utsumi H, Tsutsui H, Takeshita A. Probucol attenuates left ventricular dysfunction and remodeling in tachycardia-induced heart failure: roles of oxidative stress and inflammation. *Circulation.* 2002;106:362-367.

271. Sethi R, Takeda N, Nagano M, Dhalla NS. Beneficial effects of vitamin E treatment in acute myocardial infarction. *J Cardiovasc Pharmacol Ther.* 2000;5:51-58.

272. Vandenbroucke E, Mehta D, Minshall R, Malik AB. Regulation of endothelial junctional permeability. *Ann N Y Acad Sci.* 2008;1123:134-145.

273. Gao X, Zhang H, Belmadani S, Wu J, Xu X, Elford H, Potter BJ, Zhang C. Role of TNF-alpha-induced reactive oxygen species in endothelial dysfunction during reperfusion injury. *Am J Physiol Heart Circ Physiol.* 2008;295:H2242-2249.

274. Li JM, Fan LM, Christie MR, Shah AM. Acute tumor necrosis factor alpha signaling via NADPH oxidase in microvascular endothelial cells: role of p47phox phosphorylation and binding to TRAF4. *Mol Cell Biol.* 2005;25:2320-2330.

275. Dhingra S, Sharma AK, Singla DK, Singal PK. p38 and ERK1/2 MAPKs mediate the interplay of TNF-alpha and IL-10 in regulating oxidative stress and cardiac myocyte apoptosis. *Am J Physiol Heart Circ Physiol.* 2007;293:H3524-3531.

276. Maenpaa CJ, Shames BD, Van Why SK, Johnson CP, Nilakantan V. Oxidant-mediated apoptosis in proximal tubular epithelial cells following ATP depletion and recovery. *Free Radic Biol Med.* 2008;44:518-526.

277. Basuroy S, Bhattacharya S, Leffler CW, Parfenova H. Nox4 NADPH oxidase mediates oxidative stress and apoptosis caused by TNF-alpha in cerebral vascular endothelial cells. *Am J Physiol Cell Physiol.* 2009;296:C422-432.

278. Huang J, Min Lu M, Cheng L, Yuan LJ, Zhu X, Stout AL, Chen M, Li J, Parmacek MS. Myocardin is required for cardiomyocyte survival and maintenance of heart function. *Proc Natl Acad Sci U S A.* 2009;106:18734-18739.

279. Stehle R, Iorga B. Kinetics of cardiac sarcomeric processes and rate-limiting steps in contraction and relaxation. *J Mol Cell Cardiol*. 2010;(in press).

280. Yang J, Wang HD, Lu DX, Wang YP, Qi RB, Li J, Li F, Li CJ. Effects of neutral sulfate berberine on LPS-induced cardiomyocyte TNF-alpha secretion, abnormal calcium cycling, and cardiac dysfunction in rats. *Acta Pharmacol Sin.* 2006;27:173-178.

281. Rossi MA. Pathologic fibrosis and connective tissue matrix in left ventricular hypertrophy due to chronic arterial hypertension in humans. *J Hypertens.* 1998;16:1031-1041.

282. Brilla CG, Funck RC, Rupp H. Lisinopril-mediated regression of myocardial fibrosis in patients with hypertensive heart disease. *Circulation.* 2000;102:1388-1393.

283. Eghbali M, Czaja MJ, Zeydel M, Weiner FR, Zern MA, Seifter S, Blumenfeld OO. Collagen chain mRNAs in isolated heart cells from young and adult rats. *J Mol Cell Cardiol.* 1988;20:267-276.

284. Eghbali M, Blumenfeld OO, Seifter S, Buttrick PM, Leinwand LA, Robinson TF, Zern MA, Giambrone MA. Localization of types I, III and IV collagen mRNAs in rat heart cells by in situ hybridization. *J Mol Cell Cardiol.* 1989;21:103-113.

285. Yue P, Massie BM, Simpson PC, Long CS. Cytokine expression increases in nonmyocytes from rats with postinfarction heart failure. *Am J Physiol.* 1998;275:H250-258.

286. Deten A, Volz HC, Briest W, Zimmer HG. Cardiac cytokine expression is upregulated in the acute phase after myocardial infarction. Experimental studies in rats. *Cardiovasc Res.* 2002;55:329-340.

287. Leicht M, Greipel N, Zimmer H. Comitogenic effect of catecholamines on rat cardiac fibroblasts in culture. *Cardiovasc Res.* 2000;48:274-284.

288. Zimmet JM, Hare JM. Nitroso-redox interactions in the cardiovascular system. *Circulation.* 2006;114:1531-1544.

289. Murray J, Taylor SW, Zhang B, Ghosh SS, Capaldi RA. Oxidative damage to mitochondrial complex I due to peroxynitrite: identification of reactive tyrosines by mass spectrometry. *J Biol Chem.* 2003;278:37223-37230.

290. Okamoto T, Akaike T, Nagano T, Miyajima S, Suga M, Ando M, Ichimori K, Maeda H. Activation of human neutrophil procollagenase by nitrogen dioxide and peroxynitrite: a novel mechanism for procollagenase activation involving nitric oxide. *Arch Biochem Biophys.* 1997;342:261-274.

291. Viappiani S, Nicolescu AC, Holt A, Sawicki G, Crawford BD, Leon H, van Mulligen T, Schulz R. Activation and modulation of 72kDa matrix metalloproteinase-2 by peroxynitrite and glutathione. *Biochem Pharmacol.* 2009;77:826-834.

292. Sampieri CL, Nuttall RK, Young DA, Goldspink D, Clark IM, Edwards DR. Activation of p38 and JNK MAPK pathways abrogates requirement

for new protein synthesis for phorbol ester mediated induction of select MMP and TIMP genes. *Matrix Biol.* 2008;27:128-138.

293. Siwik DA, Colucci WS. Regulation of matrix metalloproteinases by cytokines and reactive oxygen/nitrogen species in the myocardium. *Heart Fail Rev.* 2004;9:43-51.

294. Tyagi SC, Ratajska A, Weber KT. Myocardial matrix metalloproteinase(s): localization and activation. *Mol Cell Biochem.* 1993;126:49-59.

295. Tyagi SC, Kumar S, Borders S. Reduction-oxidation (redox) state regulation of extracellular matrix metalloproteinases and tissue inhibitors in cardiac normal and transformed fibroblast cells. *J Cell Biochem.* 1996;61:139-151.

296. Clark IM, Swingler TE, Sampieri CL, Edwards DR. The regulation of matrix metalloproteinases and their inhibitors. *Int J Biochem Cell Biol.* 2008;40:1362-1378.

297. Yan C, Boyd DD. Regulation of matrix metalloproteinase gene expression. *J Cell Physiol.* 2007;211:19-26.

298. Clerk A, Cullingford TE, Fuller SJ, Giraldo A, Markou T, Pikkarainen S, Sugden PH. Signaling pathways mediating cardiac myocyte gene expression in physiological and stress responses. *J Cell Physiol.* 2007;212:311-322.

299. Fischer P, Hilfiker-Kleiner D. Survival pathways in hypertrophy and heart failure: the gp130-STAT axis. *Basic Res Cardiol.* 2007;102:393-411.

300. Moorjani N, Westaby S, Narula J, Catarino PA, Brittin R, Kemp TJ, Narula N, Sugden PH. Effects of left ventricular volume overload on mitochondrial and death-receptor-mediated apoptotic pathways in the transition to heart failure. *Am J Cardiol.* 2009;103:1261-1268.

301. Luchtefeld M, Grote K, Grothusen C, Bley S, Bandlow N, Selle T, Struber M, Haverich A, Bavendiek U, Drexler H, Schieffer B. Angiotensin II induces MMP-2 in a p47phox-dependent manner. *Biochem Biophys Res Commun.* 2005;328:183-188.

302. Bian J, Sun Y. Transcriptional activation by p53 of the human type IV collagenase (gelatinase A or matrix metalloproteinase 2) promoter. *Mol Cell Biol.* 1997;17:6330-6338.

303. Yan C, Wang H, Boyd DD. ATF3 represses 72-kDa type IV collagenase (MMP-2) expression by antagonizing p53-dependent trans-activation of the collagenase promoter. *J Biol Chem.* 2002;277:10804-10812.

304. Xie TX, Wei D, Liu M, Gao AC, Ali-Osman F, Sawaya R, Huang S. Stat3 activation regulates the expression of matrix metalloproteinase-2 and tumor invasion and metastasis. *Oncogene.* 2004;23:3550-3560.

305. En-Nia A, Reisdorff J, Stefanidis I, Floege J, Heinrich PC, Mertens PR. Mesangial cell gelatinase A synthesis is attenuated by oscillating hyperbaric pressure. *Biochem J.* 2002;362:693-700.

306. Heymans S, Schroen B, Vermeersch P, Milting H, Gao F, Kassner A, Gillijns H, Herijgers P, Flameng W, Carmeliet P, Van de Werf F, Pinto YM, Janssens S. Increased cardiac expression of tissue inhibitor of metalloproteinase-1 and tissue inhibitor of metalloproteinase-2 is related to cardiac fibrosis and dysfunction in the chronic pressure-overloaded human heart. *Circulation.* 2005;112:1136-1144.

307. Barton PJ, Birks EJ, Felkin LE, Cullen ME, Koban MU, Yacoub MH. Increased expression of extracellular matrix regulators TIMP1 and MMP1 in deteriorating heart failure. *J Heart Lung Transplant.* 2003;22:738-744.

308. Thomas CV, Coker ML, Zellner JL, Handy JR, Crumbley AJ, 3rd, Spinale FG. Increased matrix metalloproteinase activity and selective upregulation in LV myocardium from patients with end-stage dilated cardiomyopathy. *Circulation.* 1998;97:1708-1715.

309. Timms PM, Mannan N, Hitman GA, Noonan K, Mills PG, Syndercombe-Court D, Aganna E, Price CP, Boucher BJ. Circulating MMP9, vitamin D and variation in the TIMP-1 response with VDR genotype: mechanisms for inflammatory damage in chronic disorders? *QJM.* 2002;95:787-796.

310. Lindsay MM, Maxwell P, Dunn FG. TIMP-1: a marker of left ventricular diastolic dysfunction and fibrosis in hypertension. *Hypertension.* 2002;40:136-141.

311. Timms PM, Wright A, Maxwell P, Campbell S, Dawnay AB, Srikanthan V. Plasma tissue inhibitor of metalloproteinase-1 levels are elevated in essential hypertension and related to left ventricular hypertrophy. *Am J Hypertens.* 2002;15:269-272.

312. Amour A, Slocombe PM, Webster A, Butler M, Knight CG, Smith BJ, Stephens PE, Shelley C, Hutton M, Knauper V, Docherty AJ, Murphy G. TNF-alpha converting enzyme (TACE) is inhibited by TIMP-3. *FEBS Lett.* 1998;435:39-44.

313. Fedak PW, Smookler DS, Kassiri Z, Ohno N, Leco KJ, Verma S, Mickle DA, Watson KL, Hojilla CV, Cruz W, Weisel RD, Li RK, Khokha R. TIMP-3 deficiency leads to dilated cardiomyopathy. *Circulation.* 2004;110:2401-2409.

314. Schulze CJ, Wang W, Suarez-Pinzon WL, Sawicka J, Sawicki G, Schulz R. Imbalance between tissue inhibitor of metalloproteinase-4 and matrix metalloproteinases during acute myocardial [correction of myoctardial] ischemia-reperfusion injury. *Circulation.* 2003;107:2487-2492.

315. Wei Z, Al-Mehdi AB, Fisher AB. Signaling pathway for nitric oxide generation with simulated ischemia in flow-adapted endothelial cells. *Am J Physiol Heart Circ Physiol.* 2001;281:H2226-2232.

316. Goldstein BJ, Scalia R. Adipokines and vascular disease in diabetes. *Curr Diab Rep.* 2007;7:25-33.

317. Karin M. The regulation of AP-1 activity by mitogen-activated protein kinases. *J Biol Chem.* 1995;270:16483-16486.

318. Shaulian E, Karin M. AP-1 as a regulator of cell life and death. *Nat Cell Biol.* 2002;4:E131-136.

319. Karin M, Liu Z, Zandi E. AP-1 function and regulation. *Curr Opin Cell Biol.* 1997;9:240-246.

320. Li RC, Ping P, Zhang J, Wead WB, Cao X, Gao J, Zheng Y, Huang S, Han J, Bolli R. PKCepsilon modulates NF-kappaB and AP-1 via mitogen-activated protein kinases in adult rabbit cardiomyocytes. *Am J Physiol Heart Circ Physiol.* 2000;279:H1679-1689.

321. Fischer TA, Ludwig S, Flory E, Gambaryan S, Singh K, Finn P, Pfeffer MA, Kelly RA, Pfeffer JM. Activation of cardiac c-Jun NH(2)-terminal kinases and p38-mitogen-activated protein kinases with abrupt changes in hemodynamic load. *Hypertension.* 2001;37:1222-1228.

322. Yano M, Kim S, Izumi Y, Yamanaka S, Iwao H. Differential activation of cardiac c-jun amino-terminal kinase and extracellular signal-regulated kinase in angiotensin II-mediated hypertension. *Circ Res.* 1998;83:752-760.

323. Sadoshima J, Jahn L, Takahashi T, Kulik TJ, Izumo S. Molecular characterization of the stretch-induced adaptation of cultured cardiac cells. An in vitro model of load-induced cardiac hypertrophy. *J Biol Chem.* 1992;267:10551-10560.

324. Hamill D, Davis J, Drawbridge J, Suprenant KA. Polyribosome targeting to microtubules: enrichment of specific mRNAs in a reconstituted microtubule preparation from sea urchin embryos. *J Cell Biol.* 1994;127:973-984.

325. Ruknudin A, Sachs F, Bustamante JO. Stretch-activated ion channels in tissue-cultured chick heart. *Am J Physiol.* 1993;264:H960-972.

326. Sabbah HN, Sharov VG, Lesch M, Goldstein S. Progression of heart failure: a role for interstitial fibrosis. *Mol Cell Biochem.* 1995;147:29-34.

327. Swynghedauw B. Molecular mechanisms of myocardial remodeling. *Physiol Rev*. 1999;79:215-262.

328. Kira Y, Kochel PJ, Gordon EE, Morgan HE. Aortic perfusion pressure as a determinant of cardiac protein synthesis. *Am J Physiol.* 1984;246:C247-258.

329. Ruwhof C, van der Laarse A. Mechanical stress-induced cardiac hypertrophy: mechanisms and signal transduction pathways. *Cardiovasc Res.* 2000;47:23-37.

330. Sussman MA, McCulloch A, Borg TK. Dance band on the Titanic: biomechanical signaling in cardiac hypertrophy. *Circ Res.* 2002;91:888-898.

331. Kubo SH, Rector TS, Bank AJ, Williams RE, Heifetz SM. Endothelium-dependent vasodilation is attenuated in patients with heart failure. *Circulation.* 1991;84:1589-1596.

332. Xia Y, Lee K, Li N, Corbett D, Mendoza L, Frangogiannis NG. Characterization of the inflammatory and fibrotic response in a mouse model of cardiac pressure overload. *Histochem Cell Biol.* 2009;131:471-481.

333. Brower GL, Chancey AL, Thanigaraj S, Matsubara BB, Janicki JS. Cause and effect relationship between myocardial mast cell number and matrix metalloproteinase activity. *Am J Physiol Heart Circ Physiol.* 2002;283:H518-525.

334. Saavedra WF, Paolocci N, St John ME, Skaf MW, Stewart GC, Xie JS, Harrison RW, Zeichner J, Mudrick D, Marban E, Kass DA, Hare JM. Imbalance between xanthine oxidase and nitric oxide synthase signaling pathways underlies mechanoenergetic uncoupling in the failing heart. *Circ Res.* 2002;90:297-304.

335. Ekelund UE, Harrison RW, Shokek O, Thakkar RN, Tunin RS, Senzaki H, Kass DA, Marban E, Hare JM. Intravenous allopurinol decreases myocardial oxygen consumption and increases mechanical efficiency in dogs with pacing-induced heart failure. *Circ Res.* 1999;85:437-445.

336. Amado LC, Saliaris AP, Raju SV, Lehrke S, St John M, Xie J, Stewart G, Fitton T, Minhas KM, Brawn J, Hare JM. Xanthine oxidase inhibition ameliorates cardiovascular dysfunction in dogs with pacing-induced heart failure. *J Mol Cell Cardiol.* 2005;39:531-536.

337. Minhas KM, Saraiva RM, Schuleri KH, Lehrke S, Zheng M, Saliaris AP, Berry CE, Barouch LA, Vandegaer KM, Li D, Hare JM. Xanthine oxidoreductase inhibition causes reverse remodeling in rats with dilated cardiomyopathy. *Circ Res.* 2006;98:271-279.

338. Soran O, Feldman AM, Schneider VM, Hanna R, Mann DL, Korth-Bradley JM. The pharmacokinetics of etanercept in patients with heart failure. *Br J Clin Pharmacol.* 2001;51:191-192.

339. Metyas S, La D, Arkfeld DG. The use of the tumour necrosis factor antagonist infliximab in heart transplant recipients: two case reports. *Ann Rheum Dis.* 2007;66:1544-1545.

340. Hunter EA, Grimble RF. Dietary sulphur amino acid adequacy influences glutathione synthesis and glutathione-dependent enzymes during the inflammatory response to endotoxin and tumour necrosis factor-alpha in rats. *Clin Sci (Lond).* 1997;92:297-305.

341. Aruoma OI, Halliwell B, Hoey BM, Butler J. The antioxidant action of N-acetylcysteine: its reaction with hydrogen peroxide, hydroxyl radical, superoxide, and hypochlorous acid. *Free Radic Biol Med.* 1989;6:593-597.